

**UNIVERSIDAD AUTÓNOMA DE NUEVO LEÓN**

**FACULTAD DE CIENCIAS BIOLÓGICAS**



**Cr(VI) AND Cu(II) BIOREMEDIATION USING  
FUNGAL BIOMASS**

BY

**MARTHA ALICIA ESPINOZA SÁNCHEZ**

SUMMITTED IN FULFILMENT OF THE REQUIREMENTS FOR THE  
DEGREE OF DOCTOR IN BIOTECHNOOLOGY

**May, 2020**

**Cr(VI) AND Cu(II) BIOREMEDIATION USING  
FUNGAL BIOMASS  
THESIS COMMITTEE**



---

Dra. Verónica Almaguer Cantú  
Director



---

Dra. Katiushka Arevalo Niño  
Secretary



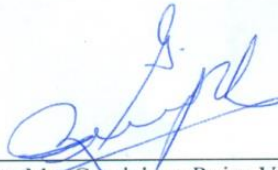
---

Dr. Ramón Gerardo Rodríguez Garza  
Vocal 1



---

Dra. Isela Quintero Zapata  
Vocal 2



---

Dra. Ma. Guadalupe Rojas Verde  
Vocal 3

## ACKNOWLEDGMENTS

This dissertation is the representative work of years where I have fed and cultivated my scientific life at its fullest so far. During these years, I have met amazing people with great minds and a beautiful motivation not only to share but to keep on learning for their improvement as humans in science. None of this would have been possible without the support of my family, my parents Marco Espinoza and Alicia Sanchez, from whom I have found my greatest motivation in life, and my brother and sister Marco and Caro for always walking with me even from far away.

I would like to express my gratitude to my PhD director Dr. Veronica Almaguer for the opportunity and trust in developing this project, along with the Faculty of Biological Sciences, the Autonomous University of Nuevo Leon and CONACYT for making this project possible.

To Dr. Katiushka Arevalo, thank you for the support, help and guidance with the struggles during this period. You have been a great inspiration as a scientist and as a woman.

I want to thank Anita for her unconditional help with every experiment and for her many hours spent in the lab. To Isabel whose help was of great importance with this work.

I want to specially thank Dr. Carlos Lopez Vazquez for the opportunity of working together at IHE-Delft along with Dr. Eldon Raj and Dr. Eric van Hullebusch. Your support and lessons have motivated me to continue into pursuing a life in science. Thank you for all the shared work and for your friendship. The opportunity that you brought to me at IHE has been my most rewarding experience.

I also want to thank the lab staff: Peter, Berend, Ferdi, Lyzzete and Frank, your expertise and knowledge made easier the challenges found in the laboratory.

I also want to thank my students; their interest and freshness was a source of motivation and a constant reminder of the reason why I do science for.

Last but not least, I would like to thank my friends Jorge, Jael and Andrea, for their constant support, understanding and appreciation through all this process.

## DEDICATORY

*To the great minds with noble hearts whose motivation keeps on feeding the curious ones.*

## SUMMARY

Heavy metal contaminated wastewaters are a consequence of the anthropogenic activities that have bred an advanced human life despite the harm that has done to the environment. Chromium and copper are classified as heavy metals. Both exist in different species and their toxicity depends on the valences. Cu(II) can be essential as micronutrient in a concentration less than  $2 \text{ mg}\cdot\text{L}^{-1}$ . Cr(VI) is a highly toxic specie and it must be limited to a concentration of  $100 \mu\cdot\text{L}^{-1}$ . The technologies used to approach the decontamination of these ions are often not efficient enough to reach the low concentrations or the high cost of operation, notwithstanding the proper disposal of the materials used to remove the metals. A green cost-effective way to remove these contaminants needs to scale up. Biosorption is the active/passive uptake of a pollutant using biological materials as adsorbents. Microorganisms have been studied as potential biosorbents in the removal of heavy metals. Fungi species were studied to evaluate their metal uptake capacity under different setups. Optimum pH, temperature, and agitation conditions were selected using factorial design experiments. Kinetic and isotherm models were used to determine the mechanisms involved in the biosorption process. Analysis of linear and non-linear equations was discussed. The highest removal of Cu(II) and Cr(VI) using *Aspergillus* biomass was 37% and 99%, respectively. Biosorption of Cu(II) peaked at 48% and 99% for Cr(VI) using *Rhizopus* sp. dead biomass. Immobilized *Rhizopus* sp. biomass in Ca-alginate beads was studied for Cr(VI) removal, reaching 62.5%. In the continuous experiments, *Trichoderma* sp. was used to be self-immobilized in fungal pellets using two sequencing batch reactors (for growth and Cr(VI) removal). The highest removal for this setup was of 30%. The presence of Cr(VI) at  $10 \text{ mg}\cdot\text{L}^{-1}$  inhibits the substrate consumption of *Trichoderma* sp. This thesis has demonstrated that fungi are potential biosorbents for heavy metal removal, however, the challenges in the scale up process should be deeply considered into the use of these microorganisms as biosorbents.

## RESUMEN

La contaminación de metales pesados en aguas residuales es un resultado de actividades antropogénicas que han cultivado una vida más avanzada para los humanos a pesar del daño que ha causado al medio ambiente. El cromo y cobre están clasificados como metales pesados. Dichos metales existen en diferentes especies y su toxicidad depende de las valencias. El ion Cu(II) puede ser utilizado como micronutriente, sin embargo, su concentración no debe excederse de  $2 \text{ mg}\cdot\text{L}^{-1}$ . El Cr(VI) es una especie altamente tóxica y debe ser limitado a una concentración de  $100 \mu\cdot\text{L}^{-1}$ . Las tecnologías utilizadas para remover estos iones de soluciones acuosas no suelen ser suficientemente eficientes para llegar a las concentraciones necesarias o para llegar al costo de operación, sin mencionar el manejo adecuado de residuos que fueron utilizados para remover los contaminantes. Esto ha llevado a la necesidad de escalar un proceso que sea factible económica y ambientalmente. La biosorción es la captación activa/pasiva de un contaminante utilizando materiales biológicos como adsorbentes. Los microorganismos han sido estudiados como potenciales biosorbentes para la remoción de metales pesados. Diferentes especies fúngicas han sido estudiadas para evaluar su capacidad de remoción en diferentes configuraciones. Las condiciones de pH, temperatura y agitación fueron seleccionadas utilizando un diseño factorial. Modelos cinéticos e isotérmicos fueron aplicados para determinar los mecanismos involucrados en el proceso de biosorción. Se realizó un análisis del uso de las ecuaciones lineales y no lineales de dichos modelos. La biomasa de *Aspergillus* sp. alcanzó una remoción de 37% y 99% para Cu(II) y Cr(VI), respectivamente. La biosorción de Cu(II) tuvo un máximo de 48% y un 99% en el caso de Cr(VI) utilizando biomasa inactiva de *Rhizopus* sp. La biomasa inmovilizada de *Rhizopus* sp. en una matriz de alginato de calcio fue utilizada para la remoción de Cr(VI), obteniendo un 62.5% de remoción. En los experimentos realizados de manera continua, dos reactores discontinuos secuenciales se montaron para la producción de *Trichoderma* sp. en pellets y para determinar su remoción con Cr(VI), cuyo máxima remoción fue 30%. Este trabajo ha demostrado que la biomasa fúngica es un potencial biosorbente para la remoción de metales pesados, no obstante, los retos en el proceso de escalamiento deben ser considerados profundamente para el uso de microorganismos como biosorbentes.

## CONTENTS

<b>AKNOWLEDGMENTS</b> .....	<b>I</b>
<b>DEDICATORY</b> .....	<b>II</b>
<b>SUMMARY</b> .....	<b>III</b>
<b>RESUMEN</b> .....	<b>IV</b>
<b>1. CHAPTER 1 General introduction</b> .....	<b>1</b>
1.1.Introduction.....	2
1.2.Problem statement.....	2
1.3.Hypothesis.....	2
1.4.Research objectives.....	3
1.5.Thesis structure .....	3
1.6.References .....	5
<b>2. CHAPTER 2 Literature review</b> .....	<b>6</b>
2.1.Introduction.....	7
2.2.Heavy metals.....	8
2.2.1. Chromium .....	8
2.2.2. Copper .....	8
2.3.Heavy metal wastewater treatment techniques .....	9
2.3.1. Chemical precipitation .....	9
2.3.2. Electrochemical processes .....	9
2.3.3. Reverse Osmosis .....	9
2.3.4. Ion exchange .....	10
2.3.5. Adsorption.....	10
2.3.6. Biological methods .....	10
2.4.Biosorption mechanisms .....	11
2.4.1. Kinetics in adsorption processes .....	11
2.4.1.1.Biosorption capacity.....	11
2.4.1.2.Kinetic models .....	12
2.4.1.2.1. Pseudo-first order .....	13
2.4.1.2.2. Pseudo-second order .....	13
2.4.1.2.3. Elovich .....	13
2.4.1.2.4. Intraparticle diffusion .....	14
2.4.2. Isotherm models .....	14
2.4.2.1.Langmuir isotherm .....	14

2.4.2.2.Freundlich isotherm .....	15
2.4.3. Thermodynamic parameters of adsorption equilibrium.....	15
2.4.4. Biomass immobilization .....	16
2.5.Bioreactors .....	17
2.5.1. Packed bed column reactor .....	17
2.5.2. Sequencing batch reactor .....	18
2.6.References.....	19
<b>3. CHAPTER 3 Cu(II) removal using dead fungal biomass .....</b>	<b>24</b>
Abstract .....	25
3.1.Introduction.....	26
3.2.Materials and methods .....	27
3.2.1. Preparation of fungal biomass.....	27
3.2.2. Synthetic Cu(II) solution.....	28
3.2.3. Analytical Cu(II) determination.....	28
3.2.4. Experimental design 2 <sup>3</sup> .....	28
3.2.5. Kinetic adsorption assays.....	28
3.2.6. Isotherm assays .....	29
3.3.Results and discussion .....	29
3.3.1. Evaluation of optimal conditions for Cu(II) adsorption.....	29
3.3.2. Adsorption kinetics .....	30
3.3.3. Isotherm analysis.....	33
3.4.Conclusions.....	36
3.5.References.....	36
<b>4. CHAPTER 4 Cr(VI) removal using dead fungal biomass .....</b>	<b>40</b>
Abstract .....	41
4.1.Introduction.....	42
4.2.Materials and methods .....	44
4.2.1. Preparation of dead fungal biomass .....	44
4.2.2. Synthetic Cr(VI) solution.....	44
4.2.3. Batch adsorption experiments.....	44
4.2.3.1.Experimental design 2 <sup>3</sup> .....	44
4.2.3.2.Kinetic assays.....	45



4.2.3.3. Equilibrium studies .....	45
4.2.4. Analytical determination .....	45
4.2.5. Characterization of dead fungal biomass .....	45
4.2.6. Statistical analysis .....	45
4.3. Results and discussion .....	46
4.3.1. Evaluation of optimal adsorption conditions for Cr(VI) adsorption .....	46
4.3.2. Adsorption kinetics .....	47
4.3.3. Isotherm analysis .....	51
4.3.4. FTIR .....	55
4.3.5. SEM-EDX .....	56
4.4. Conclusions .....	57
4.5. References .....	57
<b>5. CHAPTER 5 Cr(VI) removal using immobilized dead fungal biomass .....</b>	<b>62</b>
Abstract .....	63
5.1. Introduction .....	64
5.2. Materials and methods .....	65
5.2.1. Preparation of fungal biomass .....	65
5.2.2. Immobilization of fungal biomass .....	66
5.2.3. Synthetic Cr(VI) solution .....	67
5.2.4. Analytical Cr(VI) determination .....	67
5.2.5. Characterization of immobilized <i>Rhizopus</i> sp. biomass .....	67
5.2.6. Kinetic adsorption assays .....	67
5.2.7. Isotherm assays .....	68
5.3. Results and discussion .....	68
5.3.1. Evaluation of immobilizing agent .....	68
5.3.2. Cr(VI) adsorption kinetics onto immobilized fungal biomass .....	69
5.3.3. Analysis of adsorption isotherms .....	72
5.3.4. Thermodynamic analysis .....	73
5.3.5. Biosorbent characterization .....	74
5.4. Conclusions .....	74
5.5. References .....	75
<b>6. CHAPTER 6 Fungal pelleted sequencing batch reactors: growth and Cr(VI) removal .....</b>	<b>78</b>

Abstract .....	79
6.1.Introduction .....	80
6.2.Materials and methods .....	81
6.2.1. Pre-culture, medium and growth.....	81
6.2.2. Cr(VI) bioaccumulation .....	83
6.2.3. Bioreactor configuration and operating conditions.....	84
6.2.3.1.Cultivation of fungal pellets in SBR .....	86
6.2.3.2.Cr(VI) removal in SBPR.....	86
6.2.4. Characterization of fungal pellets biomass .....	86
6.3.Results and discussion .....	87
6.3.1. Batch glucose growth experiments .....	87
6.3.2. Cr(VI) bioaccumulation experiment .....	88
6.3.3. Cultivation of fungal pellets in SBT .....	88
6.3.4. Cr(VI) removal in SBR using fungal pellets.....	90
6.3.5. SEM-EDX.....	92
6.4.Conclusions .....	94
6.5.References .....	94
<b>7. CHAPTER 7 Conclusions and future perspectives.....</b>	<b>98</b>
7.1.Introduction .....	99
7.2.Fungal biosorption of Cu(II) and Cr(VI) in aqueous solutions.....	99
7.3.Scope for future applications in heavy metal biosorption.....	100
7.4.References .....	100

## FIGURES INDEX

		<b>Page</b>
Figure 1	Thesis structure and connection between chapters	4
Figure 2	Experimental and modelled linear kinetic models of Cu(II) adsorption onto <i>Rhizopus</i> sp. biomass (a) PFO ■ and PSO ■, (b) ID ■ and Elovich ■ models.	31
Figure 3	PFO, PSO, Elovich, and ID non-linear kinetics of Cu(II) adsorption onto <i>Rhizopus</i> sp. dead biomass.	32
Figure 4	(a) Freundlich and (b) Langmuir linear Cu(II) isotherm onto <i>Rhizopus</i> sp. at 10 °C (■), 25 °C (●) and 40 °C (▲).	33
Figure 5	(---) Freundlich and ( — ) Langmuir linear Cu(II) isotherm onto <i>Rhizopus</i> sp. at 10 °C (■), 25 °C (●) and 40 °C (▲).	33
Figure 6	Experimental and modelled linear kinetic models of Cr(VI) adsorption onto <i>Aspergillus</i> sp. and <i>Rhizopus</i> sp. (a) PFO, (b) PSO, (c) Elovich and (d) ID.	49
Figure 7	PFO, PSO, Elovich, and ID experimental and modelled non-linear kinetics of Cr(VI) adsorption onto (a) <i>Rhizopus</i> sp., (b) <i>Rhizopus</i> sp. + NaCl., (c) <i>Aspergillus</i> sp., and (d) <i>Aspergillus</i> + NaCl sp.	50
Figure 8	FTIR spectra of untreated and pre-treated <i>Rhizopus</i> sp. dead biomass before and after Cr (VI) removal.	56
Figure 9	SEM images before (a) and after (c) adsorption, (b), and (d) correspond to the respective EDX spectrums.	57
Figure 10	Ca-alginate beads of <i>Rhizopus</i> sp.	66
Figure 11	<i>Rhizopus</i> sp. immobilized biomass in contact with Cr(VI).	67
Figure 12	Cr(VI) removal using calcium alginate beads.	69
Figure 13	Cr(VI) adsorption using immobilized <i>Rhizopus</i> sp. biomass (—■— % removal, —■— removal capacity)	70
Figure 14	Non-linear kinetic analysis of immobilized fungal biomass on the adsorption of Cr(VI).	71

Figure 15	Non-linear isotherm adsorption of Cr(VI) onto immobilized <i>Rhizopus</i> sp. biomass. (a) Freundlich; (b) Langmuir.	73
Figure 16	FTIR spectra of calcium alginate, <i>Rhizopus</i> sp. biomass immobilized in Ca-alg beads before and after biosorption	74
Figure 17	Macroscopic morphology of fungi in solid media (PDA)	82
Figure 18	Macroscopic morphology of fungal pellets in liquid medium.	83
Figure 19	Experimental set up for fungal pelleted reactor: 1) reactor; 2) biocontroller; 3) influent tank; 4) air supply; 5) pH meter; 6) dO <sub>2</sub> meter; 7) peristaltic pumps; 8) effluent tank; 9) computer	84
Figure 20	Fungal pelleted reactor	85
Figure 21	Fungal growth and glucose consumption at different glucose concentrations (■ TSS (g); ▲ glucose consumption (g·L <sup>-1</sup> ))	87
Figure 22	Glucose consumption and dry weight of R1.	89
Figure 23	dO <sub>2</sub> profile cycles of R1.	89
Figure 24	Glucose consumption from day 24 to 32 on SBR with Cr(VI).	92
Figure 25	Removal of Cr(VI) in SBR reactor.	92
Figure 26	SEM of fungal pellets grown in SBR	93
Figure 27	SEM and EDX analysis of fungal biomass after being in contact with Cr(VI).	94

## TABLE INDEX

		<b>Page</b>
Table 1	Kinetic equation models	12
Table 2	Screening results of <i>Aspergillus</i> sp. and <i>Rhizopus</i> sp. in the removal of Cu(II)	30
Table 3	Kinetic parameters for the adsorption of Cu(II) onto <i>Rhizopus</i> sp.	31
Table 4	Isotherm parameters for the adsorption of Cu(II) onto dead biomass of <i>Rhizopus</i> sp.	35
Table 5	Screening results of <i>Aspergillus</i> sp. and <i>Rhizopus</i> sp. in the removal of Cr(VI)	47
Table 6	Kinetic parameters for the adsorption of Cr(VI) onto untreated and pretreated <i>Rhizopus</i> sp. and <i>Aspergillus</i> sp.	48
Table 7	Isotherm parameters for the adsorption of Cr(VI) onto dead biomass of <i>Rhizopus</i> sp. and <i>Aspergillus</i> sp. analysis.	53
Table 8	Thermodynamic parameters for Cr(VI) adsorption onto pre-treated dead <i>Rhizopus</i> sp. and untreated <i>Aspergillus</i> sp. biomass.	54
Table 9	Kinetic parameters for the adsorption of Cr(VI) onto immobilized <i>Rhizopus</i> sp. biomass.	71
Table 10	Isotherm parameters for the adsorption of Cr(VI) onto immobilized <i>Rhizopus</i> sp. biomass.	72
Table 11	Thermodynamic parameters for Cr(VI) adsorption onto immobilized <i>Rhizopus</i> sp. biomass	72

## EQUATION INDEX

	<b>Page</b>	
Equation 1	Biosorption capacity	11
Equation 2	Removal percentage	12
Equation 3	PFO Lagergren equation	13
Equation 4	PFO solving with initial conditions	13
Equation 5	PFO linearized	13
Equation 6	PSO non-linear	13
Equation 7	PSO linearized	13
Equation 8	Elovich non-linear	13
Equation 9	Elovich linearized	14
Equation 10	ID model	14
Equation 11	Langmuir linearized	14
Equation 12	Langmuir non-linear	14
Equation 13	Separation equilibrium constant	15
Equation 14	Freundlich isotherm non-linear	15
Equation 15	Freundlich isotherm linearized	15
Equation 16	Gibbs free energy	15
Equation 17	Enthalpy	16
Equation 18	Entropy	16

## APPENDIX LIST

		<b>Page</b>
Appendix A	<i>Aspergillus</i> sp. on PDA	101
Appendix B	<i>Rhizopus</i> sp. on PDA	101
Appendix C	ANOVA results of Cu(II) removal screening using <i>Aspergillus</i> sp.	102
Appendix D	ANOVA results of Cu(II) removal screening using <i>Rhizopus</i> sp.	103
Appendix E	ANOVA results of Cr(IV) removal screening using <i>Aspergillus</i> sp.	104
Appendix F	ANOVA results of Cr(IV) removal screening using <i>Rhizopus</i> sp.	105
Appendix G	Reactor 1 through continuous operation for 20 days	106
Appendix H	Reactor 2 through continuous operation for 35 days	103
Appendix I	Reactors setup	105
Appendix J	Script of program used for SBR	106
Appendix K.1	SEM image of fungal biomass	108
Appendix K.2	SEM image of fungal biomass	108
Appendix L.1	Conference certificate	109
Appendix L.2	Congress certificate	109
Appendix L.3	Congress certificate	110

**CHAPTER 1**  
**GENERAL INTRODUCTION**



## **1.1. Introduction**

Water is an elemental resource for life on this planet. Adequate water supplies for agriculture, industry and human consumption are essential for life as it is now known. Ironically, this growing globalization, which has tried to make a better life for human beings, has impacted the environment in a negative way. This impact has added many contaminants, these make more difficult to reach for this fundamental resource. This means that environmental pollution has incremented at the same scale in which industrial development has expanded.

## **1.2. Problem statement**

Industrial activities are known to be the principal source of heavy metal contamination. Usually, metals are essential in low concentrations as nutrients. They play a role in enzymatic and metabolic pathways, also acting as cofactors. Nonetheless, high concentrations of heavy metals can come as inhibitors to all forms of life and can also cause death (Mishra *et al.*, 2019). Copper is the second most important non-ferrous metal and is used in several industries like construction, electronics, and telecommunications (Sethurajan and van Hullebusch 2019). Chromium has its place in industries like plating, corrosion inhibitors, burning of coal, fuel additive, petrochemical fertilizers, steel industries and cooling towers (Javed and Usmani, 2019). The removal of these contaminants can be accomplished by using various techniques to treat industrial wastewaters by chemical means, ion exchange, separation processes and electrochemical technologies (Azizi *et al.*, 2016). The challenges for these technologies can be: 1) in the presence of low concentrations these techniques are not feasible; 2) the cost is not affordable in all countries; 3) the disposal of the materials used usually require treatment before dumping. Bioremediation involves the use of microorganisms or their enzymes as a potential technique to detoxify industrial wastewaters (Sharma and Malaviya, 2016). Therefore, fungi are employed in bioremediation because of their versatility adapting and growing in various extreme conditions of temperature, pH and nutrients, including high metal concentrations (Salvadori *et al.*, 2014). Deeper discussion about the stated problem as well as possible alternative technologies are exposed in *Chapter 2*.

### **1.3. Hypothesis**

Demonstrate that the immobilized fungal biomass in a fixed bed column reactor can remove heavy metals in aqueous solutions.

### **1.4. Research objectives**

#### **1.4.1. General**

Characterization and evaluation of a fixed bed column reactor assessing heavy metal biosorption using fungal biomass.

#### **1.4.2. Specific objectives:**

- Produce inactive biomass of *Aspergillus* sp. and *Rhizopus* sp.
- Execute kinetic bioassays that allow the calculation of the kinetic constants using free biomass, immobilizing agent, and immobilized biomass.
- Elaborate experimental adsorption isotherms to determine the affinity and maximum biosorbent capacity in heavy metal removal.
- Evaluate susceptible parameters in order to scale up the system into a continuous fixed-bed column reactor.
- Set up and up-flow fixed-bed column reactor with immobilized fungal biomass.
- Monitor the performance of the reactor through kinetics measurements and at different hydraulic retention times.
- Analyze and interpret the results in terms of thermodynamic parameters.

### **1.5. Thesis structure**

This dissertation is comprised of seven chapters. Figure 1 shows the diagram of the structure of this work. *Chapter 1* describes a general view of the content of this work, including the problem statement, hypothesis, research objectives, and the thesis outline. *Chapter 2* provides a literature review where a deeper background of the assessed problem is acknowledged, also the use of different technologies for wastewater treatment are exposed. *Chapter 3* consists in the description of the Cu(II) removal process using *Rhizopus* sp. and *Aspergillus* sp. biomass in batch experiments. *Chapter 4* corresponds to the analysis of kinetic and isotherm experiments using the same strains in the removal of Cr(VI) in aqueous solutions, in this chapter the use of pre-treated *Rhizopus* sp. biomass

was selected to continue with further experiments. A modified version of this chapter was published as Espinoza-Sanchez *et al.* (2019). *Chapter 5* describes the Cr(VI) adsorption process in immobilized fungal biomass using calcium alginate, this information was crucial in the scope for future applications of the biosorbent. *Chapter 6* explores the potential of fungal pellets in the removal of Cr(VI) using an SBR where self-immobilization was the main motivation of this part of the work. *Chapter 7* summarizes the gathered information in this thesis and provides insights on the potential use of fungal biomass as heavy metal biosorbents.

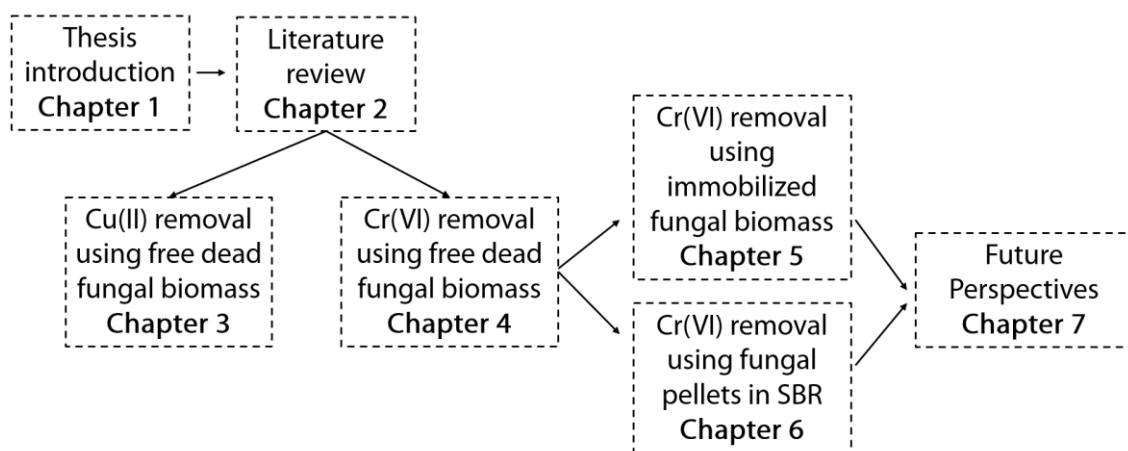


Figure 1. Thesis structure and connection between chapters

## 1.6. References

1. Azizi, S., Kamika, I., Tekere, M., 2016. Evaluation of heavy metal removal from wastewater in a modified packed bed biofilm reactor. *PLoS One* 11, 1–13. <https://doi.org/10.1371/journal.pone.0155462>
2. Javed, M., Usmani, N., 2019. An overview of the adverse effects of heavy metal contamination on fish health. *Proc. Natl. Acad. Sci. India Sect. B - Biol. Sci.* 89, 389–403. <https://doi.org/10.1007/s40011-017-0875-7>
3. Mishra, S., Bharagava, R.N., More, N., Yadav, A., Zainith, S., Mani, S., Chowdhary, P., 2019. Heavy Metal Contamination: An Alarming Threat to Environment and Human Health. *Environ. Biotechnol. Sustain. Futur.* 103–125. [https://doi.org/10.1007/978-981-10-7284-0\\_5](https://doi.org/10.1007/978-981-10-7284-0_5)
4. Salvadori, M.R., Ando, R. a, Oller Do Nascimento, C. a, Corrêa, B., 2014. Bioremediation from wastewater and extracellular synthesis of copper nanoparticles by the fungus *Trichoderma koningiopsis*. *J. Environ. Sci. Health. A. Tox. Hazard. Subst. Environ. Eng.* 49, 1286–95. <https://doi.org/10.1080/10934529.2014.910067>

5. Sethurajan, M., van Hullebusch, E.D., 2019. Leaching and selective recovery of Cu from printed circuit boards. *Metals (Basel)*. 9, 25–26. <https://doi.org/10.3390/met9101034>
6. Sharma, S., Malaviya, P., 2016. Bioremediation of tannery wastewater by chromium resistant novel fungal consortium. *Ecol. Eng.* 91, 419–425. <https://doi.org/10.1016/j.ecoleng.2016.03.005>

**CHAPTER 2**  
**LITERATURE REVIEW**

## 2.1. Introduction

According to UN-Water (2017), high-income countries treat about 70% of the municipal and industrial wastewater they generate. The ratio goes down to 38% in the case of upper-middle-income countries and even to 28% in lower-middle-income countries. In low-income countries, only 8% of the used water undergoes treatment of any kind. This means that worldwide, over 80% of all the wastewater is discharged without treatment. As the population keeps growing, the demand for clean water also accelerates the demand in the reuse of wastewater and freshwater to meet with the needs of the population. In order to supply this necessity, more novel techniques and framework for water treatment technologies are required to reach its final stage, this can possible make an adequate water treatment to fit into daily human and environmental needs (Karri *et al.*, 2019). The contamination of water can be caused by several means: industrial wastes, mining activities, sewage and wastewater, pesticides and chemical fertilizers, energy usage, radioactive waste, urban development, etc. As the water is used gets polluted, any activity will produce an effluent, in which many occasions this contains an undesirable amount of toxic pollutants (Crini and Lichtfouse, 2019). In developing countries, the impact of increased pollution is particularly problematic because these populations do not have the resources to effectively treat contaminated water or access to clean drinking water systems that can supply it to their homes (Joseph *et al.*, 2019).

Heavy metals are the main group of inorganic contaminants in wastewater and are defined as any metallic element that has a high density and is characterized as toxic. It is crucial to acknowledge the effects of toxic substances in different organisms that are present in diverse ecosystems (Muñoz-Nájera *et al.*, 2018). Contrary to organic contaminants, heavy metals are not biodegradable and have a propensity to accumulate in living organisms. Among the toxic heavy metals, there is a specific concern in the treatment of industrial wastewaters that contain zinc, copper, nickel, mercury, cadmium, lead, and chromium (Fu and Wang, 2011).

## **2.2. Heavy metals**

### **2.2.1. Chromium**

The tanning industry has been greatly examined for its environmental impact and it is marked as one of the worst anthropogenic polluters. The tanning process, whether is chrome tanning or vegetable tanning, follows beamhouse operations of soaking, liming, reliming, unhairing, and fleshing. The combined wastewater from tannery operations is described with a strong color and high chemical oxygen demand (COD), biochemical oxygen demand (BOD), dissolved and suspended solids, and chromium. Chromium toxicity is one of the major causes of human health hazards caused by tannery wastewaters (Sharma and Malaviya, 2016). Produced wastewaters from washing and rinsing operations of plating processes contain Cr(VI) in elevated concentrations and different metal salts in low amounts at a pH between 3.0 and 5.0. The high toxicity of Cr(VI) makes its reduction or removal mandatory, in order to discharge the effluent meeting with the permissible limits (Liu *et al.*, 2016). Physical processes, which reduce the amount of available Cr(VI), can mask the processes responsible for biological and chemical Cr(VI) reduction (Lu *et al.*, 2018).

### **2.2.2. Copper**

Undesirable concentrations of copper ions are found in the wastewater produced by mining wastes, drainage discharges, plating baths, fertilizers, paint, and pigment industries (Blázquez *et al.*, 2011). Part of the copper that enters aquatic systems gets washed off from surfaces during storm events, yet, the rest is directed to wastewater treatment facilities (WWTFs) where it is further combined with both household sources of copper and leached copper from copper piping. Since not all the metal is removed in WWTFs, copper is discharged with the treated effluent (Mosbrucker, 2016). There are different forms of copper and their toxicity differs among them, nonetheless, most of the copper produces a complex with organic and inorganic species. Some of these species are considered toxic to some extent, but the cupric ion is commonly considered the most toxic species (Paquin *et al.*, 2002). Nowadays, there is not a specific method able to deliver an adequate treatment, mainly because of the complex nature of industrial effluents. This implies that only a combination of methods can reach the required quality of water needed to discharge (Crini and Lichtfouse, 2019).

## **2.3. Heavy metal wastewater treatment techniques**

### **2.3.1. Chemical precipitation**

The most used industrial method to remove heavy metals is chemical precipitation. It consists in the removal of a certain substance, adding a specific reagent, which will ease the removal of the target substance by separation methods. According to Chen *et al.* (2018), the simplicity of process control, effectivity varying temperature and the low-cost operations are the characteristics that make this method attractive. Notwithstanding, commercial precipitants lack the necessary binding sites or bring environmental hazards, which makes it a not completely safe technology to use. This has led to studies of new and more effective precipitants to be synthesized in order to meet the discharged law requirements (Fu and Wang, 2011).

### **2.3.2. Electrochemical processes**

The basis of this technology is to apply electricity through a metal bearing aqueous solution, which contains a cathode plate and an insoluble anode, causing reduction and oxidation in both cathode and anode. The heavy metals will precipitate in a weakly acidic or neutralized electrolyte as hydroxides (Tran *et al.*, 2017). The electrochemical process based on deposition for removing heavy metals has advantages such as: rapid removal enabled by electric-field migration instead of random diffusion, high capacity due to the reducing nature of the process that can change the metal ions to its zerovalent form, and the multiple heavy metals treating feature that makes it possible not to be removed but to be recovered from wastewater (Liu *et al.*, 2019).

### **2.3.3. Reverse Osmosis**

Reverse osmosis is a well-known technology for its use on wastewater treatments and more recurrent in desalination applications. The process is driven by pressure, where a membrane rejects dissolved constituents in water. Rejection can occur by size exclusion, charge exclusion, and physicochemical interactions between solute, solvent, and the membrane itself (Radjenović *et al.*, 2008). The efficiency depends on parameters like the density of the membrane and the functional groups introduced into the polymer structure, which are responsible for the strength in the membrane charge (Malaeb and Ayoub, 2011).



#### **2.3.4. Ion exchange**

The foundation of this process consists in a reversible ion interchange between phases (solid and liquid). The insoluble substance removes ions from an electrolytic solution and releases other ions of similar charge in a chemically equivalent amount without any structural change of the resin (Vigneswaran *et al.*, 2004). Chelating resins contain ligands that bond particularly with certain types of metal cations. The choice of the resin will determine the affinity for a given metal. This technology is commonly used in continuous processes using fixed bed plants. By using this set-up the selectivity for the noxious species increases, which at the same time diminishes the interference of other cations present in the effluent (Malaviya and Singh, 2011).

#### **2.3.5. Adsorption**

The application of this technology can be found in the treatment of wastewaters, groundwater, and industrial effluents along with the generation of drinking water. The adjustability in design, low-energy requirements, and cost-effectiveness are some of the advantages that adsorption has (Bonilla-Petriciolet *et al.*, 2017). It works as a mass transfer process where an adsorbate is bound to a solid surface (adsorbent) by physical and chemical interactions (Kurniawan *et al.*, 2006). Activated carbon is well-known for its high efficiency in the removal of contaminants, however, the adsorbent comes to be expensive, hereby the need of low-cost adsorbents (El-Naggar *et al.*, 2018). The use of biological materials for adsorption processes has gained a lot of attention in the last decades.

#### **2.3.6. Biological methods**

According to Kikuchi and Tanaka (2012), the biological treatments for the removal of metals in water and sediments can be found in the following classifications: biosorption, bioaccumulation, oxidation/reduction, leaching, precipitation, volatilization, degradation, and phytoremediation. Bioaccumulation and biosorption have been considered as novel technologies with economic feasibility along with efficiency and as an eco-friendly alternative to treat heavy metals from wastewaters (Kanamarlapudi *et al.*, 2018).

## 2.4. Biosorption mechanisms

The concept of biosorption has been explained as the potential of biological materials to accumulate heavy metals from wastewater in either active or inactive (metabolically) mediated pathways (Shamim, 2016). The mechanisms involved depend on the origin of the biomass used and its processing. The metal uptake follows several complex mechanisms like ion exchange, chelation, adsorption by physical forces; the ion entrapment in the capillaries of the surface can result in a gradient of concentration and diffusion through the matrix of the biosorbent (Volesky and Holan, 1995). The factors affecting the process include pH, temperature, ionic strength, initial metal concentration, biosorbent dosage and size, agitation speed, and also the possible interaction with other contaminants present in the solution (Park *et al.*, 2010). There is a great variety of biological materials that can be used as sorbents in heavy metal removal. Different types of plants, animals, microbial biomass and its derivatives; wastes from plants, agricultural and industrial activities; and byproducts that are discharged can be used as biosorbents. Fungal biomass has many polysaccharides and glycoproteins, these hold metal-binding groups (carboxyls, amines, hydroxyl, phosphate, etc.). Fungal production is present in many industrial processes, this makes it possible to be used in the removal of contaminants at large volumes of wastewaters (Kanamarlapudi *et al.*, 2018). Biosorption has been considered as a promising alternative technique for heavy metal ions removal due to its cost-effectiveness, high metal adsorption capacity, high efficiency at low concentrations, ecologically friendly nature and the possible biosorbent regeneration, as well as the possible metal recovery (El-Naggar *et al.*, 2018).

### 2.4.1. Kinetics of biosorption

#### 2.4.1.1. Biosorption capacity

The biosorption capacity refers to the quality of the biosorbent to capture the target metal ion (amount of adsorbed material per mass of adsorbent ( $Q_e$ )), and it is calculated using the difference between the initial and remaining concentrations of the contaminant in aqueous solution. This is calculated using Eq. (1). The removal efficiency of the metal removal is calculated as Eq. (2) shows.

$$Q_e = \frac{C_i - C_f}{M} V \quad (1)$$

$$\text{Removal efficiency (\%)} = \frac{C_i - C_f}{C_i} \times 100 \quad (2)$$

Where  $C_i$  and  $C_f$  are the initial and final concentrations of the metal ion respectively,  $M$  is the biomass dosage and  $V$  is the work volume.

#### 2.4.1.2. Kinetic models

The adsorption process can be explained in stages. In the first, the sorbate is transferred from the solution to the external surface of the sorbent. In the second stage, the internal diffusion of the sorbate to the sorption sites occurs, and finally, the sorption itself takes place. Some mathematical models assume that the sorption is the limiting step, some others, take the diffusion as the rate-limiting step (Largitte and Pasquier, 2016). This is the basis for the wide use of adsorption kinetic studies, the understanding of the involved mechanisms for the further design of future large-scale adsorption facilities. The most common models used for adsorption studies are the pseudo-first order (PFO), pseudo-second order (PSO), intraparticle diffusion (ID) and Elovich models (Riahi *et al.*, 2017). The equations used to model in this work are shown in Table 1.

Table 1. Kinetic equation models

Kinetic model	Equation	Linearized form
Pseudo-first order	$q_t = q_e(1 - e^{-k_1 t})$	$\log(q_e - q_t) = \log(q_e) - \frac{k_1}{2.303} t$
Pseudo-second order	$q_t = \frac{k_2 q_e^2 t}{1 + k_2 q_e t}$	$\frac{t}{q_t} = \frac{1}{k_{II} q_e^2} + \frac{1}{q_e} t$
Intra-particle diffusion	$q_t = k_d t^{\frac{1}{2}}$	$q_t = k_d t^{\frac{1}{2}} + C$
Elovich	$q_t = a e^{-\beta q}$	$q_t = \frac{1}{\beta} \ln(\alpha \beta) + \frac{1}{\beta} \ln(t)$

#### 2.4.1.2.1. Pseudo-first order

The PSO equation suggested by Lagergren in 1898 infers that the rate of solute uptake is proportional to the gradient in saturation concentration and it is described by the following differential equation.

$$\frac{dq_t}{dt} = k_1(q_e - q_t) \quad (3)$$

Where  $q_t$  = adsorption capacity ( $\text{mg} \cdot \text{g}^{-1}$ );  $t$  = time (min) and  $k_1$  is the rate constant ( $1 \cdot \text{min}^{-1}$ ). After solving with the initial conditions of  $q_t = 0$ , when  $t = 0$ , Eq. (3) becomes Eq. (4).

$$q = q_e(1 - \exp(-k_1 t)) \quad (4)$$

Its linearized form is:

$$\ln\left(\frac{q_e}{q_e - q_t}\right) = k_1 t \quad (5)$$

Plotting  $\ln(q_e - q)$  vs  $t$  can determine the values of  $k_1$ .

#### 2.4.1.2.2. Pseudo-second order

The PSO model based on adsorption capacity has the form (Wu *et al.*, 2009).

$$\frac{dq_t}{dt} = k_2(q_e - q)^2 \quad (6)$$

After the integration of Eq. (6), followed by the application of the initial conditions, the following equation is attained.

$$\frac{t}{q_t} = \left(\frac{1}{k_2 q_e^2}\right) + \left(\frac{1}{q_e}\right) t \quad (7)$$

Since the equation is linear, the calculation of  $k_2$  and  $q_e$  in Eq. (7) can be obtained from the intercept and slope in the plot  $(t \cdot q_t^{-1})$  vs  $t$ .

#### 2.4.1.2.3. Elovich model

The Elovich model describes a process of chemical adsorption of molecules, first explained with the adsorption rate of carbon monoxide onto manganese dioxide by Zeldowitsch (1934), who developed the Elovich equation (Bonilla-Petriciolet *et al.*, 2017), the following differential equation represents this model.

$$\frac{dq}{dt} = a e^{-\beta q} \quad (8)$$

Where  $q$  ( $\text{mg}\cdot\text{g}^{-1}$ ) expressed the adsorption capacity at time  $t$ ,  $a$  is the desorption constant, and  $\beta$  is the initial adsorption rate. Assuming  $a\beta t \gg 1$ , Eq. (8) was integrated with the initial conditions of  $q = 0$  at  $t = 0$  and  $q = q$  at  $t = t$  resulting in Eq. (9).

$$q_t = \left(\frac{1}{\beta}\right) \text{Ln}(\alpha\beta) + \left(\frac{1}{\beta}\right) \text{Ln}(t) \quad (9)$$

This model is used to describe the adsorption process of various molecules from aqueous solutions. The constants  $\alpha$  and  $\beta$  are calculated from the slope and intercept of the linear plot of  $q_t$  vs  $\text{Ln}(t)$ .

#### 2.4.1.2.4. Intra-particle diffusion equation

The mechanisms of the intraparticle diffusion phenomena are developed by compelling pore volume diffusion, surface diffusion, or a merge of both mechanisms (Bonilla-Petriciolet *et al.*, 2017). The initial rate of the intra-particle diffusion is defined by the Eq. (10).

$$q_t = k_d t^{\frac{1}{2}} + C \quad (10)$$

where  $k_d$  is the intra-particle diffusion rate constant ( $\text{mg}\cdot(\text{g}\cdot\text{min}^{1/2})^{-1}$ ) and  $C$  is linked to the boundary layer thickness ( $\mu\cdot\text{mg}$ ).

### 2.4.2. Isotherm models

#### 2.4.2.1. Langmuir isotherm

The Langmuir adsorption isotherm is a model that has been widely used to deduce the performance of different sorbents and it is based on the hypothesis that the uptake of sorbates occurs on a homogenous surface by monolayer sorption without interaction between the adsorbed molecules (Hamdaoui and Naffrechoux, 2007; Farouq and Yousef, 2015). The Langmuir isotherm equations can be expressed as follows in its linear and non-linear form.

$$\frac{1}{q_e} = \frac{1}{K_L \times q_m} \cdot \frac{1}{C_e} + \frac{1}{q_m} \quad (11)$$

$$q_e = \frac{q_{max} \cdot K_L \cdot C_e}{1 + K_L \cdot C_e} \quad (12)$$

where  $K_L$  is the adsorption constant ( $\text{L}\cdot\text{mg}^{-1}$ ) related to the adsorption energy,  $q_m$  is the maximum adsorption capacity ( $\text{mg}\cdot\text{g}^{-1}$ ) and  $C_e$  the metal concentration at equilibrium.

The Langmuir isotherm can be exhibited in terms of equilibrium parameter  $R_L$ , which is a dimensionless constant, considered as a separation equilibrium parameter (Dada *et al.*, 2012), which can be calculated with Eq. (13).

$$R_L = \frac{1}{1+(1+K_L C_o)} \quad (13)$$

Where:

$C_o$  is the initial Cr(VI) concentration and  $K_L$  is Langmuir constant. The  $R_L$  value indicates if the adsorption is unfavorable  $R_L > 1$ , linear if  $R_L = 1$ , favorable if  $0 < R_L < 1$  and irreversible if  $R_L = 0$ .

#### 2.4.2.2. Freundlich isotherm

The Freundlich sorption isotherm model explains the adsorption process in heterogeneous surfaces (Hamdaoui and Naffrechoux, 2007); Farouq and Yousef, 2015), the exponential distribution of active sites and their energies, and is expressed by the following equations (Bilgili *et al.*, 2012).

$$q_e = K_f C_e^{1/n} \quad (14)$$

$$\log q_e = \log K_f + \frac{1}{n_f} \log C_e \quad (15)$$

The values of  $K_f$  and  $n_f$  are calculated from the slope and intercept of the linear plot  $\log q_e$  versus  $\log C_e$ . The linear least-squares method and the linearly transformed equations have been widely applied to correlate sorption data where  $1 \cdot n^{-1}$  is a heterogeneity parameter, the smaller the  $1 \cdot n^{-1}$ , the greater the expected heterogeneity (Dada *et al.*, 2012).

#### 2.4.3. Thermodynamic parameters of adsorption equilibrium

The thermodynamic characteristics of an adsorption system are needed to incorporate complex microscopic interactions, this leads to adsorption studies focusing on these properties to identify the affinity of the adsorbent for the adsorbate (Liu and Lee, 2014). With the fitted parameters for the Langmuir isotherm, the standard Gibbs free energy of adsorption is calculated by Eq. (16).

$$\Delta G^0 = -RT \ln K_L \quad (16)$$

Where  $K_L$  is the adsorption equilibrium constant. The isotheric heat of adsorption can be derived as follows.

$$\Delta H^0 = R \frac{d \ln K_L}{d(1/T)} \quad (17)$$

Therefore, when adsorption efficiency increases with temperature  $\Delta H^0 > 0$ , the process is endothermic; any other way, it is exothermic. Based on equations (16) and (17), the difference in the entropy adsorption process is calculated with Eq. (18).

$$\Delta S^0 = \left( -\frac{\Delta G^0}{T} \right) - \left( -\frac{\Delta H^0}{T} \right) \quad (18)$$

#### 2.4.4. Biomass immobilization

The understanding of the mechanisms that rule biosorption is without a doubt a crucial point in the study of the biosorption. However, the use of free biomass has a disadvantage when the biosorbent has to be separated from the bulk solution. In order to be able to use biomass as a biosorbent for heavy metal treatment in an industrial application, the biomass must have certain mechanical, chemical, and thermodynamic characteristics, which, usually are not found in dry biomass. This leads to the need of an immobilization matrix that can enhance the removal of the ion and maintain its removal properties after the desorption of the pollutant. The appropriate immobilization agent shall be considered if the combination of both biomass and immobilization agent has no negative effect on the uptake removal of the heavy metal. Immobilization is defined as the entrapment of material in a fixed matrix through physical or chemical means. There are several methods to immobilize living or dead cells and different organic, inorganic, and composite carriers (chitin, agar, ceramic, activated charcoal, zeolite, clay, alginate, etc.) that allow the microorganisms immobilization (Bouabidi *et al.*, 2019). Self-immobilization also has been reported in several studies, in this process cell-cell interaction in the microorganism results in the aggregation of what is known as a granule. Aerobic granulation has been regarded as one of the most promising biotechniques in the wastewater treatment area (de Kreuk and van Loosdrecht, 2004; Sharma *et al.*, 2019). The biomass immobilization provides to the biosorbent the facility to reuse and the possibility to separate the biomass from the liquid bulk (Prakasham *et al.*, 1999). Live and dead microbial biomass has been immobilized and self-immobilized to evaluate its potential as a wastewater treatment in continuous set-ups.

## 2.5. Bioreactors

According to McDuffie (1991), a reactor in which a biological reaction takes place is defined as a bioreactor. In wastewater treatment, the water is recycled in aerobic or anaerobic conditions, in which free or immobilized microbial biomass enhances the removal of a contaminant. The principal characteristics that must be considered in the design of biological reactors are the following: operating conditions, pH, size of the reactor, mixing and mass transfer for oxygen uptake, temperature, sterility, influent and effluent feeds, oxygen concentrations, and illumination. The use of bioreactors in wastewater treatment appears in different types of bioreactors:

- Fluidized bed reactor (FBR)
- Packed bed reactor (PBR)
- Bubble column reactor (BCR)
- Membrane bioreactor (MBR)
- Rotating biological contactor (RBC)
- Continuous stirred tank bioreactor (CSTR)
- Sequencing batch reactor (SBR)
- Photo-bioreactor

Each of these reactors has a specific target to remove, in order to assess the removal of any contaminant, the design of the reactor will play an essential role. In the present work, the use of PBR and SBR is analyzed using fungal species to remove heavy metals.

### 2.5.1. PBR

This type of reactors usually have a tubular geometry and are packed with immobilized biosorbent. This design is popular between chemical engineers because of the versatile applications that the configuration covers. The reactor consists of a chamber filled with the pellets and a liquid solution that flows through the catalyst. The efficiency of the adsorbent used is measured by a breakthrough curve, which exhibits its maximum when the adsorbent is saturated. The use of PBR with biosorbents has been reported in the removal of different contaminants. A mixed biosorbent from tea waste, maple leaves and mandarin peels was used by Abdolali *et al.*, (2017) to remove heavy metals in a PBR. *Aspergillus niger* immobilized in a polysulfone matrix was used in a column to study the



biosorption of Cd, Cu, Pb, and Ni (Kapoor and Viraraghavan, 1998). Removal of Cr(VI) was studied in a PBR using *Hibiscus Cannabinus* Kenaf in a column containing a working volume of 6 mL (Omidvar Borna *et al.*, 2016). The use of microbial biomass immobilized in external materials like alginate, chitosan, polyurethane, and pectin could be restricted when a large-scale production is needed due to the high cost of the materials. This leads to a more suitable, novel and economical treatment using fungal-based pellets (Wang *et al.*, 2019).

### **2.5.2. SBR**

The activated sludge process (ASP) is a biological treatment of wastewaters, where a microbial suspension is added to a vessel to be aerated (to oxidize organic matter), after aeration, there is solid-liquid separation to discharge the clarified effluent, the exceeding waste is removed and the biomass is returned to the aeration tank (Tantak *et al.*, 2014). The SBR can be considered as an improvement of the ASP, considering that there is no need to discharge the effluent to another container because the whole treatment is accomplished in the same reactor. This process consists of a sequence of filling, mixing, reaction, clarification, and withdrawal (Wang *et al.*, 1995). The SBR is one of the most popular technologies to treat municipal wastewater and is very adjustable in processes like nitrification and denitrification, the possibility to use aerobic, anaerobic, and anoxic setups makes it a very attractive technology. Enhanced biological phosphorus removal (EBPR) has been reported as a sustainable process in activated sludge processes. The use of glycogen-accumulating organisms (GAO) and phosphorus accumulating organisms (PAO) in SBR was reported by Lopez-Vazquez *et al.* (2008). The removal of inorganic compounds has been gaining attention using SBR set ups. Zhang *et al.* (2019) used activated sludge from a wastewater treatment plant in a SBR to investigate the nitrification process in the presence of Cd. *Trametes versicolor* immobilized in sorghum was used to evaluate the removal of humic acids from synthetic and real wastewater under non-sterile conditions, these contaminants form complexes with heavy metals increasing their transport in water (Zahmatkesh *et al.*, 2018). *Phanerochaete chrysosporum* was produced in the form of fungal pellets to remove selenite and tellurite in an up-flow reactor by Espinosa-Ortíz *et al.* (2015). However, there is no report on the use of fungal self-immobilized pellets in SBR for heavy metal removal.

## 2.6. References

1. Abdolali, A., Ngo, H.H., Guo, W., Zhou, J.L., Zhang, J., Liang, S., Chang, S.W., Nguyen, D.D., Liu, Y., 2017. Application of a breakthrough biosorbent for removing heavy metals from synthetic and real wastewaters in a lab-scale continuous fixed-bed column. *Bioresour. Technol.* 229, 78–87. <https://doi.org/10.1016/j.biortech.2017.01.016>
2. Bilgili, M.S., Varank, G., Sekman, E., Top, S., Özçimen, D., Yazıcı, R., 2012. Modeling 4-chlorophenol removal from aqueous solutions by granular activated carbon. *Environ. Model. Assess.* 17, 289–300. <https://doi.org/10.1007/s10666-011-9293-z>
3. Blázquez, G., Martín-Lara, M.A., Dionisio-Ruiz, E., Tenorio, G., Calero, M., 2011. Evaluation and comparison of the biosorption process of copper ions onto olive stone and pine bark. *J. Ind. Eng. Chem.* 17, 824–833. <https://doi.org/https://doi.org/10.1016/j.jiec.2011.08.003>
4. Bonilla-Petriciolet, A., Mendoza-Castillo, D., Reynel, H., 2017. Adsorption Processes for Water Treatment and Purification. DOI 10.1007/978-3-319-58136-1\_1
5. Bouabidi, Z.B., El-Naas, M.H., Zhang, Z., 2019. Immobilization of microbial cells for the biotreatment of wastewater: A review. *Environ. Chem. Lett.* 17, 241–257. <https://doi.org/10.1007/s10311-018-0795-7>
6. Chen, Q., Yao, Y., Li, X., Lu, J., Zhou, J., Huang, Z., 2018. Comparison of heavy metal removals from aqueous solutions by chemical precipitation and characteristics of precipitates. *J. Water Process Eng.* 26, 289–300. <https://doi.org/10.1016/j.jwpe.2018.11.003>
7. Crini, G., Lichtfouse, E., 2019. Advantages and disadvantages of techniques used for wastewater treatment. *Environ. Chem. Lett.* 17, 145–155. <https://doi.org/10.1007/s10311-018-0785-9>
8. Dada, A.O., Olalekan, O.P., Olatunya, A.M., Dada, O., 2012. Langmuir, Freundlich, Temkin and Dubinin–Radushkevich isotherms studies of equilibrium sorption of Zn<sup>2+</sup> unto phosphoric acid modified rice husk. *IOSR J. Appl. Chem.* 3, 38–45. <https://doi.org/10.9790/5736-0313845>
9. de Kreuk, M.K., van Loosdrecht, M.C.M., 2004. Selection of slow growing organisms as a means for improving aerobic granular sludge stability. *Water Sci. Technol.* 49, 9–17.
10. El-Naggar, N.E.A., Hamouda, R.A., Mousa, I.E., Abdel-Hamid, M.S., Rabei, N.H., 2018. Biosorption optimization, characterization, immobilization and application of *Gelidium amansii* biomass for complete Pb<sup>2+</sup> removal from aqueous solutions. *Sci. Rep.* 8, 1–19. <https://doi.org/10.1038/s41598-018-31660-7>
11. Espinosa-Ortiz, E.J., Rene, E.R., van Hullebusch, E.D., Lens, P.N.L., 2015. Removal of selenite from wastewater in a *Phanerochaete chrysosporium* pellet based fungal

- bioreactor. *Int. Biodeterior. Biodegrad.* 102, 361–369. <https://doi.org/10.1016/j.ibiod.2015.04.014>
12. Farouq, R., Yousef, N.S., 2015. Equilibrium and kinetics studies of adsorption of copper (II) ions on natural biosorbent. *Int. J. Chem. Eng. Appl.* 6, 319–324. <https://doi.org/10.7763/IJCEA.2015.V6.503>
  13. Fu, F., Wang, Q., 2011. Removal of heavy metal ions from wastewaters: A review. *J. Environ. Manage.* 92, 407–418. <https://doi.org/10.1016/j.jenvman.2010.11.011>
  14. Hamdaoui, O., Naffrechoux, E., 2007. Modeling of adsorption isotherms of phenol and chlorophenols onto granular activated carbon. Part I. Two-parameter models and equations allowing determination of thermodynamic parameters. *J. Hazard. Mater.* 147, 381–394. <https://doi.org/10.1016/j.jhazmat.2007.01.021>
  15. Joseph, L., Jun, B.M., Flora, J.R.V., Park, C.M., Yoon, Y., 2019. Removal of heavy metals from water sources in the developing world using low-cost materials: A review. *Chemosphere* 229, 142–159. <https://doi.org/10.1016/j.chemosphere.2019.04.198>
  16. Kanamarlapudi, S.L.R.K., Chintalpudi, V.K., Muddada, S., 2018. Application of Biosorption for Removal of Heavy Metals from Wastewater. *Biosorption*. <https://doi.org/10.5772/intechopen.77315>
  17. Kapoor, A., Viraraghavan, T., 1998. Removal of heavy metals from aqueous solutions using immobilized fungal biomass in continuous mode. *Water Res.* 32, 1968–1977. [https://doi.org/10.1016/S0043-1354\(97\)00417-X](https://doi.org/10.1016/S0043-1354(97)00417-X)
  18. Karri, R.R., Shams, S., Sahu, J.N., 2019. Overview of Potential Applications of Nano-Biotechnology in Wastewater and Effluent Treatment, *Nanotechnology in Water and Wastewater Treatment*. Elsevier Inc. <https://doi.org/10.1016/b978-0-12-813902-8.00004-6>
  19. Kikuchi, T., Tanaka, S., 2012. Biological removal and recovery of toxic heavy metals in water environment. *Crit. Rev. Environ. Sci. Technol.* 42, 1007–1057. <https://doi.org/10.1080/10643389.2011.651343>
  20. Kurniawan, T.A., Chan, G.Y.S., Lo, W.-H., Babel, S., 2006. Physico-chemical treatment techniques for wastewater laden with heavy metals. *Chem. Eng. J.* 118, 83–98. <https://doi.org/https://doi.org/10.1016/j.cej.2006.01.015>
  21. Largitte, L., Pasquier, R., 2016. A review of the kinetics adsorption models and their application to the adsorption of lead by an activated carbon. *Chem. Eng. Res. Des.* 109, 495–504. <https://doi.org/10.1016/j.cherd.2016.02.006>
  22. Liu, C., Fiol, N., Poch, J., Villaescusa, I., 2016. A new technology for the treatment of chromium electroplating wastewater based on biosorption. *J. Water Process Eng.* 11, 143–151. <https://doi.org/10.1016/j.jwpe.2016.05.002>
  23. Liu, C., Wu, T., Hsu, P.C., Xie, J., Zhao, J., Liu, K., Sun, J., Xu, J., Tang, J., Ye, Z., Lin, D., Cui, Y., 2019. Direct/alternating current electrochemical method for removing and recovering heavy metal from water using graphene oxide electrode. *ACS Nano* 13, 6431–6437. <https://doi.org/10.1021/acsnano.8b09301>

24. Liu, X., Lee, D., 2014. Thermodynamic parameters for adsorption equilibrium of heavy metals and dyes from wastewaters. *Bioresour. Technol.* 160, 24–31. <https://doi.org/10.1016/j.biortech.2013.12.053>
25. Lopez-Vazquez, C.M., Song, Y. Il, Hooijmans, C.M., Brdjanovic, D., Moussa, M.S., Gijzen, H.J., Van Loosdrecht, M.C.M., 2008. Temperature effects on the aerobic metabolism of glycogen-accumulating organisms. *Biotechnol. Bioeng.* 101, 295–306. <https://doi.org/10.1002/bit.21892>
26. Lu, Y.Z., Chen, G.J., Bai, Y.N., Fu, L., Qin, L.P., Zeng, R.J., 2018. Chromium isotope fractionation during Cr(VI) reduction in a methane-based hollow-fiber membrane biofilm reactor. *Water Res.* 130, 263–270. <https://doi.org/10.1016/j.watres.2017.11.045>
27. Malaeb, L., Ayoub, G.M., 2011. Reverse osmosis technology for water treatment: State of the art review. *Desalination* 267, 1–8. <https://doi.org/10.1016/j.desal.2010.09.001>
28. Malaviya, P., Singh, A., 2011. Physicochemical technologies for remediation of chromium-containing waters and wastewaters. *Crit. Rev. Environ. Sci. Technol.* 41, 1111–1172. <https://doi.org/10.1080/10643380903392817>
29. McDuffie, N.G., 1991. Introduction. *Bioreact. Des. Fundam.* 1–3. <https://doi.org/10.1016/b978-0-7506-9107-9.50005-0>
30. Mosbrucker, A.M., 2016. Copper speciation in wastewater-impacted surface waters. PhD diss., Oregon State University.
31. Muñoz-Nájera, M.A., Barrera-Escorcía, G., Ramírez-Romero, P., Tapia-Silva, F.O., Rosas-Cedillo, R., 2018. Heavy metal bioaccumulation in *Oreochromis niloticus* from Tenango Dam, Puebla, Mexico. *Environ. Monit. Assess.* 190. <https://doi.org/10.1007/s10661-018-6670-y>
32. Omidvar Borna, M., Pirsahab, M., Vosoughi Niri, M., Khosravi Mashizie, R., Kakavandi, B., Zare, M.R., Asadi, A., 2016. Batch and column studies for the adsorption of chromium(VI) on low-cost Hibiscus Cannabinus kenaf, a green adsorbent. *J. Taiwan Inst. Chem. Eng.* 68, 80–89. <https://doi.org/10.1016/j.jtice.2016.09.022>
33. Paquin, P.R., Gorsuch, J.W., Apte, S., Batley, G.E., Bowles, K.C., Campbell, P.G.C., Delos, C.G., Di Toro, D.M., Dwyer, R.L., Galvez, F., Gensemer, R.W., Goss, G.G., Hogstrand, C., Janssen, C.R., McGeer, J.C., Naddy, R.B., Playle, R.C., Santore, R.C., Schneider, U., Stubblefield, W.A., Wood, C.M., Wu, K.B., 2002. The biotic ligand model: A historical overview. *Comp. Biochem. Physiol. - C Toxicol. Pharmacol.* 133, 3–35. [https://doi.org/10.1016/S1532-0456\(02\)00112-6](https://doi.org/10.1016/S1532-0456(02)00112-6)
34. Park, D., Yun, Y.-S., Park, J.M., 2010. The past, present, and future trends of biosorption. *Biotechnol. Bioprocess Eng.* 15, 86–102. <https://doi.org/10.1007/s12257-009-0199-4>

35. Prakasham, R.S., Merrie, J.S., Sheela, R., Saswathi, N., Ramakrishna, S. V., 1999. Biosorption of chromium VI by free and immobilized *Rhizopus arrhizus*. Environ. Pollut. 104, 421–427. [https://doi.org/10.1016/S0269-7491\(98\)00174-2](https://doi.org/10.1016/S0269-7491(98)00174-2)
36. Radjenović, J., Petrović, M., Ventura, F., Barceló, D., 2008. Rejection of pharmaceuticals in nanofiltration and reverse osmosis membrane drinking water treatment. Water Res. 42, 3601–3610. <https://doi.org/10.1016/j.watres.2008.05.020>
37. Riahi, K., Chaabane, S., Thayer, B. Ben, 2017. A kinetic modeling study of phosphate adsorption onto *Phoenix dactylifera* L. date palm fibers in batch mode. J. Saudi Chem. Soc. 21, S143–S152. <https://doi.org/10.1016/j.jscs.2013.11.007>
38. Shamim, S., 2016. Comparative analysis of metal resistance, accumulation and antioxidant enzymes in *Cupriavidus metallidurans* CH34 and *Pseudomonas putida* mt2 during cadmium stress. J Basic Microbiol. 55:374–381. <https://doi.org/10.1002/jobm.201300038>
39. Sharma, S., Malaviya, P., 2016. Bioremediation of tannery wastewater by chromium resistant novel fungal consortium. Ecol. Eng. 91, 419–425. <https://doi.org/10.1016/j.ecoleng.2016.03.005>
40. Sharma, S., Sarma, S.J., Tay, J.H., 2019. Aerobic granulation in wastewater treatment: A general overview, Microbial Wastewater Treatment. Elsevier Inc. <https://doi.org/10.1016/B978-0-12-816809-7.00004-X>
41. Tantak, N., Chandan, N., Raina, P., 2014. An Introduction to Biological Treatment and Successful Application of the Aqua EMBR System in Treating Effluent Generated from a Chemical Manufacturing Unit: A Case Study, Industrial Wastewater Treatment, Recycling and Reuse. Elsevier Ltd. <https://doi.org/10.1016/B978-0-08-099968-5.00009-X>
42. Tran, T.K., Chiu, K.F., Lin, C.Y., Leu, H.J., 2017. Electrochemical treatment of wastewater: Selectivity of the heavy metals removal process. Int. J. Hydrogen Energy 42, 27741–27748. <https://doi.org/10.1016/j.ijhydene.2017.05.156>
43. UN-Water, 2017. Wastewater - The Untapped Resources, The United Nations World Water Development Report. Wastewater. The Untapped Resource. <https://doi.org/10.1017/CBO9781107415324.004>
44. Volesky, B., Holan, Z.R., 1995. Biosorption of heavy metals. Biotechnol. Prog. 11, 235–50. <https://doi.org/10.1021/bp00033a001>
45. Vigneswaran S., Ngo H.H., Chaudhary D.S., Hung YT. (2005) Physicochemical Treatment Processes for Water Reuse. In: Wang L.K., Hung YT., Shammas N.K. (eds) Physicochemical Treatment Processes. Handbook of Environmental Engineering, vol 3. Humana Press
46. Wang, L., Kurylko, L., Wang Mu, H.S., 1995. 5354458 Sequencing batch liquid treatment. Environ. Int. 21, XXVIII. [https://doi.org/10.1016/0160-4120\(95\)99321-r](https://doi.org/10.1016/0160-4120(95)99321-r)

47. Wang, L., Yu, T., Ma, F., Vitus, T., Bai, S., Yang, J., 2019. Novel self-immobilized biomass mixture based on mycelium pellets for wastewater treatment: A review. *Water Environ. Res.* 91, 93–100. <https://doi.org/10.1002/wer.1026>
48. Wu, F.C., Tseng, R.L., Huang, S.C., Juang, R.S., 2009. Characteristics of pseudo-second-order kinetic model for liquid-phase adsorption: A mini-review. *Chem. Eng. J.* 151, 1–9. <https://doi.org/10.1016/j.cej.2009.02.024>
49. Zahmatkesh, M., Spanjers, H., van Lier, J.B., 2018. A novel approach for application of white rot fungi in wastewater treatment under non-sterile conditions: immobilization of fungi on sorghum. *Environ. Technol. (United Kingdom)* 39, 2030–2040. <https://doi.org/10.1080/09593330.2017.1347718>
50. Zhang, L., Fan, J., Nguyen, H.N., Li, S., Rodrigues, D.F., 2019. Effect of cadmium on the performance of partial nitrification using sequencing batch reactor. *Chemosphere* 913–922. <https://doi.org/10.1016/j.chemosphere.2019.02.006>

**CHAPTER 3**  
**Cu(II) REMOVAL USING DEAD FUNGAL BIOMASS**

## **Abstract**

The contamination of water by heavy metals is a problem that needs to be assessed in a serious way. Copper is one of the most used metals in industry and the increasing anthropogenic activities demand a new approach to deal with this situation. Microorganisms have been reported as biosorbents in the removal of several pollutants. The removal of Cu(II) onto dead biomass of *Aspergillus* sp. and *Rhizopus* sp. was studied through discontinuous experiments. The operational conditions for the removal of Cu(II) were determined by a factorial design in which pH, temperature, and agitation were the independent variables, having the adsorption capacity as the response variable. The highest removal was at pH 5.0 for both strains. The ANOVA demonstrated that pH is a variable that affects significantly the biosorption process with the two strains. The biomass with greater adsorption in the screening was *Rhizopus* sp., which reached 48.63% of Cu(II) removal. Linear and non-linear equations of the kinetic and isotherm models were evaluated to extrapolate which model and regression approach was the most reliable method to describe the adsorption experiments of Cu(II) onto *Rhizopus* sp. The kinetic results showed that the ID model fitted the experimental data. The isotherm modelling demonstrated the heterogeneity of the fungal biomass surface, since the Freundlich model had the highest coefficient of determination in both equations used.



### 3.1. Introduction

The unceasing production of wastewater containing metals and other contaminants poses a serious threat not only to the environment but even to the industrial world who discharge these contaminated wastewaters. Heavy metals can be found in the environment by natural and anthropogenic activities. Copper is the third most used metal in the world, this includes many industries like construction, machinery, electronics, and telecommunication (Sethurajan and van Hullebusch, 2019). Cu(II) is an essential micronutrient needed in the growth of plants and animals, however, in high doses can cause several diseases like anemia, or produce damage in both kidney and liver along with stomach and intestinal irritation (Saad *et al.*, 2019). The World Health Organization (WHO) provided a guideline in which the Cu(II) intake should not exceed  $2 \text{ mg}\cdot\text{L}^{-1}$  (WHO, 2011).

The conventional methods such as chemical precipitation, ion exchange, electrodeposition, and membrane filtration require expensive equipment, monitoring, complex reagents, and the generation of secondary contaminants (Xu *et al.*, 2018). For this reason, the need to research a different and more economical approach to remove heavy metals from wastewater is increasing. Bioremediation is mainly applied in matrixes such as soil, sludges and several types of residual waters (Zhang *et al.*, 2017). This access through biotechnology can be very attractive due to its ecofriendly nature and low-cost operation, distinctively if applied *in-situ* (Quintella *et al.*, 2019). Biosorption is a physicochemical process that involves electrostatic interactions between an extracellular surface and the metal ions (Lacerda *et al.*, 2019). This process represents the ability of biological materials in removing heavy metals from aqueous effluents, biosorbents have high efficiency, selectivity, and its natural affinity to metal ions (Matouq *et al.*, 2015). Biomass (live or dead) of bacteria, algae, fungi, and plants have been highly reported as potential biosorbents able to sequester metal ions at trace level from contaminated effluents. These biosorbents, unlike ion exchange resins, contain several functional sites (carboxyl, imidazole, sulfhydryl, amino, etc.) (Gazem and Nazareth, 2012). Fungal dead biomass has been reported as profitable in wastewater treatment considering that the biomass is less affected by toxic wastes, along with its potential regeneration and reutilization (Dhal *et al.*, 2018). Even though heavy metal removal can be achieved by

living or dead biological matrixes, large scale feasibility of biosorptive processes have shown that the use of dead biomass could be more suitable than the bioaccumulation approach, this is due to the nutrient requirements of the living cells in a bioreactor (Ayangbenro and Babalola, 2017). A great number of studies reported in literature have shown the use of biosorbents like *Mucor indicus*, *Rhizopus arrhizus*, *Rhizopus oryzae* in the removal of heavy metals (Behnam *et al.*, 2015).

The adsorption process is a surface phenomenon, which consists in the transfer of soluble substances into a solid adsorbent. Adsorption is widely used to remove pollutants from aqueous solutions, hence, the study of kinetic and isotherm equilibrium experiments is essential to design an optimal adsorption system (Guo and Wang, 2019). The different adsorption isotherm equations have been studied with the fundamental idea to optimize the design of the parameters for adsorption (Subramanyam and Das, 2014). The accuracy of the model parameters will depend on the appropriate selection of the conceptual model, the data reliability, and whether the correct parameter estimation method was used (Bolster and Hornberger, 2007).

This work aims to research the biosorption potential of *Rhizopus* sp. and *Aspergillus* sp. in the removal of Cu(II) from aqueous solutions. The optimum conditions were determined using a factorial design varying pH, temperature, and agitation. The kinetic constants were calculated using the linear and non-linear equations of the PFO, PSO, Elovich and ID kinetic models. The Langmuir and Freundlich model isotherm models were modelled also in their linear and non-linear equations to predict the equilibrium constants that ruled the isotherm experiments.

## **3.2. Materials and methods**

### **3.2.1. Preparation of fungal biomass**

The fungal strains used in this study were *Rhizopus* sp and *Aspergillus* sp. These strains were isolated from soil. The sampling and isolation of the strains were carried out in Monterrey, Nuevo León, México by Castro-González *et al.* (2017). The strains were cultivated in 500 mL Erlenmeyer flasks with liquid sterile media containing the following concentrations in g·L<sup>-1</sup>: sucrose (40), K<sub>2</sub>HPO<sub>4</sub> (4), MgSO<sub>4</sub>·7H<sub>2</sub>O (75), NH<sub>4</sub>Cl (1), citric acid (3), cysteine (0.5), yeast extract (1.5), NaCl (1), and CaCl<sub>2</sub> (0.1). The Erlenmeyer

flasks containing 200 mL of culture media were incubated for 7 days at 30 °C in a MaxQ 8000 stackable shaker (Thermo Scientific). The biomass it was inactivated by autoclaving (1.0207 atm., 121 °C). After, it was filtrated using Vacuum Filter Units with 0.22 µm Cellulose acetate membrane. Finally, the biomass was dried in an oven at 60 °C for 24 h and powdered into ~10 µm particles using a mortar and pestle.

### **3.2.2. Synthetic Cu(II) solution**

The chemicals used were of analytical grade. A stock solution (1000 mg·L<sup>-1</sup>) of Cu (II) was prepared with 3.9308 g of CuSO<sub>4</sub>. The pH of the solutions was adjusted using HCl and NaOH at 0.1 M.

### **3.2.3. Analytical Cu(II) determination**

The determination of the residual Cu(II) ions after being in contact with the biomass was quantified using Atomic Absorption Spectroscopy (Spectra AA 50 Varian) at a wavelength of 324.8 nm.

### **3.2.4. Experimental design 2<sup>3</sup>**

In order to get the optimal conditions for Cu(II) removal, an experimental screening varying pH, temperature, and agitation conditions was conducted. These experiments were carried out by using Corning 15 mL centrifuge tubes, containing 10 mL of Cu(II) solution of 50 mg·L<sup>-1</sup> at pH 3.0 and 5.0, the dosage of fungal biomass was of 0.05 g·L<sup>-1</sup>. The solution was in contact with the fungal biomass for 120 min in orbital shakers at 50 and 150 rpm, with temperatures of 20 °C and 40 °C, afterwards the tubes were centrifuged in a Compact II Centrifuge (Clay Adams) and the remaining Cu(II) was analyzed.

### **3.2.5. Kinetic adsorption assays**

Kinetic experiments were conducted with 10 mL of 50 mg·L<sup>-1</sup> Cu(II) solution at pH 5.0, 120 rpm, and 25 ± 2°C. The biomass dosage was 0.05 g and contact times were designed to sample at different time intervals in a total time of 8 h. The experimental kinetic data were modeled using the equations in Table 1 of *Chapter 2*.

### 3.2.6. Isotherm assays

The isotherm studies were carried out with 0.05 g of dead biomass into 10 mL of Cu(II) solutions with concentrations between 12.5 mg·L<sup>-1</sup> and 300 mg·L<sup>-1</sup> at pH 5.0, temperature was set up at 10, 25 and 40 °C. The biomass was in contact with the solution for 240 min. Langmuir and Freundlich isotherm models were used to analyze the data collected from the experiments.

## 3.3. Results and discussion

### 3.3.1. Evaluation of optimal conditions for Cu(II) adsorption

The experimental screening was executed to choose the conditions in which the adsorption phenomenon has optimal results. These results were analyzed with IBM SPSS Statistics 22 using one-way ANOVA. According to the screening analysis for *Aspergillus* sp., the only variable that presented a statistical significance was pH, the model had an  $R^2$  of 0.98 ( $F_{1,7} = 305.05$ ,  $p < 0.05$ ) demonstrating that Cu(II) removal onto *Aspergillus* sp. is affected solely by pH, these results are shown in Table 2. The maximum removal for this strain was a 37.6% at the conditions of pH 5.0, 20 °C and 150 rpm, the removal capacity was a  $q$  of 3.71 mg·g<sup>-1</sup>. The variance analysis for the screening parameters of *Rhizopus* sp. dead biomass had an  $R^2$  of 0.94 ( $F_{1,7} = 40.38$ ,  $p < 0.05$ ) showed that the significant variables were pH and temperature. A noticeable increase in adsorption can be observed at higher pH, as shown in the work of Song *et al.*, (2014), where the sorption of metal ions increased at pH 4.0 for Pb(II) and at 5.0 for Cu(II). There is influence of pH in the chemical speciation of metals, the increase in biosorption of Cu(II) with the increase in pH can be due to the gradually exposed ligands (carboxyl, sulfhydryl, phosphate groups, etc.) resulting in greater attraction between metal ions and ligands (Xu *et al.*, 2018). In the work of Tu *et al.* (2018), it was shown that in the pH range of 3.0–5.0, the Cu(II) removal extent of the strain NT-1 increased significantly with increasing pH and reached a peak value of 24.4% at pH = 5.0. There are three species of copper present in solution: Cu<sup>2+</sup>, CuOH<sup>+</sup> and Cu(OH)<sub>2</sub>, from pH 2.5 to 3.5 H<sup>+</sup> compete with Cu<sup>2+</sup> ions for the biosorption sites. Nonetheless, the effect is diminished by the increase of pH (4.0–6.0), since the rise of density in negative charges on the cell surface offer more binding sites (Kapoor and Viraraghavan, 1995; Li *et al.*, 2015). Since the dead biomass

of *Rhizopus* sp. exhibited better results in the removal of Cu(II), this strain was selected for the next set of experiments.

Table 2. Screening results of *Aspergillus* sp. and *Rhizopus* sp. in the removal of Cu(II).

pH	Temperature (°C)	RPM	<i>Aspergillus</i> sp.		<i>Rhizopus</i> sp.	
			% Removal	$Q$ (mg·g <sup>-1</sup> )	% Removal	$Q$ (mg·g <sup>-1</sup> )
3.0	20	50	23.60	2.21	40.18	3.77
		150	27.64	2.59	39.32	3.69
	40	50	32.56	3.06	47.40	4.45
		150	27.41	2.57	42.77	3.99
5.0	20	50	37.61	3.71	46.70	4.59
		150	29.99	2.96	40.62	4.01
	40	50	34.60	3.41	48.63	4.78
		150	34.64	3.61	48.33	4.73

### 3.3.2. Adsorption kinetics

The biosorption capacity of the *Rhizopus* sp. was evaluated at different times. The results of the kinetic models used to analyze this experiment are shown in Table 3. The process is time-dependent, however, the rate of adsorption had a rapid increase during the first 120 min, where the removal reached 25%, the highest removal was at 480 min with a 35% removal, showing a decrease in the adsorption rate. The linear and non-linear analysis of the kinetic models showed different results with the collected data. The graphs of the modelled kinetics are shown in Figure 2 and 3. The ID model in the non-linear analysis was the one with a better fit for this data, reaching a regression coefficient of 0.97, followed by the Elovich model (0.96), the PSO (0.93), and finally PFO (0.87). These non-linear analysis results speculate that the adsorption process is ruled by the ID model. In contrast, the linearized equations of the models assume that the best fit for the data was with both PSO and Elovich model ( $R^2 = 0.97$ ), followed by the PFO (0.96) and finally the ID model with a coefficient of 0.95. The PFO linear model shows a  $q_e$  of 2.2 mg·g<sup>-1</sup>, while the non-linear model has a 2.9 mg·g<sup>-1</sup>, which is closer to the experimental  $q_e = 3.26$  mg·g<sup>-1</sup>.

Table 3. Kinetic parameters for the adsorption of Cu(II) onto *Rhizopus* sp. biomass.

	Non-linear	Linear
Kinetic model	<i>Rhizopus</i> sp.	
<i>Pseudo-first order model</i>		
$K_1$ ( $\text{min}^{-1}$ )	0.0110	0.0043
$q_e$ ( $\text{mg}\cdot\text{g}^{-1}$ )	2.9081	2.2799
$R^2$	0.8753	0.9688
<i>Pseudo-second order model</i>		
$K_{II}$ ( $\text{g}\cdot(\text{mg}\cdot\text{min})^{-1}$ )	0.0038	0.0021
$q_e$ ( $\text{mg}\cdot\text{g}^{-1}$ )	3.4373	3.8343
$R^2$	0.9349	0.9775
<i>Intra-particle diffusion model</i>		
$K_d$	0.1129	0.1205
$R^2$	0.9724	0.9573
<i>Elovich model</i>		
$\alpha$ ( $\text{mg}\cdot(\text{g}\cdot\text{min})^{-1}$ )	0.2717	0.0808
$\beta$ ( $\text{g}\cdot\text{mg}^{-1}$ )	0.6316	1.2683
$R^2$	0.9647	0.9775
$q_{e,exp}$		3.2674

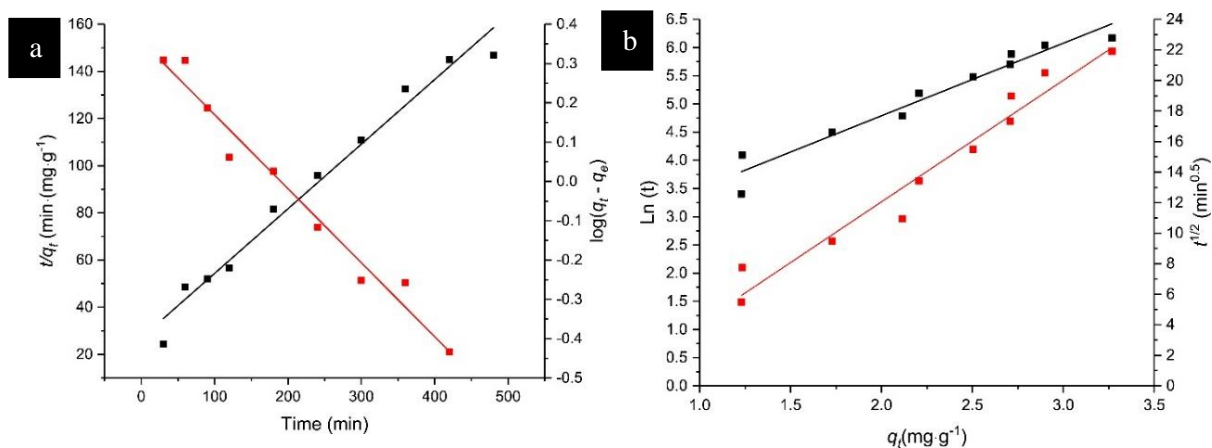


Figure 2. Experimental and modelled linear kinetic models of Cu(II) adsorption onto *Rhizopus* sp. biomass

(a) PFO ■ and PSO ■, (b) ID ■ and Elovich ■ models.

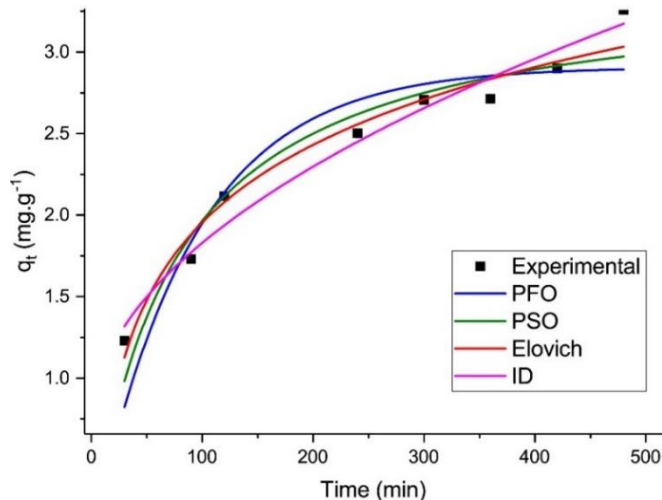


Figure 3. PFO, PSO, Elovich and ID non-linear kinetics of Cu(II) adsorption onto *Rhizopus* sp. dead biomass

The models which have consistency within both linear and non-linear analysis are in the next order: ID > Elovich > PSO > PFO, this behaviour in the fitting of the data has been previously observed for the PSO also by Chowdhury and Saha (2011). The model that reported the greatest error in the comparison of the different regression approach was the PFO, analogous results have been reported, where Lin and Wang (2009) studied the adsorption of basic dye onto activated carbon. There are two different adsorption phases within this phenomenon through time. The first one compasses the high availability of the many free sites and the high Cu(II) concentration, after, the removal rate is reduced when the sites are occupied and the sorbate needs to penetrate the inner layers of the adsorbent (Kannamba *et al.*, 2010; Behnam *et al.*, 2015). The increase in contact time did not show a significant increment in the adsorption capacity, demonstrating that the lower adsorption rate at the final stage was because of the metal ions laboriousness into occupying the active vacant sites remaining, due to the forces between the biosorbent and the sorbate (Rashid *et al.*, 2016). The decrease in the adsorption capacity at the latter stage could be attributed to the intraparticle diffusion process during the second phase of adsorption (Haq Nawaz *et al.*, 2011; Noreen *et al.*, 2013). The effect of contact time has been explained with the presumption that the active sites at the beginning of the process are available to bind with the ions, as in the second slower phase, the vacant sites that still remain are not able to bind anymore, also there could be repulsive forces between the solute of solid and the bulk phase (Gupta and Balomajumder, 2015).

### 3.3.3. Isotherm analysis

The isotherm analysis of Cu(II) biosorption onto *Rhizopus* sp. was mathematically expressed in terms of the Langmuir and Freundlich isotherm models, in both linear and non-linear equations. The objective was to evaluate the higher coefficient of determination in the experimental data set. Figures 4 and 5 show the graphs for the linearized and non-linearized models, respectively. The calculated constants of the modelled equations are presented in Table 4.

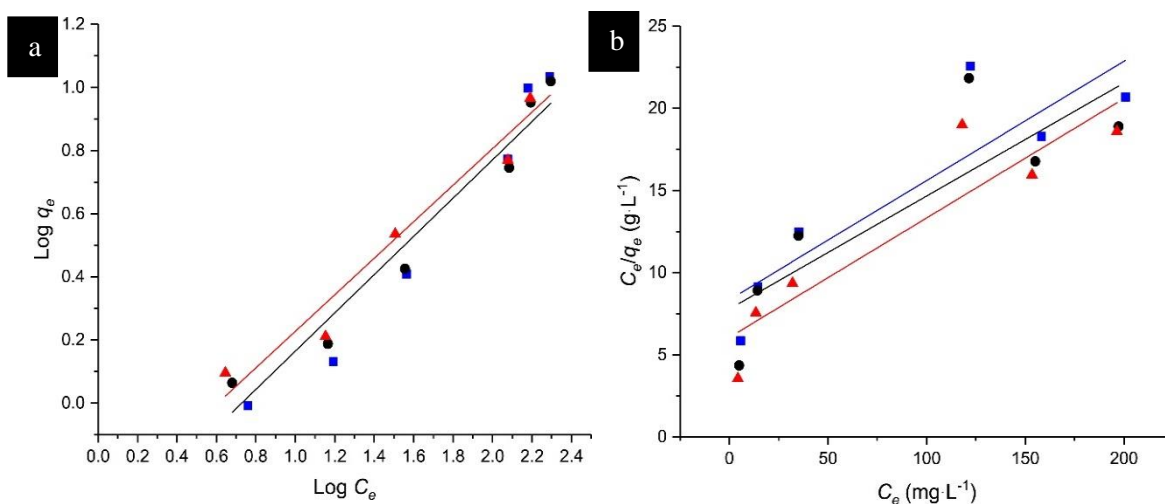


Figure 4. (a) Freundlich and (b) Langmuir linear Cu(II) isotherm onto *Rhizopus* sp. at 10 °C (■), 25 °C (●) and 40 °C (▲).

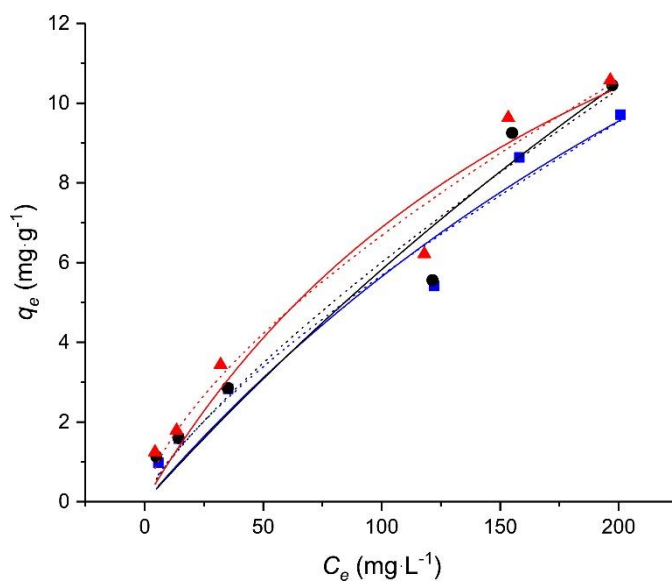


Figure 5. (---) Freundlich and (—) Langmuir linear Cu(II) isotherm onto *Rhizopus* sp. at 10 °C (■), 25 °C (●) and 40 °C (▲).



The Langmuir model has at least four different linearized equations, which, each bring a different output, showing that the linearization of the Langmuir isotherm model affects the interpretation of data sets while using linearized equations. The characteristic plot of  $C_e/Q_e$  vs  $C_e$  has the feature that the model formulation can artificially create a high correlation between the independent and dependent variables and, thereupon, a high correlation of the model predictions with the experimental data (Osmari *et al.*, 2013). Consequently, the Langmuir linearized equation chosen to model the biosorption of Cu(II) onto *Rhizopus* sp. was using the plot mentioned above. However, this linearized equation, which usually shows a very good correlation, did not fit with the experimental data since the  $q_m$  calculated with both equations were higher than the  $q_{m,exp}$  (10.57 mg·g<sup>-1</sup>). In the non-linear approach of the Langmuir model, the  $R^2$  was better than the one in the linear equation, nonetheless, the  $q_m$  shows values even greater than the ones calculated in the linear expression, thus, this model is not considered suitable to explain this isotherm experiments. One of the reasons that could explain the very different calculated parameters is that the linear regression method makes an approximation of the scattered points around the line, assuming that the data follows a Gaussian distribution and the standard deviation at every value of  $C_e$ , this is not a real behavior with equilibrium isotherm models (Nagy *et al.*, 2017). Consequently, the model which had the best coefficient of determination ( $R^2 > 0.95$ ) was the Freundlich model for the three temperatures in both linear and non-linear equations. The intensity of sorption, denoted by “n”, is related to the distribution of bound ions on the sorbent surface, was greater than the unity in all the modelled data, indicating that there is favorable sorption of copper onto *Rhizopus* sp. The Freundlich constant  $1/n$  decreased with the increase in temperature, indicating more specific surface heterogeneity of the sorbent at high temperature, supporting an endothermic chemisorption, similar results were reported in the adsorption of europium(III) onto 1-(2-pyridylazo)-2-naphthol impregnated polyurethane foam by Saeed and Ahmed (2006).

Xu *et al.* (2018) reported the biosorption of Cu(II) and Cr(VI) using *Penicillium chrysogenum* XJ-1, where the experimental data of Cu(II) biosorption had a better fit with the Freundlich equation in its linear form, comparing to three different linearized equations of the Langmuir isotherm. Gupta *et al.* (2015) reported the isotherm analysis of

Cu(II) using living *Aspergillus niger* biomass, in this study the correlation coefficients obtained were higher for the Freundlich isotherm. Similar results were also shown by Gazem and Nazareth (2012), where the biosorption of Pb(II) and Cu(II) were studied using lyophilized *Aspergillus versicolor* biomass and had also a better fit with the Freundlich isotherm equation. The work of Naeem *et al.* (2016), showed the sorption properties of iron impregnated activated carbon in the removal of methylene blue followed the Freundlich model, since it fitted closely as compared with the Langmuir model. In this case, the heterogeneous distribution of iron content on activated carbon caused is attributable to the affinity of the model. *Moringa* pods were used to remove heavy metals, evaluated by four different isotherm models (Langmuir, Freundlich, Temkin and Dubinin-Radushkevich), in the case of copper removal the Freundlich and the Temkin equations delivered the best correlation (Matouq *et al.*, 2015). The transformation of non-linear isotherm model to a linear equation seems to implicitly alter the error functions as well as the error variance and normality assumptions of the least-squares methods (Subramanyam and Das, 2014).

Table 4. Isotherm parameters for the adsorption of Cu(II) onto dead biomass of *Rhizopus* sp.

Isotherm model	Temperature (°C)					
	Linear			Non-Linear		
	10	25	40	10	25	40
<i>Langmuir</i>						
$K_L$ (L·mg <sup>-1</sup> )	0.0087	0.0088	0.0120	0.0022	0.0012	0.0047
$q_m$ (mg·g <sup>-1</sup> )	13.7778	14.5375	13.7517	30.9833	53.3012	21.2380
$R^2$	0.7911	0.7215	0.8397	0.9471	0.9379	0.9393
$R_L$	0.22–0.47	0.21–0.47	0.18–0.46	0.60–0.97	0.74–0.98	0.42–0.95
<i>Freundlich</i>						
$K_F$ (mg·g <sup>-1</sup> )	0.2282	0.3619	0.4453	0.1820	0.1607	0.3141
$n$	1.4005	1.6504	1.7284	1.3387	1.2702	1.5066
$R^2$	0.9678	0.9563	0.9626	0.9625	0.9501	0.9626

### 3.4. Conclusions

The biosorption potential of *Rhizopus* sp. and *Aspergillus* sp. dead biomass was studied for the removal of Cu(II). The optimal conditions for pH, temperature and agitation were chosen from the ANOVA analysis of a factorial design. The removal of the ion using *Aspergillus* sp. was inferior compared to the results using *Rhizopus* sp.. Both strains were affected significantly by the change of pH and the maximum removal was at pH 5.0. Further analyses were carried out using only *Rhizopus* sp. biomass. The results of the kinetic analysis showed that the coherence in the kinetic models, both linear and non-linear analysis are in the next order: ID > Elovich > PSO > PFO. Assuming that the adsorption phenomenon is instantaneous at the beginning, followed by a step where intraparticle diffusion behaves as gradual adsorption, leading to the last phase, where equilibrium is reached due to the slow adsorption rate. The isotherm assay showed that the model with better fit was the Freundlich model in the two equations considered, displaying a heterogenous surface and favorable adsorption of Cu(II) onto *Rhizopus* sp.

### 3.5. References

1. Ayangbenro, A.S., Babalola, O.O., 2017. A new strategy for heavy metal polluted environments: A review of microbial biosorbents. *Int. J. Environ. Res. Public Health* 14. <https://doi.org/10.3390/ijerph14010094>
2. Behnam, S., Zamani, A., Karimi, K., Mehrabani-Zeinabad, A., 2015. Copper removal using different fungal-based adsorbents: a comparative and detailed study. *J. Dispers. Sci. Technol.* 36, 866–876. <https://doi.org/10.1080/01932691.2014.930351>
3. Bolster, C.H., Hornberger, G.M., 2007. On the use of linearized Langmuir equations. *Soil Sci. Soc. Am. J.* 71, 1796–1806. <https://doi.org/10.2136/sssaj2006.0304>
4. Castro-Gonzalez, I., Rojas-Verde, G., Quintero-Zapata, I., Almaguer-Cantu, V., 2017. A comparative study on removal efficiency of Cr(VI) in aqueous solution by *Fusarium* sp. and *Myrothecium* sp. *Water Air Soil Pollut.* 228. <https://doi.org/10.1007/s11270-017-3476-4>
5. Chowdhury, S., Saha, P., 2011. Adsorption kinetic modeling of safranin onto rice husk biomatrix using pseudo-first- and pseudo-second-order kinetic models: comparison of linear and non-linear methods. *Clean - Soil, Air, Water* 39, 274–282. <https://doi.org/10.1002/clen.201000170>
6. Dhal, B., Abhilash, Pandey, B.D., 2018. Mechanism elucidation and adsorbent characterization for removal of Cr(VI) by native fungal adsorbent. *Sustain. Environ. Res.* 28, 289–297. <https://doi.org/10.1016/j.serj.2018.05.002>

7. Gazem, M.A.H., Nazareth, S., 2012. Isotherm and kinetic models and cell surface analysis for determination of the mechanism of metal sorption by *Aspergillus versicolor*. World J. Microbiol. Biotechnol. 28, 2521–2530. <https://doi.org/10.1007/s11274-012-1060-z>
8. Guo, X., Wang, J., 2019. Comparison of linearization methods for modeling the Langmuir adsorption isotherm. J. Mol. Liq. 296, 111850. <https://doi.org/10.1016/j.molliq.2019.111850>
9. Gupta, A., Balomajumder, C., 2015. Simultaneous bioremediation of Cr(VI) and phenol from single and binary solution using *Bacillus* sp.: multicomponent kinetic modeling. J. Environ. Chem. Eng. 3, 2180–2186. <https://doi.org/10.1016/j.jece.2015.07.025>
10. Gupta, P., Kumar, P., Singh, N., 2015. Adsorption of copper metal by living *Aspergillus niger* L. biomass 5, 1122–1133. <https://doi.org/10.6088/ijes.2014050100106>
11. Haq Nawaz, B., Rubina, K., Muhammad Asif, H., 2011. Biosorption of Pb(II) and Co(II) on red rose waste biomass. Iran. J. Chem. Chem. Eng. 30, 81–88.
12. Kannamba, B., Reddy, K.L., AppaRao, B. V., 2010. Removal of Cu(II) from aqueous solutions using chemically modified chitosan. J. Hazard. Mater. 175, 939–948. <https://doi.org/10.1016/j.jhazmat.2009.10.098>
13. Kapoor, A., Viraraghavan, T., 1995. Fungal biosorption - an alternative treatment option for heavy metal bearing wastewaters: a review. Bioresour. Technol. 53, 195–206. [https://doi.org/10.1016/0960-8524\(95\)00072-M](https://doi.org/10.1016/0960-8524(95)00072-M)
14. Lacerda, E.C.M., dos Passos Galluzzi Baltazar, M., dos Reis, T.A., do Nascimento, C.A.O., Côrrea, B., Gimenes, L.J., 2019. Copper biosorption from an aqueous solution by the dead biomass of *Penicillium ochrochloron*. Environ. Monit. Assess. 191. <https://doi.org/10.1007/s10661-019-7399-y>
15. Li, X., Li, A., Long, M., Tian, X., 2015. Equilibrium and kinetic studies of copper biosorption by dead *Ceriporia lacerata* biomass isolated from the litter of an invasive plant in China. J. Environ. Heal. Sci. Eng. 13, 1–8. <https://doi.org/10.1186/s40201-015-0191-1>
16. Lin, J., Wang, L., 2009. Comparison between linear and non-linear forms of pseudo-first-order and pseudo-second-order adsorption kinetic models for the removal of methylene blue by activated carbon. Front. Environ. Sci. Eng. China 3, 320–324. <https://doi.org/10.1007/s11783-009-0030-7>
17. Matouq, M., Jildeh, N., Qtaishat, M., Hindiyeh, M., Al Syouf, M.Q., 2015. The adsorption kinetics and modeling for heavy metals removal from wastewater by *Moringa* pods. J. Environ. Chem. Eng. 3, 775–784. <https://doi.org/10.1016/j.jece.2015.03.027>

18. Naeem, S., Baheti, V., Militky, J., Wiener, J., Behera, P., Ashraf, A., 2016. Sorption properties of iron impregnated activated carbon web for removal of methylene blue from aqueous media. *Fibers Polym.* 17, 1245–1255. <https://doi.org/10.1007/s12221-016-6423-x>
19. Nagy, B., Mânzatu, C., Măicăneanu, A., Indolean, C., Barbu-Tudoran, L., Majdik, C., 2017. Linear and nonlinear regression analysis for heavy metals removal using *Agaricus bisporus* macrofungus. *Arab. J. Chem.* 10, S3569–S3579. <https://doi.org/10.1016/j.arabjc.2014.03.004>
20. Noreen, S., Bhatti, H.N., Nausheen, S., Sadaf, S., Ashfaq, M., 2013. Batch and fixed bed adsorption study for the removal of Drimarine Black CL-B dye from aqueous solution using a lignocellulosic waste: A cost effective adsorbent. *Ind. Crops Prod.* 50, 568–579. <https://doi.org/10.1016/j.indcrop.2013.07.065>
21. Osmari, T.A., Gallon, R., Schwaab, M., Barbosa-Coutinho, E., Severo, J.B., Pinto, J.C., 2013. Statistical analysis of linear and non-linear regression for the estimation of adsorption isotherm parameters. *Adsorpt. Sci. Technol.* 31, 433–458. <https://doi.org/10.1260/0263-6174.31.5.433>
22. Quintella, C.M., Mata, A.M.T., Lima, L.C.P., 2019. Overview of bioremediation with technology assessment and emphasis on fungal bioremediation of oil contaminated soils. *J. Environ. Manage.* 241, 156–166. <https://doi.org/10.1016/j.jenvman.2019.04.019>
23. Rashid, A., Bhatti, H.N., Iqbal, M., Noreen, S., 2016. Fungal biomass composite with bentonite efficiency for nickel and zinc adsorption: a mechanistic study. *Ecol. Eng.* 91, 459–471. <https://doi.org/10.1016/j.ecoleng.2016.03.014>
24. Saad, A.M., Saad, M.M., Ibrahim, N.A., El-hadedy, D., Ibrahim, E.I., El-din, A.Z.K., Hassan, H.M., 2019. Evaluation of *Aspergillus tamaris* NRC 3 biomass as a biosorbent for removal and recovery of heavy metals from contaminated aqueous solutions 5.
25. Saeed, M.M., Ahmed, R., 2006. Temperature effected sorption of europium ( III ) onto 1- ( 2-pyridylazo ) -2-naphthol impregnated polyurethane foam 267, 147–153.
26. Sethurajan, M., van Hullebusch, E.D., 2019. Leaching and selective recovery of Cu from printed circuit boards. *Metals (Basel)*. 9, 25–26. <https://doi.org/10.3390/met9101034>
27. Song, H.L., Liang, L., Yang, K.Y., 2014. Removal of several metal ions from aqueous solution using powdered stem of *Arundo donax* L: As a new biosorbent, *Chemical Engineering Research and Design. Institution of Chemical Engineers.* <https://doi.org/10.1016/j.cherd.2014.04.027>
28. Subramanyam, B., Das, A., 2014. Linearised and non-linearised isotherm models optimization analysis by error functions and statistical means. *J. Environ. Heal. Sci. Eng.* 12, 1–6. <https://doi.org/10.1186/2052-336X-12-92>

29. Tu, C., Liu, Y., Wei, J., Li, L., Scheckel, K.G., Luo, Y., 2018. Characterization and mechanism of copper biosorption by a highly copper-resistant fungal strain isolated from copper-polluted acidic orchard soil. *Environ. Sci. Pollut. Res.* 25, 24965–24974. <https://doi.org/10.1007/s11356-018-2563-4>
30. World Health Organization, 2011. Guidelines for drinking-water quality 4<sup>th</sup> ed. World Health Organization. <https://apps.who.int/iris/handle/10665/44584>, accessed 4<sup>th</sup> July 2019.
31. Xu, X., Zhang, Z., Huang, Q., Chen, W., 2018. Biosorption performance of multimetal resistant fungus *Penicillium chrysogenum* XJ-1 for removal of Cu<sup>2+</sup> and Cr<sup>6+</sup> from aqueous solutions. *Geomicrobiol. J.* 35, 40–49. <https://doi.org/10.1080/01490451.2017.1310331>
32. Zhang, S., Gedalanga, P.B., Mahendra, S., 2017. Advances in bioremediation of 1,4-dioxane-contaminated waters. *J. Environ. Manage.* 204, 765–774. <https://doi.org/10.1016/j.jenvman.2017.05.033>

**CHAPTER 4**  
**Cr(VI) REMOVAL USING DEAD FUNGAL BIOMASS**

## Abstract

The highly toxic species of chromium in its hexavalent state is an important hazard on the flora and fauna, causing a rupture in balance especially in aquatic environments. The removal of Cr(VI) ions from aqueous solutions using dead fungal biomass of *Rhizopus* sp. and *Aspergillus* sp. was investigated under batch experiments. The biomass was produced and treated with NaCl to compare pre-treated and untreated biosorbents capacity. Adsorption of Cr(VI) was investigated with a 2<sup>3</sup> experimental design to determine the best operational parameters including pH [2.0 & 4.0], temperature [20 & 40 °C], and agitation [50 & 150 rpm]. Maximum Cr(VI) uptake (99%) indicated that pH 2.0 is the optimal for Cr(VI) removal. Linear and non-linear kinetic models were evaluated. The best fitting for linear kinetics was the pseudo-second order linear equation and the Elovich model in its non-linear form, suggesting chemisorption as the controlling step of adsorption. Results followed Langmuir isotherm equation, the  $q_m$  was 9.95 (mg·g<sup>-1</sup>) for *Rhizopus* sp. and 9.76 (mg·g<sup>-1</sup>) for *Aspergillus* sp. Thermodynamic parameters were calculated using the adsorption equilibrium constant obtained from Langmuir isotherm and indicated that the adsorption process was spontaneous and endothermic. The surface characteristics of the biomass were analyzed by Fourier transformed infrared (FTIR) spectra; the analysis showed the involvement of amino groups in the bonding with Cr(VI). SEM and EDX analysis confirmed the presence of Cr(VI) in the biomass after adsorption. The results of these experiments may be utilized for modeling, simulation and scale-up processes in the future.



#### 4.1. Introduction

The main water pollutants present in industrial effluents are heavy metals, these contaminants can be assignable to processes like electroplating, mineral processing, metal mining, tanning in the leather industry, wood preservative, cooling water, dyeing in textile industry and pigment manufacture, contributing to the discharge of inorganic, organic and biological waste (Enniya *et al.*, 2018; García *et al.*, 2019). As the addressed case of a contaminated aquifer, attributed to Cr ore processing residue piles (COPRP), the aquifer is beneath a chromate factory in Buenavista, León located in the central-western part of the Mexican state of Guanajuato (Villalobos-Aragón *et al.*, 2012). It has been shown that heavy metals can cause severe damage to human health if not treated properly (Volesky, 2001). The removal of some ionic species of heavy metals such as  $\text{Cr}^{6+}$ ,  $\text{Cd}^{2+}$ ,  $\text{Pb}^{2+}$ ,  $\text{Zn}^{2+}$ ,  $\text{Ni}^{2+}$ , and  $\text{Cu}^{2+}$  has attracted interest due to their highly toxic potential in human health in addition to the ecological imbalance that they cause especially in aquatic ecosystems. Chromium exists in valences from +2 to +6, Cr(III), and Cr(VI) are the two stable oxidation states, being Cr(VI) not only toxic but carcinogenic, mutagenic and teratogenic in nature (Verma *et al.*, 2014). The guiding value for drinking water is  $50 \text{ mg}\cdot\text{L}^{-1}$  for total chromium (WHO, 2011). The concentration of chromium in the nearby area of COPRP in Guanajuato is above the limit permitted for drinking water, reporting values up to  $95.1 \text{ mg}\cdot\text{L}^{-1}$  (Armienta and Rodríguez-Castillo R., 1995; Villalobos-Aragón *et al.*, 2012; Lara *et al.*, 2017). The Environmental Protection Agency (EPA) limits total chromium to a standard of  $100 \text{ }\mu\text{g}\cdot\text{L}^{-1}$  and is based on the dermatological effects (USEPA, 2018). Contemplating the noxious effects of heavy metals, their concentrations must be limited to levels inside the admissible margins prescribed by the environmental agencies, before their discharge into water.

There are multiple physical and/or chemical technologies that have been developed to treat contaminated water such as adsorption, precipitation, complexation, membrane filtration, ion exchange, reverse osmosis, chemical reduction, solvent extraction, etc. The treatment processes that accomplish the removal of pollutants in great quantities come to be expensive and ineffective when the target is removing contaminants at a trace level, these levels are established by environmental legislations (Michalak *et al.*, 2013). Biosorption, that has been defined as the sorption of pollutants from solutions using

biological material, is considered to be a rising technology due to the great availability of biomass, low cost, high-quality effluent and adaptable operational procedures (Fomina and Gadd, 2014; Espinosa-Ortiz *et al.*, 2016). Biological remediation of chromium from water has gained popularity and interest due to its advantages over the conventional techniques (Sen *et al.*, 2018).

Both active and inactive biological materials have been used to remove heavy metal from aqueous solutions. Biosorbents like litchi peels can be easily obtained in large quantities and used as an inexpensive sorbent for the biosorption of Cr(VI) from synthetic tannery wastewater (Manikandan *et al.*, 2016). Microorganisms like bacteria, fungi, and yeast have demonstrated the ability to detoxify liquid wastes (Shankar *et al.*, 2014; Sivakumar, 2016). Fourier transform infrared spectroscopy (FTIR) analysis has proved that functional groups found in biosorbents take the principal role in the removal of heavy metals. The essential functional groups are hydroxyl, carboxyl, sulfate amine and phosphate groups (He and Chen, 2014). Metal ions biosorption is influenced by other factors rather than the surface of the biosorbent cell wall, such as the physical-chemical properties of the solutions, temperature, pH, presence of nutrients, biosorbent concentration and equilibrium time (Kapoor *et al.*, 1999; Wang and Chen, 2006; Fomina and Gadd, 2014).

The main aim of this research is to analyze through mathematical models the adsorption mechanisms involved in the Cr(VI) removal onto untreated and pre-treated dead fungal biomass in batch experiments. In accordance with the scope of the research: (1) the optimal conditions of pH, temperature and agitation for the Cr(VI) removal were evaluated by a  $2^3$  factorial design, (2) kinetic studies were performed to determine linear and non-linear constants for the PFO, PSO, ID and the Elovich models, (3) equilibrium studies were carried out to evaluate the thermodynamic parameters using constants from the Langmuir isotherm model. The possible mechanisms entangled in Cr(VI) adsorption were discussed on the specific modifications of the biomass by FTIR spectroscopic analysis, scanning electron microscopy (SEM) and energy-dispersive X-Ray (EDX).

## **4.2. Materials and methods**

### **4.2.1. Preparation of the dead fungal biomass**

The fungal strains used in this study were *Rhizopus* sp. and *Aspergillus* sp. These strains were isolated from soil, the samples were obtained from 5 random sampling points carried out in Monterrey Nuevo León México (Castro-González *et al.*, 2017). The strains were cultivated in 500 mL Erlenmeyer flasks with liquid sterile media containing the following concentrations in g·L<sup>-1</sup>: sucrose (40), K<sub>2</sub>HPO<sub>4</sub> (4), MgSO<sub>4</sub>·7H<sub>2</sub>O (75), NH<sub>4</sub>Cl (1), citric acid (3), cysteine (0.5), yeast extract (1.5), NaCl (1), and CaCl<sub>2</sub> (0.1). The Erlenmeyer flasks containing 200 mL of culture media were incubated for 7 days at 30 °C in a MaxQ 8000 stackable shaker (Thermo Scientific, Monterrey, México). The biomass was inactivated by autoclaving (1.0207 atm., 121 °C). After, it was filtrated using Vacuum Filter Units with 0.22 µm Cellulose acetate membrane. After the filtration, half of each of the fungal biomass obtained was washed with a 0.8 M solution of NaCl, followed by a wash with generous deionized water. Finally, the biomass was dried in an oven at 60 °C for 24 h and powdered into ~10 µm particles using a mortar and pestle.

### **4.2.2. Synthetic Cr(VI) solution**

The chemicals used were of analytical grade. A stock solution (1000 mg·L<sup>-1</sup>) of Cr (VI) was prepared with 2.828 g of K<sub>2</sub>Cr<sub>2</sub>O<sub>7</sub>. The pH of the solutions was adjusted to 4.0 and 2.0 using HCl 0.1 M or NaOH 0.1 M.

### **4.2.3. Batch adsorption experiments**

The biosorption capacity of *Rhizopus* sp. and *Aspergillus* sp. was investigated by various batch experiments, beginning with a screening with a 2<sup>3</sup> experimental design, followed by kinetic assay. All the adsorption tests were performed in triplicate in a MaxQ 4000 Benchtop Orbital Shaker (Thermo Scientific).

#### **4.2.3.1. Experimental design 2<sup>3</sup>**

In order to get the optimal conditions for Cr(VI) removal, an experimental screening varying pH, temperature, and agitation was conducted. These experiments were carried out by using Corning 15 mL centrifuge tubes, containing 10 mL of Cr(VI) solution of 50 mg·L<sup>-1</sup> at pH 2.0 and 4.0, the dosage of fungal biomass was of 10 mg·L<sup>-1</sup>. The

solution was in contact with the fungal biomass for 120 min in orbital shakers at 50 and 150 rpm, with temperatures of 20 °C and 30 °C, afterwards the tubes were centrifuged in a Compact II Centrifuge (Clay Adams) and the remaining Cr(VI) was analyzed.

#### **4.2.3.2. Kinetic assays**

Kinetic experiments were conducted with 10 mL of 50 mg·L<sup>-1</sup> Cr(VI) solution at pH 2.0, 120 rpm and 25 ± 2°C, the biomass dosage was of 0.05 g and contact times were designed as 0.25, 0.5, 0.75, 1.0, 1.25, 1.50, 1.75, 2.0, 3.0, 4.0, 5.0, 6.0, 7.0 and 8.0 h respectively. The experimental kinetic data were modeled using the equations on Table 1 of Chapter 2.

#### **4.2.3.3. Equilibrium studies**

The equilibrium isotherm was performed by adding 0.05 g of dead biomass into 10 mL of Cr(VI) solutions with concentrations ranging from 12.5 mg·L<sup>-1</sup> to 300 mg·L<sup>-1</sup>, at pH 2.0 and at 10, 25 and 30 °C. The experiment was conducted for 240 min, which was the equilibrium time established in preliminary experiments. The results were analyzed by Langmuir and Freundlich isotherm models. The thermodynamic analysis was performed using the Langmuir constant to calculate the free energy, entropy and enthalpy.

#### **4.2.4. Analytical determination**

The determination of the residual Cr(VI) ions after biosorption were quantified spectrophotometrically using a UV-VIS Spectrophotometer Evolution 60S (Thermo Scientific) at 540 nm after complexation with 1, 5- diphenylcarbazide agent, following the 3500-Cr B. Colorimetric Method (APHA/AWWA/WEF, 2012).

#### **4.2.5. Characterization of the dead fungal biomass**

The chemical characteristics of the untreated and pre-treated dead biomass of *Rhizopus* sp. and *Aspergillus* sp. were scanned before and after being in contact with Cr(VI). The infrared scan was made in transmission mode using a Fourier Transform Infrared spectrometer Nicolet iS10 (Thermo Scientific), using wavelengths between the range of 400 to 4000 cm<sup>-1</sup>. IR spectra of control and metal treated biomass were compared.

The biomass surface characteristics before and after Cr(VI) adsorption were analyzed using SEM coupled with EDX using JSM 6510 LV (JEOL). The biomass samples were prepared in aluminum stub followed by gold coat under vacuum conditions.

#### **4.2.6. Statistical analysis**

The error functions are vital to determine which mathematical model has the best fit with the experimental results. Statistical functions of Microsoft Excel 2013, OriginPro2017, and IBM SPSS Statistics 22 were used to calculate the coefficient of determination ( $R^2$ ) of the linear and non-linear kinetic and isotherm models.

### **4.3. Results and discussion**

#### **4.3.1. Evaluation of optimal conditions for Cr(VI) adsorption**

This experiment was undertaken to choose the optimum work conditions for the kinetic and isotherm studies. A factorial design of  $2^3$  was made varying pH, temperature, and agitation in two levels each one. The screening results of the untreated dead biomass were evaluated in IBM SPSS Statistics 22 using one-way ANOVA and  $F$  test in order to know which factors were affecting the biosorption process. The results of this experiment are shown in Table 5. The removal of Cr(VI) onto *Rhizopus* sp. dead biomass reached 82% and 99% removal and for *Aspergillus* sp. the removal went from 53% to 99%, at pH 4.0 and 2.0 respectively, the ANOVA model for *Rhizopus* sp. had an  $R^2$  of 0.96, the  $F$  test ( $F_{1,7} = 60.54$ ,  $p < 0.005$ ), in the case of *Aspergillus* sp. the  $R^2$  was of 0.99 while the  $F$  test ( $F_{1,7} = 237.69$ ,  $p < 0.005$ ), with this information has been demonstrated that the only variable with statistical significance was pH. According to Tylak *et al.* (2015), the variations in the sorption removal in the analyzed pH range may be related to the pH dependency of chromium species present in water solutions. The pH is considered an important parameter for the adsorption of metal ions from aqueous solutions due to the solubility effects on metal ions, concentration of the counter-ions on the biosorbent functional groups, and the degree of ionization of the adsorbent during the reaction (Dewangan *et al.*, 2011). The lower uptake of Cr(VI) at higher pH can be explained by the increase in the number of competitive hydroxyl anions along with the unfavorable negative charge over the fungal cell wall, therefore, the electrostatic repulsion will be higher, decreasing the amount of metal adsorbed. This means that the high adsorption at

acidic pH can be ascribed to the three ionic states of Cr(VI) in low pH ( $\text{HCrO}_4^-$ ,  $\text{Cr}_2\text{O}_7^{2-}$  and  $\text{CrO}_4^{2-}$ ), increasing the electrostatic attraction between sorbent and sorbate (Verma *et al.*, 2014; Fernández-López *et al.*, 2014). Also, accordingly with the results of the present study, where the highest Cr(VI) adsorption was at pH 2.0.

Table 5. Screening results of *Aspergillus* sp. and *Rhizopus* sp. in the removal of Cr(VI)

pH	Temperature (°C)	RPM	<i>Aspergillus</i> sp.		<i>Rhizopus</i> sp.	
			% Removal	$Q$ (mg·g <sup>-1</sup> )	% Removal	$Q$ (mg·g <sup>-1</sup> )
2.0	20	50	99.35	86.75	99.32	86.76
		150	99.39	86.82	99.36	86.80
	30	50	99.40	86.83	99.29	86.78
		150	99.38	86.82	99.32	86.76
4.0	20	50	55.41	39.05	83.65	58.96
		150	59.38	41.85	82.44	58.10
	30	50	53.89	37.98	82.44	58.10
		150	54.78	38.61	83.46	58.82

#### 4.3.2. Adsorption kinetics

The values of the experimental sorption capacity of Cr(VI) by *Rhizopus* sp. and *Aspergillus* sp. dead biomass showed that the adsorption process is time-dependent. Most of the Cr(VI) uptake is taking place within the first 30 min of contact time, the uptake of the ion metal keeps increasing for greater periods but the rate of adsorption is slower. Adsorption equilibrium started to stabilize after approximately 240 min for both treated and untreated biomass. To fit the data obtained from the experimental adsorption assays the PFO, PSO, ID, and the Elovich kinetic models were used. The calculated rate constants from the linear and non-linear models along with the coefficient of determination  $R^2$  have been listed in Table 6. In Figure 6, the results of the linear fit are shown as (a) PFO, (b) PSO, (c) Elovich and (d) ID model. In Figure 7, non-linear fit of (a) *Rhizopus* sp., (b) *Rhizopus* sp. + NaCl, (c) *Aspergillus* sp., and (d) *Aspergillus* sp. + NaCl are displayed.

Table 6. Kinetic parameters for the adsorption of Cr(VI) onto untreated and pretreated *Rhizopus* sp. and *Aspergillus* sp.

Kinetic model	Non-linear				Linear			
	<i>Rhizopus</i> sp.	<i>Rhizopus</i> sp. + NaCl	<i>Aspergillus</i> sp.	<i>Aspergillus</i> sp. + NaCl	<i>Rhizopus</i> sp.	<i>Rhizopus</i> sp. + NaCl	<i>Aspergillus</i> sp.	<i>Aspergillus</i> sp. + NaCl
<i>PFO</i>								
$K_l$ (min <sup>-1</sup> )	0.0396	0.0520	0.0592	0.0381	0.0056	0.0080	0.0063	0.0059
$q_e$ (mg·g <sup>-1</sup> )	5.0458	6.7593	5.9816	4.4157	1.7165	2.7925	1.6175	2.2929
$R^2$	0.9396	0.9125	0.7629	0.5933	0.8826	0.8830	0.9096	0.9050
<i>PSO</i>								
$K_{II}$ (g·(mg·min) <sup>-1</sup> )	0.0113	0.0114	0.0165	0.0111	0.0103	0.0085	0.0154	0.0079
$q_e$ (mg·g <sup>-1</sup> )	5.4509	7.3067	6.3361	4.9054	5.5679	7.5852	6.4170	5.1899
$R^2$	0.9865	0.9765	0.9668	0.8316	0.9975	0.9982	0.9996	0.9934
<i>ID</i>								
$K_d$	0.1943	0.2329	0.1044	0.1339	0.1943	0.1408	0.1044	0.1339
$R^2$	0.7501	0.6565	0.8232	0.8948	0.7501	0.6564	0.8232	0.8948
<i>Elovich</i>								
$\alpha$ (mg·(g·min) <sup>-1</sup> )	8.0790	39.4870	114.3199	4.1285	3.2209	17.1490	49.6485	3.7971
$\beta$ (g·mg <sup>-1</sup> )	0.6066	0.5324	0.7073	0.6043	1.1531	1.2426	1.6288	1.3914
$R^2$	0.9953	0.9958	0.9484	0.9252	0.9808	0.9729	0.9484	0.9252
$q_{e,exp}$	5.5080	7.4580	6.3924	5.1503	5.5080	7.4580	6.3924	5.1503

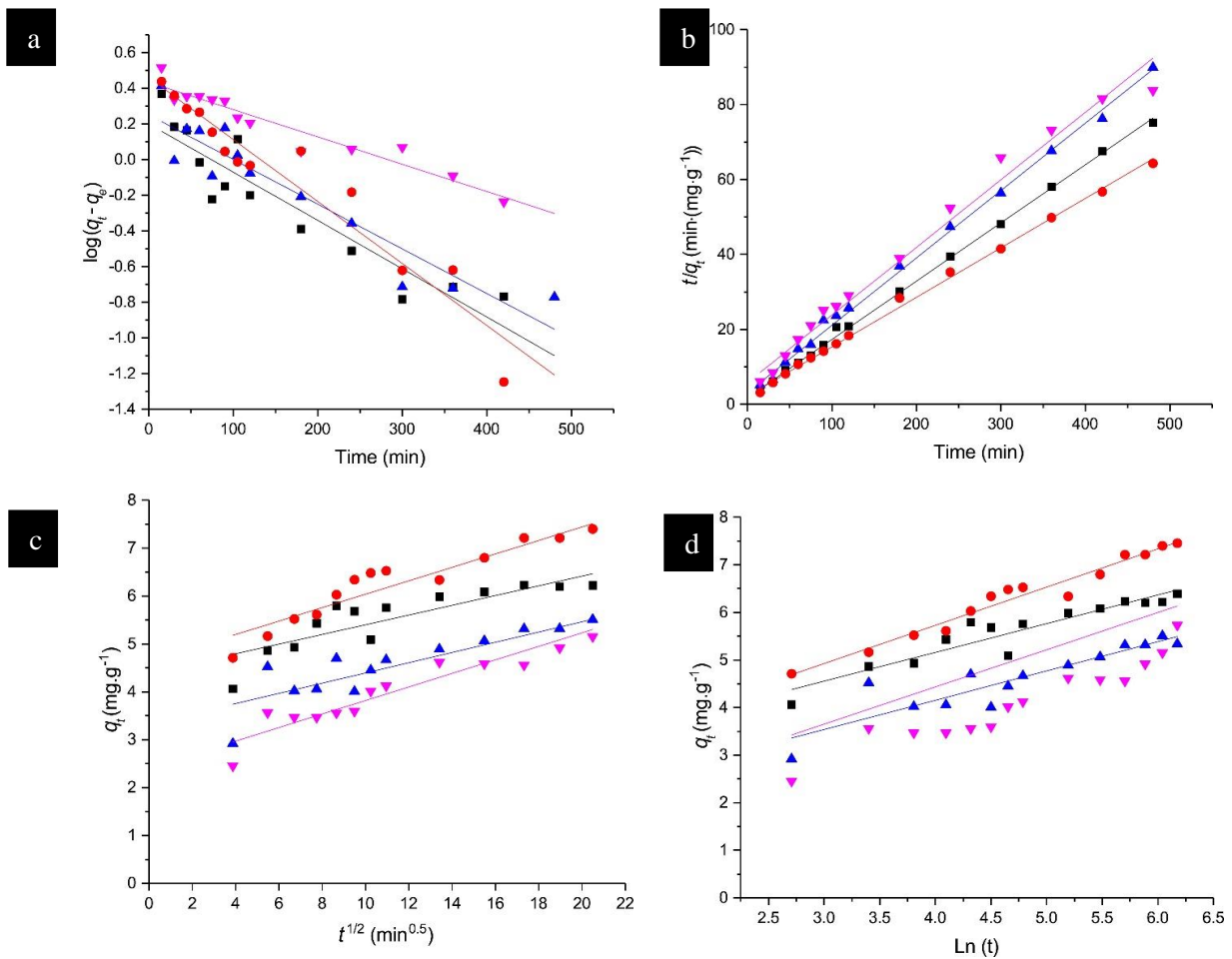


Figure 6. Experimental and modelled linear kinetic models of Cr(VI) adsorption onto *Aspergillus* sp. and *Rhizopus* sp. (a) PFO, (b) PSO, (c) Elovich and (d) ID (■ *Aspergillus* sp., ▼ *Aspergillus* sp. + NaCl, ● *Rhizopus* sp., ▲ *Rhizopus* sp. + NaCl).

The values of  $k_1$  were calculated by plotting  $\ln(q_e - q)$  vs  $t$  for the PFO linear equation. The  $R^2$  for the PFO linear equations is 0.88 for both *Rhizopus* sp. biomasses, in the case of *Aspergillus* sp. the  $R^2$  was of 0.90 also for both untreated and pretreated biomass, however, there is a great difference between the  $q_e$  and the  $q_{e,exp}$ . The nonlinear approach has an  $R^2$  value of 0.93 and 0.91 for the pre-treated and untreated *Rhizopus* sp. biomass, *Aspergillus* sp. untreated biomass reached an  $R^2$  of 0.76 and a 0.59 for pre-treated biomass. Even though this regression coefficient is not as high as the linear one, it is important to pay attention to the fact that in this case the  $q_e$  for the four biosorbents is closer to the  $q_{e,exp}$ , this suggests that the nonlinear equation of PFO must be considered



for further discussion. According to Largette (2016), the use of non-linear expressions should be favored.

For the PSO linear model, the coefficient of determination was the highest ( $R^2 > 0.99$ ), fitting with the experimental data obtained with the biosorbents used. The data of the linear equation is plotted in Figure 6 and indicates that the adsorption phenomenon of the metal ion onto the biosorbents is controlled by chemisorption (working as the rate-limiting step of the adsorption). Involving valences forces, through sharing or exchanging the electrons between adsorbent and adsorbate (Arshadi *et al.*, 2014; Bhainsa and D'Souza, 2008). Similarly to this work, adsorption of Cr(VI) by *Aspergillus niger* biomass showed that Ho and McKay pseudo-second order model was a better kinetic expression (Khambhaty *et al.*, 2009).

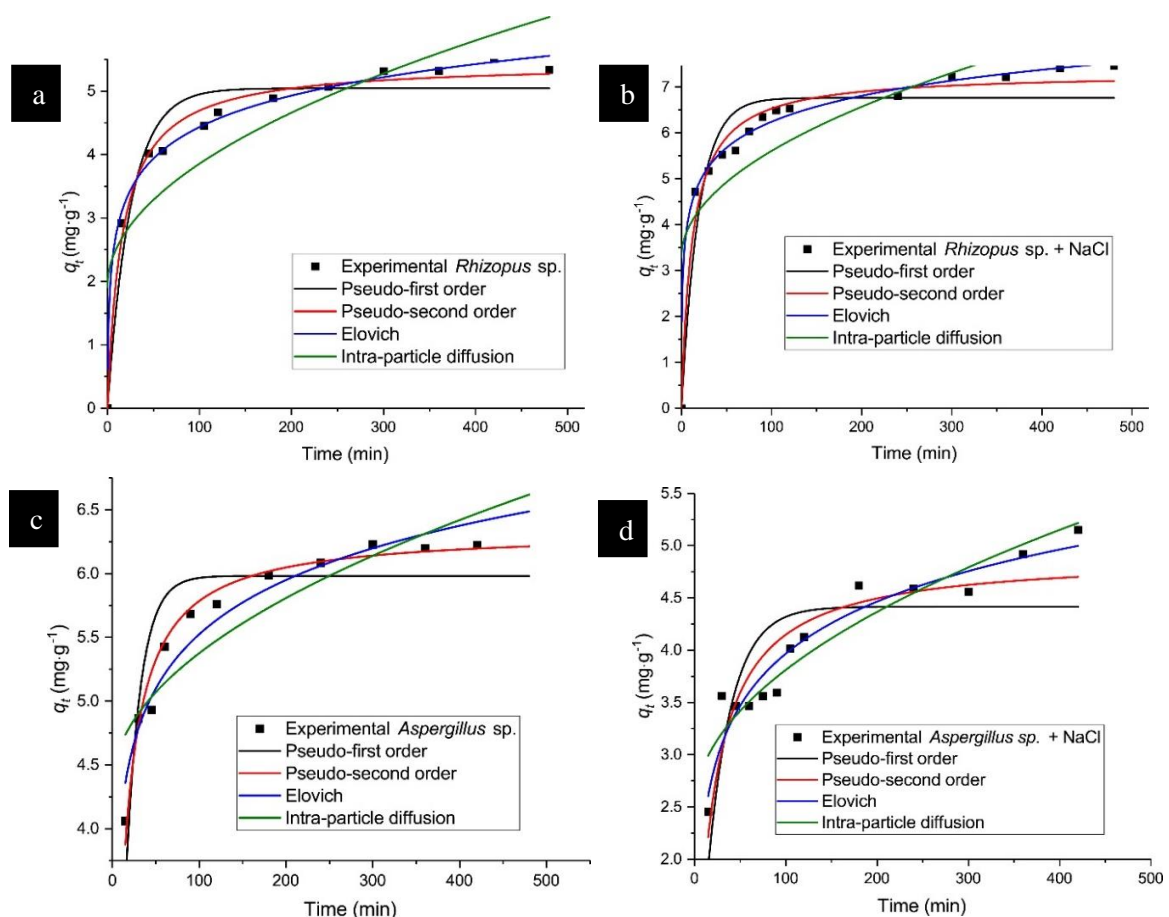


Figure 7. PFO, PSO, Elovich and ID experimental and modelled non-linear kinetics of Cr(VI) adsorption onto (a) *Rhizopus* sp., (b) *Rhizopus* sp. + NaCl., (c) *Aspergillus* sp., and (d) *Aspergillus* + NaCl sp.

The Elovich equation is suitable to describe adsorption behavior that concurs with the nature of chemical adsorption (Aharoni and Tompkins, 1970; Chien and Clayton, 1980; Wu *et al.*, 2009). The values presented in Table 6 show an  $R^2$  of 0.98 and 0.97 for *Rhizopus* sp. and *Rhizopus* sp. + NaCl on its linear form, likewise, *Aspergillus* sp. reached a  $R^2$  of 0.94 and 0.92 for untreated and pre-treated biomass. On the non-linear equation model the  $R^2$  was 0.99 for both *Rhizopus* sp. biomasses, the fit for *Aspergillus* sp. was of 0.94 and 0.92 for untreated and pre-treated respectively, in the case of *Aspergillus* sp. the  $R^2$  for linear and non-linear equations was the same. The fit with the Elovich model indicates that the adsorption process of Cr(VI) onto both strains biomasses is by chemisorption. The ID model explains the diffusion mechanism, the plots ( $q_t$  vs  $t^{1/2}$ ) represent multi-linearity, which indicated two or more steps occurring in the adsorption process (Hameed *et al.*, 2009; Shukla and Kisku, 2015). Values of  $C$  give an idea about the boundary layer effect (Dorrajati *et al.*, 2017). The intraparticle diffusion constant was calculated using the linear equation showed in Table 1. The results are plotted in Figure 6. The calculated  $R^2$  values for this model were the lowest for both linear and non-linear equations, in the case of *Rhizopus* sp., with 0.65 for the pre-treated and 0.75 in the case of untreated biomass, implying that the adsorption mechanism is not by intra-particle diffusion, denoting that more than one step affected the adsorption process. The calculated constants of the ID model for *Aspergillus* sp. biomass on both linear and non-linear models were the same, the untreated biomass had a  $R^2$  of 0.82 while the pre-treated biomass reached 0.89, according to this results both of the mathematical approaches get to the same results, this means that for the ID model both linear and non-linear equations can be used. According to Delgado (2019), non-linear regression analysis has been previously applied in literature as a useful tool when adsorption kinetics and equilibrium cannot be clearly defined using traditional methods.

#### **4.3.3. Isotherm analysis**

Adsorption isotherms imply the mechanism of the molecules subjected to adsorption, specifying how the particles distribute themselves between liquid and solid phases, at equilibrium time. They give some insight into the adsorption mechanism, as well as the surface characteristics and affinities of the adsorbent (Aly *et al.*, 2014).

The supportive Langmuir model, which was the one with better coefficient of determination, indicated that the adsorption energy was equally distributed throughout the surface, this means that there was no interaction nor transmigration of chromium ions onto the fungal surface after monolayer adsorption (Verma *et al.*, 2014). According to the Langmuir isotherm constants in Table 7, the maximum adsorption capacity for *Rhizopus* sp. was a  $q_m$  of 9.95 mg·g<sup>-1</sup>,  $K_L$  was 0.15 at 10 °C with a  $R^2$  of 0.93. The  $R_L$  values in the present study were between 0.0041 and 0.3040, which indicates a favorable adsorption process of Cr(VI) onto pre-treated *Rhizopus* sp. biomass. In the case of *Aspergillus* sp. the  $q_m$  was of 9.76 which does not differ radically from the other strain, however, in this case the highest  $R^2$  was 0.88 with a  $K_L$  value of 0.03. For both strains, the Langmuir model had a better linear fit.

The values of  $K_F$  and  $n_f$  are shown in Table 7, since the best fitting was a  $R^2$  of 0.82 at 10 °C, suggests that the adsorption process is not following the Freundlich isotherm equation, since Langmuir has a greater coefficient of determination. As Yang *et al.* (2015) reported with the adsorption of Cr(VI) onto activated carbon, the process can be described better with the Langmuir model than with Freundlich model, surface adsorption occurs on specific homogeneous sites.

The values of  $\Delta G^0$ ,  $\Delta H^0$  and  $\Delta S^0$  are shown in Table 8. The positive value of the enthalpy ( $\Delta H$ ) indicates that the adsorption process of Cr(VI) onto *Rhizopus* sp. biomass is endothermic, for *Aspergillus* sp. the value was positive, this means that the process is exothermic. The negative values of  $\Delta G^0$  indicate that the sorption process is spontaneous and the increase in the negative value of  $\Delta G^0$  with raise in the temperature makes the biosorption of Cr(VI) favorable, which was the same for both biosorbents. The positive value of entropy  $\Delta S^0$  indicates an increase of disorder between the adsorbed species and the solution during the biosorption (Seo *et al.*, 2013).

Table 7. Isotherm parameters for the adsorption of Cr(VI) onto dead biomass of *Rhizopus sp.* and *Aspergillus sp.* analysis

Isotherm model	<i>Rhizopus sp.</i>			<i>Aspergillus sp.</i>		
	10 °C	25 °C	40 °C	10 °C	25 °C	40 °C
<i>Langmuir model</i>						
$K_L$ (L·mg <sup>-1</sup> )	0.15	0.77	1.2303	0.1477	0.1075	0.0315
$q_m$ (mg·g <sup>-1</sup> )	9.95	8.05	9.3811	6.0414	7.3493	9.7637
$R^2$	0.93	0.84	0.8930	0.5863	0.8117	0.8834
$R_L$	0.0316 – 0.3040	0.0064 – 0.1169	0.0041 – 0.0819	0.0173 – 0.2070	0.0718 – 0.4256	0.0309 – 0.2769
<i>Freundlich</i>						
$K_F$ (mg·g <sup>-1</sup> )	1.9281	1.3518	0.9489	2.7093	1.6094	-1.3243
$n$	2.0796	1.9598	3.0158	1.2025	2.7762	-1.2189
$R^2$	0.8243	0.7888	0.8018	0.5009	0.6501	0.7849

Table 8. Thermodynamic parameters for Cr(VI) adsorption onto pre-treated dead *Rhizopus* sp. and untreated *Aspergillus* sp. biomass.

Isotherm model	<i>Rhizopus</i> sp.			<i>Aspergillus</i> sp.		
	10 °C	25 °C	40 °C	10 °C	25 °C	40 °C
<i>Langmuir model</i>						
$\ln K_L$	8.8921	10.5238	10.9663	8.9464	8.6285	7.4038
$\Delta G^0$ (kJ·mol <sup>-1</sup> )	-20933.1	-26085.5	-28551.3	-207.97	-211.21	-190.35
$\Delta S^0$ (J·mol <sup>-1</sup> ·K <sup>-1</sup> )		256.94			0.5875	
$\Delta H^0$ (kJ·mol <sup>-1</sup> )		50522.35			-378.34	

#### 4.3.4. FTIR

The FTIR spectroscopic bands of the native, pre-treated, and chromium bounded biomass are shown in Figure 8. The analysis indicated the involvement of amino groups in the Cr(VI) bonding with the *Rhizopus* sp. cell wall. The band at 3275  $\text{cm}^{-1}$  indicates the existence of the amine group. The peaks at 2922 and 2853  $\text{cm}^{-1}$  indicate the  $-\text{CH}$  stretching, also found in the biomass of *Phanerochaete chrysosporium* after Cr(VI) adsorption reported by Verma *et al.* (2014). A band at 1713  $\text{cm}^{-1}$  can be attributed to  $\text{C}=\text{O}$  of the carboxyl groups. The peak at 1622  $\text{cm}^{-1}$  is an amide band that is a  $\text{C}=\text{O}$  stretch. Proteins and hexosamines are abundant cell wall constituents, hence, the contributory role of amino groups in Cr binding could be assumed (Bai and Abraham, 2002; Shroff and Vaidya, 2012). At bands 1065 and 1031  $\text{cm}^{-1}$  phosphate ( $-\text{PO}_4^{3-}$ ) is identified in the spectrum of absorption. The stoichiometric interactions that occur between the functional groups of the biosorbents and the chromate ions are an important contribution to understand the biosorption mechanisms (Ferraz *et al.*, 2015). In several fungal strains, chromium ions bind to carboxyl, phosphate, amine, amide, and alkane groups (Ahluwalia and Goyal, 2010).

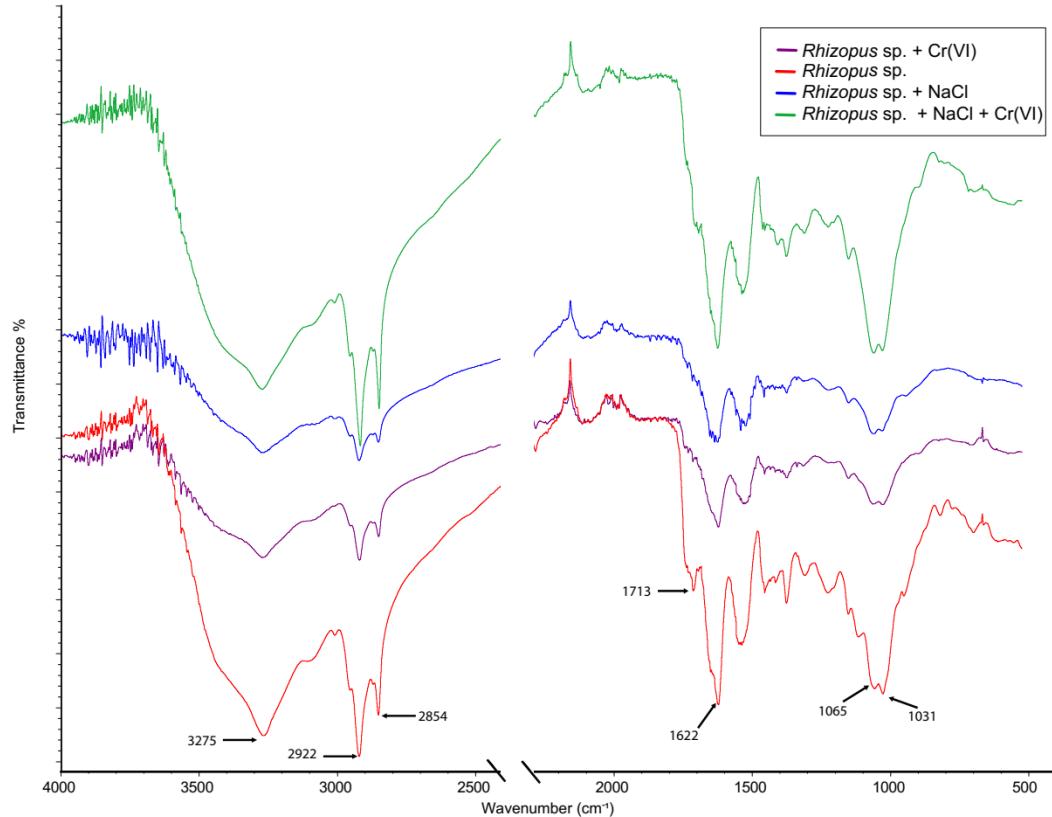


Figure 8. FTIR spectra of untreated and pre-treated *Rhizopus* sp. biomass before and after Cr(VI) removal.

#### 4.3.5. SEM-EDX

The biomass of *Rhizopus* sp. before and after Cr(VI) adsorption was characterized by SEM-EDX, in order to analyze the morphological changes caused by adsorption of the metal. In Figure 9, the SEM images and the EDX graph show the differences in the surface structure of the biomass shown in (a) and (b) before being in contact with the ion, and in (c) and (d) after Cr(VI) adsorption, similar alterations in the matrix of the biomass are found in the work of Manorama *et al.* (2016), where a plaster looking like structure is found after adsorption. The EDX analysis for the pre-treated biomass before adsorption showed the presence of Na and Cl, the peaks of these elements after adsorption decreased, probably due to the interaction with Cr(VI). The presence of Cr(VI) in the biomass was confirmed in EDX after adsorption experiments.

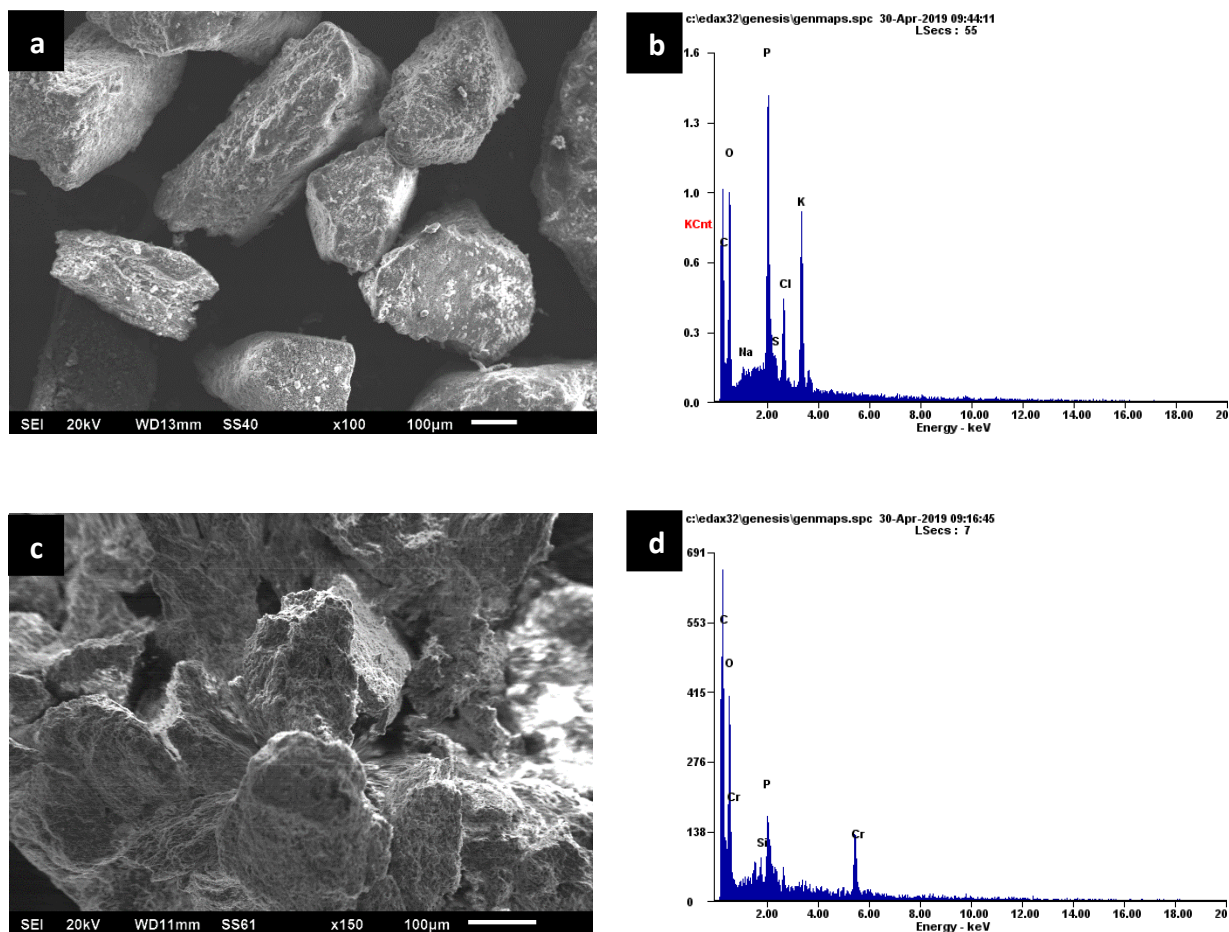


Figure 9. SEM images before (a) and after (c) adsorption, (b) and (d) correspond to the respective EDX spectrums

#### 4.4. Conclusion

The properties of untreated and pre-treated *Rhizopus* sp. and *Aspergillus* sp. biomass were studied for the enhancement of Cr(VI) biosorption. The operating conditions as pH, agitation, temperature, and time contact were evaluated. The optimal Cr(VI) adsorption process was at pH 2.0, being the process highly pH-dependent. The kinetic analysis extract that the best fitting to the models is in the next order PSO > Elovich > ID > PFO, deducing that the adsorption process is based on the sorption capacity on the solid phase and agrees with a chemisorption mechanism being the rate-controlling step. The best fit for isotherm modeling was Langmuir, with a maximum adsorption capacity of  $9.95 \text{ mg} \cdot \text{g}^{-1}$  for *Rhizopus* sp. biomass. The thermodynamic parameters indicated that the process is spontaneous and endothermic for *Rhizopus* sp. and exothermic for



*Aspergillus* sp. The pre-treated dead biomass of *Rhizopus* sp. is a promising and potential attractive biosorbent for Cr(VI) in this study, however, further tests should be carried out on to modeling of Cr(VI) removal in a continuous study.

## 5. References

1. Aharoni, C., Tompkins, F.C., 1970. Kinetics of adsorption and desorption and the Elovich equation. *Adv. Catal.* 21, 1–49.
2. Ahluwalia, S.S., Goyal, D., 2010. Removal of Cr(VI) from aqueous solution by fungal biomass. *Eng. Life Sci.* 10(5), 480–485.
3. Aly, Z., Graulet, A., Scales, N., Hanley, T., 2014. Removal of aluminum from aqueous solutions using PAN-based adsorbents: Characterisation, kinetics, equilibrium and thermodynamic studies. *Environ. Sci. Pollut. Res.* 21, 3972–3986.
4. APHA, AWWA, WEF, 2012. *Standard Methods for the Examination of Water and Wastewater*. Twentieth ed. United Book Press, Inc., Baltimore.
5. Armienta, M.A., Rodríguez-Castillo R., 1995. Environmental exposure to chromium compounds in the valley of León, México. *Environ. Health Perspect.* 103, 47-51.
6. Arshadi, M., Amiri, M.J., Mousavi, S., 2014. Kinetic, equilibrium and thermodynamic investigations of Ni(II), Cd(II), Cu(II) and Co(II) adsorption on barley straw ash. *Water Resour. Ind.* 6, 1–17.
7. Arul Manikandan, N., Alemu, A.K., Goswami, L., Pakshirajan, K., Pugazhenthii, G., 2016. Waste litchi peels for Cr(VI) removal from synthetic wastewater in batch and continuous systems: Sorbent characterization, regeneration and reuse study. *J. Environ. Eng.* 142(9), C4016001.
8. Bai, R.S., Abraham, T.E., 2002. Studies on enhancement of Cr(VI) biosorption by chemically modified biomass of *Rhizopus nigricans*. *Water Res.* 36, 1224–1236.
9. Bhainsa, K.C., D'Souza, S.F., 2008. Removal of copper ions by the filamentous fungus, *Rhizopus oryzae* from aqueous solution. *Bioresour. Technol.* 99, 3829–3835.
10. Bonilla-Petriciolet, A., Mendoza-Castillo, D., Reynel-Ávila, H., 2017. *Adsorption Processes for Water Treatment and Purification*, vol 1. Springer International Publishing.
11. Castro-González, I., Rojas-Verde, G., Quintero-Zapata, I., Almaguer-Cantú, V., 2017. A comparative study on removal efficiency of Cr(VI) in aqueous solution by *Fusarium* sp. and *Myrothecium* sp. *Water Air Soil Pollut.* 228:301–310.
12. Chien, S.H., Clayton, W.R., 1980. Application of Elovich equation to the kinetics of phosphate release and sorption in soils. *Soil Sci. Soc. Am. J.* 44, 265–268.
13. Dewangan, T., Tiwari, A., Bajpai, A.K., 2011. Removal of chromium(VI) ions by adsorption onto binary biopolymeric beads of sodium alginate and carboxymethyl cellulose. *J. Disper. Sci. Technol.* 32(8), 1075–1082.

14. Enniya, I., Rghioui., Jourani, A., 2018. Adsorption of hexavalent chromium in aqueous solution on activated carbon prepared from apple peels. *Sustain. Chem. Pharm.* 7, 9–16.
15. Espinosa-Ortiz, E.J., Shakya, M., Jain, R., Rene, E.R., van Hullebusch, E.D., Lens, P.N.L., 2016. Sorption of zinc onto elemental selenium nanoparticles immobilized in *Phanerochaete chrysosporium* pellets. *Environ. Sci. Pollut. Res.* 23, 1–12.
16. Fernández-López, J.A., Angosto, J. M., Avilés, M.D., 2014. Biosorption of hexavalent chromium from aqueous medium with *Opuntia* biomass. *Sci. World J*
17. Ferraz, A.I., Amorim, C., Tavares, T., Teixeira, J.A., 2015. Chromium(III) biosorption onto spent grains residual from brewing industry: equilibrium, kinetics and column studies. *Int. J. Environ. Sci. Technol.* 12, 1591–1602.
18. Fomina, M., Gadd, G.M., 2014. Biosorption: current perspectives on concept, definition and application. *Bioresour. Technol.* 160, 3–14.
19. García, F.E., Senn, A.M., Meichtry, J.M., Scott, T.B., Pullin, H., Leyva, A.G., Halac, E. B., Ramos, C.P., Sacanell, J., Mizrahi, M., Requejo, F.G., Litter, M.I., 2019. Iron-based nanoparticles prepared from yerba mate extract. Synthesis, characterization and use on chromium removal. *J. Environ. Manage.* 235, 1–8.
20. Hameed, B.H., Krishni, R.R., Sata, S.A., 2009. A novel agricultural waste adsorbent for the removal of cationic dye from aqueous solutions. *J. Hazard. Mater.* 162, 305–311.
21. He, J., Chen, J.P., 2014. A comprehensive review on biosorption of heavy metals by algal biomass: materials, performances, chemistry, and modeling simulation tools. *Bioresour. Technol.* 160, 67–78.
22. Kapoor, A., Viraraghavan, T., Cullimore, D.R., 1999. Removal of heavy metals using the fungus *Aspergillus niger*. *Bioresour. Technol.* 70, 95–104.
23. Khambhaty, Y., Mody, K., Basha, S., Jha, B., 2009. Biosorption of Cr(VI) onto marine *Aspergillus niger*: Experimental studies and pseudo-second order kinetics. *World J. Microbiol. Biotechnol.* 25, 1413–1421.
24. Lara, P., Morett, E., Juárez, K., 2017. Acetate biostimulation as an effective treatment for cleaning up alkaline soil highly contaminated with Cr(VI). *Environ. Sci. Pollut. Res.* 24, 25513–25521.
25. Largitte, L., Pasquier, R., 2016. A review of the kinetics adsorption models and their application to the adsorption of lead by an activated carbon. *Chem. Eng. Res. Des.* 109, 495–504.
26. Liu, X., Lee, D., 2014. Thermodynamic parameters for adsorption equilibrium of heavy metals and dyes from wastewaters. *Bioresour. Technol.* 160, 24–31.
27. Markandeya, Shukla, S.P., Kisku, G.C., 2015. Linear and non-linear kinetic modeling for adsorption of disperse dye in batch process. *Res. J. Environ. Toxicol.* 9(6), 320–331.
28. Manorama, B.A., Sucharita, P.S., Aradhana, B., Kumar, D.N., 2016. Kinetics and surface studies on biosorption of Cr (VI) by using dead fungal biomass from chromium mine waste, Sukinda, India. *Res. J. Chem. Environ.* 20, 42–50.

29. Michalak, I., Chojnacka, K., Witek-Krowiak, A., 2013. State of the art for the biosorption process - A review. *Appl. Biochem. Biotechnol.* 170, 1389–1416.
30. Pradhan, D., Sukla, L.B., Sawyer, M., Rahman, P.K.S.M., 2017. Recent bioreduction of hexavalent chromium in wastewater treatment: A review. *J. Ind. Eng. Chem.* 55, 1–20.
31. Sen, G., Sen, S., Thakurta, S.G., Chakrabarty, J., Dutta, S., 2018. Bioremediation of Cr(VI) using live cyanobacteria: Experimentation and kinetic modeling. *J. Environ. Eng.* 144(9), 1–12.
32. Seo, H., Lee, M., Wang, S., 2013. Equilibrium and kinetic studies of the biosorption of dissolved metals on *Bacillus drentensis* immobilized in biocarrier beads. *Environ. Eng. Res.* 18, 45–53.
33. Seyed Dorraji, M.S., Amani-Ghadim, A.R., Hanifehpour, Y., Woo Joo, S., Figoli, A., Carraro, M., Tasselli, F., 2017. Performance of chitosan based nanocomposite hollow fibers in the removal of selenium (IV) from water. *Chem. Eng. Res. Des.* 117, 309–317.
34. Shankar, D., Sivakumar, D., Yuvashree, R., 2014. Chromium (VI) removal from tannery industry wastewater using fungi species. *Pollut. Res.* 33(3), 505-510.
35. Shroff, K.A., Vaidya, V.K., 2012. Effect of pre-treatments on the biosorption of chromium (VI) ions by the dead biomass of *Rhizopus arrhizus*. *J. Chem. Technol. Biotechnol.* 87, 294–304.
36. Sivakumar, D., 2016. Biosorption of hexavalent chromium in a tannery industry wastewater using fungi species. *Glob. J. Environ. Sci. Manag.* 2(2), 105–124.
37. Tytlak, A., Oleszczuk, P., Dobrowolski, R., 2015. Sorption and desorption of Cr(VI) ions from water by biochars in different environmental conditions. *Environ. Sci. Pollut. Res.* 22, 5985–5994.
38. Vendruscolo, F., Rocha Ferreira, G.L., Antoniosi Filho, N.R., 2017. Biosorption of hexavalent chromium by microorganisms. *Int. Biodeterior. Biodegrad.* 119, 87–95.
39. Verma, D.K., Hasan, S.H., Ranjan, D., Banik, R.M., 2014. Modified biomass of *Phanerochaete chrysosporium* immobilized on luffa sponge for biosorption of hexavalent chromium. *Int. J. Environ. Sci. Technol.* 11, 1927–1938.
40. Villalobos-Aragón, A., Ellis, A.S., Armienta, M.A., Morton-Bermea, O., Johnson, T.M., 2012. Geochemistry and Cr stable isotopes of Cr-contaminated groundwater in León valley, Guanajuato, México. *Appl. Geochemistry* 27, 1783–1794.
41. Volesky, B., 2001. Detoxification of metal-bearing effluents: Biosorption for the next century. *Hydrometallurgy* 59, 203–216.
42. Wang, J., Chen, C., 2006. Biosorption of heavy metals by *Saccharomyces cerevisiae*: A review. *Biotechnol. Adv.* 24, 427–451.
43. Wu, F.C., Tseng, R.L., Huang, S.C., Juang, R.S., 2009a. Characteristics of pseudo-second-order kinetic model for liquid-phase adsorption: A mini-review. *Chem. Eng. J.* 151, 1–9.

44. Wu, F.C., Tseng, R.L., Juang, R.S., 2009b. Characteristics of Elovich equation used for the analysis of adsorption kinetics in dye-chitosan systems. *Chem. Eng. J.* 150, 366–373.
45. Yang, J., Yu, M., Chen, W., 2015. Adsorption of hexavalent chromium from aqueous solution by activated carbon prepared from longan seed: Kinetics, equilibrium and thermodynamics. *J. Ind. Eng. Chem.* 21, 414–422.

**CHAPTER 5**  
**Cr(VI) REMOVAL USING IMMOBILIZED FUNGAL BIOMASS**

## **Abstract**

The removal of Cr(VI) using Ca-alginate beads with and without pre-treated *Rhizopus* sp. biomass was evaluated through kinetic and thermodynamic experiments. Spherical Ca-alginate beads containing pre-treated (NaCl) *Rhizopus* sp. were produced to investigate the feasibility of immobilized fungal biomass in the removal of Cr(VI). The Ca-alginate beads reached a removal of 45% but it dropped to 15% after 8 hours, showing a reversible process. The immobilized biomass removed up to 62.5% in a lapse of 7 days, with a  $q_e$  of  $0.53 \text{ mg}\cdot\text{g}^{-1}$ . The PSO had an  $R^2$  of 0.99 in its linear form, however, the ID model showed a good fit with an  $R^2$  of 0.93 in the linear and non-linear expression. The Freundlich model presented a better fit than the Langmuir model, exposing the heterogeneous nature of the biosorbent. The thermodynamic analysis revealed that the process was endothermic and spontaneous. The functional groups interacting in the adsorption process were analyzed using FT-IR before and after Cr(VI) adsorption. This study provided the comprehension of the use of immobilized *Rhizopus* sp. biomass entrapped in calcium-alginate to remove Cr(VI) in aqueous solutions, furthermore, these results can be used in future discussions.

## 5.1. Introduction

Throughout the last years, the treatment processes to remove metal ions and organic compounds from water using low-cost sorbents have been in development and improvement (Escudero *et al.*, 2017). Natural weathering of rocks and soils that occur through contact with water is considered to be the main natural contamination resource to heavy metals, these are irresolvable and gradually accumulate in the body of living creatures, (Gasemloo *et al.*, 2019). There are three thermodynamically stable forms of chromium, Cr(0), Cr(III), and Cr(VI), there are used commercially and are present in the environment (Zhitkovich, 2011). Hexavalent chromium is the most dangerous and toxic metal that can be found as dichromates and strong oxides (Ravikumar *et al.*, 2018).

Due to the increase in environmental awareness, stringent governmental policies, and penalties imposed for the discharge of untreated wastewater cause a large financial pressure on industrialists and there has been an emphasis on the development of new environmentally friendly and cost-effective ways to decontaminate waters (Shroff and Vaidya, 2012). Among different wastewater treatment technologies, adsorption has evolved as a cost-effective method for removing chromium from aqueous solutions (Valentín-Reyes *et al.*, 2019). In the same way, biosorption has emerged as a complementary, economic and eco-friendly mean for controlling the mobility and bioavailability of metal ions in wastewater treatment processes because of its simplicity, analogous operation to conventional ion exchange technology and apparent efficiency (Gadd, 2009).

In the previous chapters, the use of free dead fungal biomass in the removal of Cr(VI) was studied, however, the powder on a large scale is limited by process engineering difficulties such as dispersion, cost of regeneration and clogging of the reactor, which makes its utilization harder for this purpose. Furthermore, powdered adsorbents are not recoverable and reusable through centrifugation or filtration, which in turn produce a huge amount of waste and create another problem for the environment (Nasrullah *et al.*, 2018) This is enough reason to consider the immobilization of the biosorbent in a matrix that can support the fungal biomass. The choice of immobilization matrix is a key factor in environmental application of immobilized biomass. The polymeric matrix determines the

mechanical strength and chemical resistance of the final biosorbent particle, which is to be utilized for successive sorption–desorption process (Bai and Abraham, 2003).

Biopolymeric materials and microbial cells can accumulate metal ions by precipitating or binding the metal ions owing to the presence of carboxyl, hydroxyl, amino, and other negatively charged sites (Yu *et al.*, 2017). Alginate is a natural polymer and can be converted into a hydrogel crosslinking it with divalent calcium cations. The use of this immobilizing agent was chosen over other types of materials due to several properties like biodegradability, hydrophilicity, the presence of carboxylic groups, and natural origin (Arica *et al.*, 2004). Encompassed by other advantages, the alginates have low density and mechanical stability which makes them highly convenient for biotechnological applications (Katircioğlu *et al.*, 2012). Ca-alginate beads not only are used to entrap microorganism’s biomass, but also other adsorbent materials, as goethite, which is one of the most important iron oxides in soil and sediment and it was used by Munagapati and Kim (2017) to remove congo red from aqueous solutions. Likewise, Gopalakannan and Viswanathan (2015), used magnetic composite beads of Fe<sub>3</sub>O<sub>4</sub> immobilized in calcium alginate using Ce(III) as a cross-linking agent, making the material more stable and improving the uptake capacity of hexavalent chromium.

The objective of this work was to study the potential Cr(VI) removal of immobilized *Rhizopus* sp. biomass, using alginate as the immobilizing agent. As it was shown in Chapter 4, the removal of Cr(VI) onto pretreated free *Rhizopus* sp. biomass reached a 99%, however, the immobilization of the biomass is a crucial part for the scale-up process, since it is not possible to use the free fungal biomass, an immobilization agent was needed to entrap the biomass into small pellet-shaped biosorbent.

## **5.2. Materials and methods**

### **5.2.1. Preparation of fungal biomass**

The fungal strain used in this study was *Rhizopus* sp. This strain was isolated from soil, the sampling and isolation of this strain were carried out in Monterrey, Nuevo León, México by Castro-González *et al.* (2017). The strain was cultivated and treated as mentioned in Chapter 4.



### 5.2.2. Immobilization of fungal biomass

The immobilization agent (sodium alginate) was taken as a control to study its effect in the removal of Cr(VI), 1.5 g of sodium alginate was mixed in a distilled water solution to make alginate beads. The fungal biomass was immobilized by mixing 1:1 (w/w) of *Rhizopus* sp. pre-treated dried biomass and sodium alginate in 100 mL of deionized distilled water. The alginate-biomass blend was mixed and stirred with a magnetic bar to ensure complete mixing. After the mixing, the solution was dropped in 500 mL of CaCl<sub>2</sub> (0.01 M) using a peristaltic pump. Spherical beads containing pre-treated (NaCl) *Rhizopus* sp. were formed immediately by a phase inversion process as the alginate was cross-linked by Ca<sup>2+</sup> ion. The immobilized biomass was stored at 4 °C in distilled water until further use. The Ca-alginate beads are shown in Figure 10.



Figure 10. Ca-alginate beads of *Rhizopus* sp.

### 5.2.3. Synthetic Cr(VI) solution

The chemicals used were of analytical grade. A stock solution (1000 mg·L<sup>-1</sup>) of Cr (VI) was prepared with 2.828 g of K<sub>2</sub>Cr<sub>2</sub>O<sub>7</sub>. The pH of the solutions was adjusted to 2.0 using HCl 0.1 M.

### 5.2.4. Analytical Cr(VI) determination

The determination of the residual Cr(VI) ions after being in contact with the immobilized biomass was quantified by spectrophotometrically means using a UV-VIS Spectrophotometer Evolution 60S (Thermo Scientific) at a wavelength of 540 nm after

the complexation with the 1,5-diphenylcarbazide agent, following the 3500-Cr B. Colorimetric Method (APHA/AWWA/WEF, 2012).

#### 5.2.5. Characterization of immobilized *Rhizopus* sp. biomass

The chemical properties of the immobilized agent, *Rhizopus* sp biomass, and the Ca-alginate beads with *Rhizopus* sp. before and after contact with Cr(VI) were analyzed using a Fourier Transform Infrared spectrometer Nicolet iS10 (Thermo Scientific). Figure 11 shows *Rhizopus* sp. pellets interacting with Cr(VI) solution.

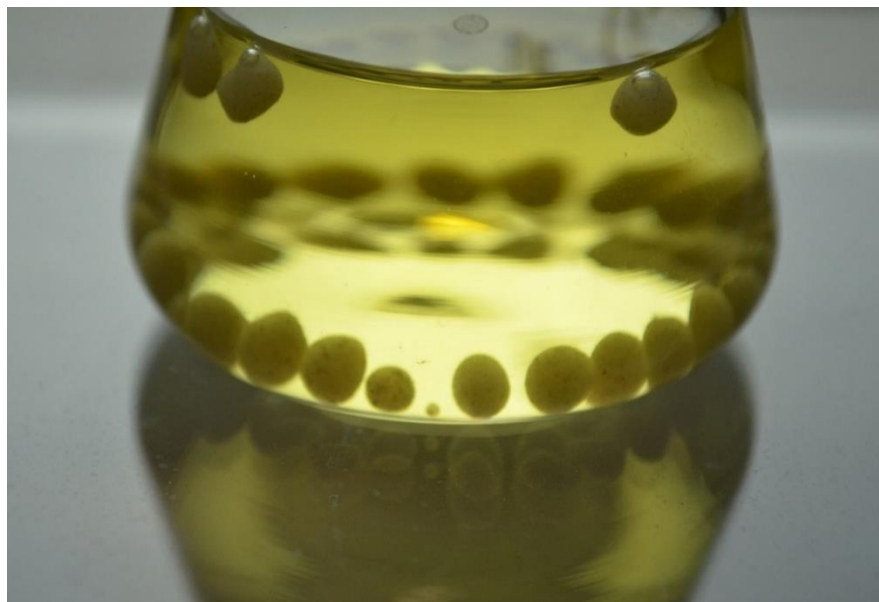


Figure 11. *Rhizopus* sp. immobilized biomass in contact with Cr(VI).

#### 5.2.6. Kinetic adsorption assays

Two different kinetic experiments were performed. In the first one, Ca-alginate beads were in contact with Cr(VI) for a total time of 8 hours, sampling every hour. For the experiments with the *Rhizopus* sp. Ca-alginate beads, the total time was of 7 days, the sampling was every day. The Cr(VI) concentration was  $50 \text{ mg}\cdot\text{L}^{-1}$  at a pH of 2.0. The average weight of biosorbent used was 0.4 g for both kinetic experiments.

The experimental data obtained with these assays was evaluated using the four most frequent mathematical models for adsorption kinetics: (1) pseudo-first order (PFO); (2) pseudo-second order (PSO); (3) Elovich model; and (4) the intraparticle diffusion (ID) models, which are fully described in previous chapters.

### 5.2.7. Isotherm assays

The equilibrium assays were executed with 0.4 g of Ca-alginate *Rhizopus* sp. beads into 10 mL of Cr(VI) solutions with ranging concentrations from 12.5 to 300 mg·L<sup>-1</sup>, at pH 2.0 and using the following three temperatures 10, 25 and 40 °C for 240 min. The results of these experiments were analyzed by Langmuir and Freundlich isotherm models. The thermodynamic characteristics of the adsorption system were analyzed with the fitted isotherm parameters calculating the entropy, enthalpy, and standard Gibbs free energy.

## 5.3. Results and discussion

The contact time between adsorbent and sorbate is of crucial importance to the adsorption process, this is because of the different types of adsorbents used in a system. The effect of contact time on the adsorption of Cr(VI) onto *Rhizopus* sp. biomass immobilized in Ca-alginate beads was studied, along with the isotherm assays under different concentrations (12.5 – 300 mg·g<sup>-1</sup>). These assays allowed the analysis of the data from a mathematical perspective, which are presented below.

### 5.3.1. Evaluation of immobilizing agent

Biosorption of hexavalent chromium onto immobilized fungal biomass was studied using kinetic and isotherm assays. The immobilizing agent was evaluated first, in order to know if there was an important interaction of the Ca-alginate beads with Cr(VI). The removal of Cr(VI) using Ca-alginate beads as biosorbents is shown in Figure 12, where the highest removal (45%) was at the first sampling of the kinetic experiment. The graph shows a decrease in the removal of the ion through time, this could mean that the sorption interaction of the chromium anion onto the alginate beads was reversible, increasing the Cr(VI) concentration in the solution, leading to a decrease in the removal thorough time. The sorption of hexavalent chromium onto calcium alginate beads is also reported by Escudero *et al.*, (2017), where the removal of the ion was 20% at a pH of 3.0, this could be caused by electrostatic interactions. The adsorption on biopolymeric beads is ruled by electrostatic attraction; the low adsorption efficiency at pH 2.0 could be attributable to the weak interaction between the carboxyl groups of the biopolymeric beads and chromium ions (Dewangan *et al.*, 2011).

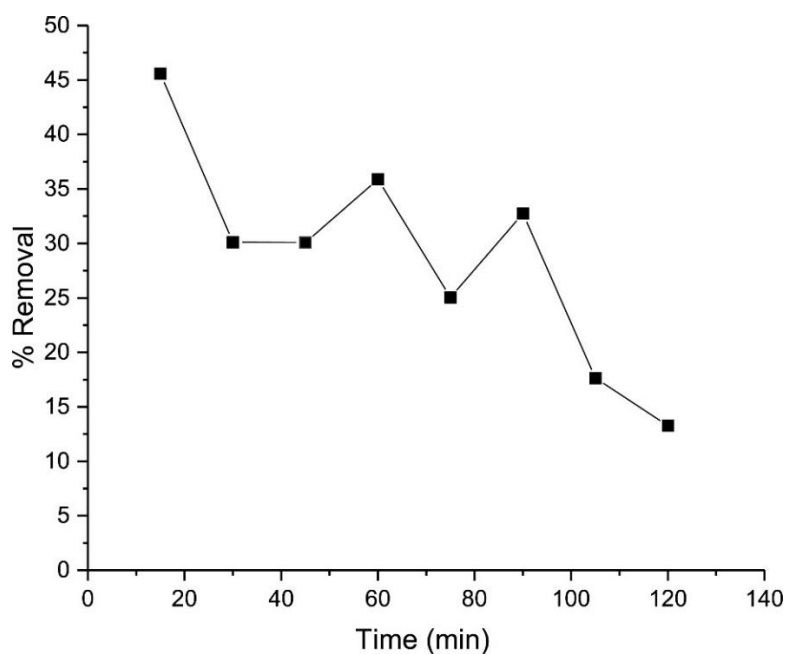


Figure 12. Cr(VI) removal using calcium alginate beads.

### 5.3.2. Cr(VI) adsorption kinetics onto immobilized fungal biomass

The removal rate of Cr(VI) onto immobilized biomass of *Rhizopus* sp. was assessed using diverse mathematical models like the PFO, PSO, Elovich, and ID. In Figure 13, the removal percentage and the adsorption capacity of the immobilized fungal biomass are shown. The highest removal was 62.5% after 7 days of contact. Bishnoi *et al.*, (2007), reported a 71.1% Cr(VI) removal using immobilized biomass of *Trichoderma viride* entrapped in Ca-alginate beads. The biosorption capacity reached its maximum with  $0.53 \text{ mg} \cdot \text{g}^{-1}$ . The analysis of this data set is shown in Table 9, along with the non-linear models (Figure 14). The analysis with the non-linear PFO model was not possible since the algorithm for the non-linear regression could not find an accurate fit to the equation. The PSO model has a determination coefficient of 0.99 with the linear equation, however, the non-linear analysis exhibited an  $R^2$  of 0.31. In the case of the ID model, both linear and non-linear analysis seemed to fit better with the collected data, this indicated that the intraparticle diffusion took place in the biosorption process. Similar results of the fitting were obtained by Tsekova *et al.* (2010), where the ability of *Aspergillus niger* biomass entangled with polyvinyl alcohol was studied for the removal of Cu(II) and Cd(II). In the specific case of this study, the process appears to be ruled by chemisorption and expressly with the intraparticle diffusion model, since both linear and non-linear  $R^2$  are 0.93.

In the work published by Bishnoi *et al.* (2007), where Ca-alginate beads and immobilized biomass of *Trichoderma viride* in Ca-alginate beads were compared in the biosorption of Cr(VI), the data indicated that immobilized fungal biomass was better adsorbent than the cell-free Ca-alginate beads for Cr(VI). Similar results were obtained by Arica *et al.* (2003), where a significant increase in the  $q_m$  was observed when *Phanerochaete chrysosporium* was entrapped in Ca-alginate beads. This may be due to the more available sites on the immobilized biomass. Bai and Abraham (2003) did adsorption-desorption studies of Cr(VI) using immobilized *Rhizopus nigricans* biomass in different types of immobilizing agents, the best removal was also for free biomass, followed by polysulfone among others, in the case of sodium alginate the percentage of adsorption was of 70.07%.

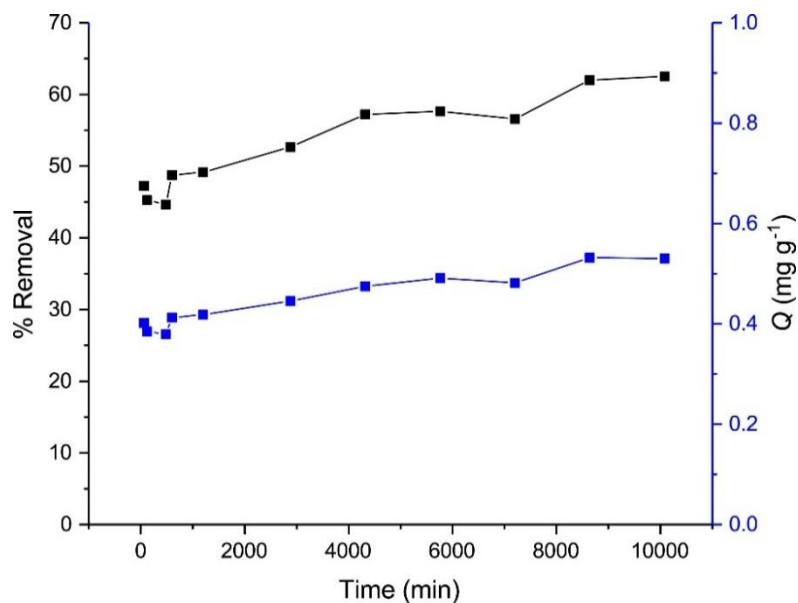


Figure 13. Cr(VI) adsorption using immobilized *Rhizopus* sp. biomass (—■— % removal, —■— removal capacity)

Table 9. Kinetic parameters for the adsorption of Cr(VI) onto immobilized *Rhizopus* sp. biomass.

	Non-linear	Linear
<b>Kinetic model</b>		
<i>Pseudo-first order</i>		
$K_I$ ( $\text{min}^{-1}$ )	-	0.0003
$q_e$ ( $\text{mg}\cdot\text{g}^{-1}$ )	-	0.1816
$R^2$	-	0.8003
<i>Pseudo-second order</i>		
$K_{II}$ ( $\text{g}\cdot(\text{mg}\cdot\text{min})^{-1}$ )	0.1566	0.0094
$q_e$ ( $\text{mg}\cdot\text{g}^{-1}$ )	0.4774	0.5238
$R^2$	0.3168	0.9951
<i>Intra-particle diffusion</i>		
$K_d$	0.0014	0.0015
$R^2$	0.9386	0.9390
<i>Elovich</i>		
$\alpha$ ( $\text{mg}\cdot(\text{g}\cdot\text{min})^{-1}$ )	2195.8470	703.0501
$\beta$ ( $\text{g}\cdot\text{mg}^{-1}$ )	17.0637	38.6288
$R^2$	0.7468	0.8050
$q_{e,exp}$		0.5300

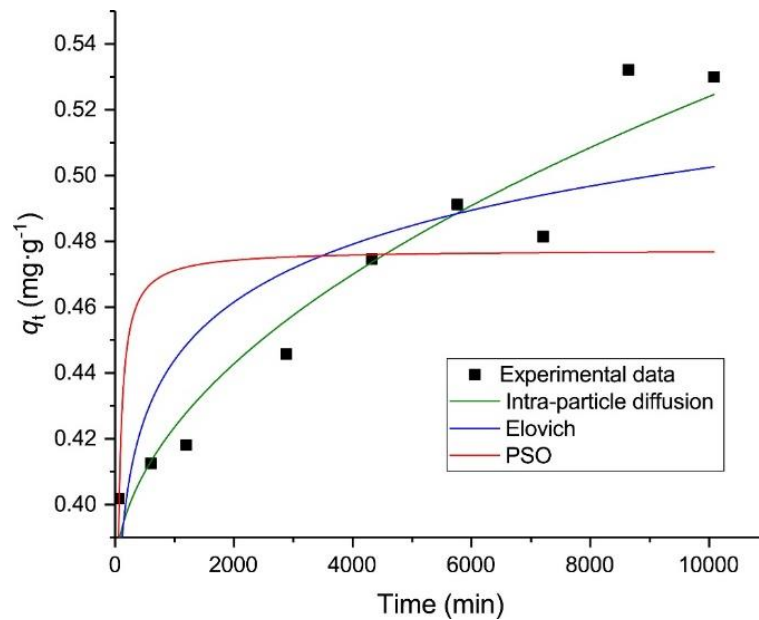


Figure 14. Non-linear kinetic analysis of immobilized fungal biomass on the adsorption of Cr(VI).

### 5.3.3. Analysis of adsorption isotherms

The adsorption isotherm data of Cr(VI) using immobilized *Rhizopus* sp. biomass at different initial concentrations of hexavalent chromium was analyzed using Langmuir and Freundlich equations. The estimated values for each model are shown in Table 10. The best linear regression was for the Freundlich model, which is based upon sorption on a heterogeneous surface.

Table 10. Isotherm parameters for the adsorption of Cr(VI) onto immobilized *Rhizopus* sp. biomass.

Isotherm model	Temperature					
	Lineal			Non-linear		
	10 °C	25 °C	40 °C	10 °C	25 °C	40 °C
<i>Langmuir model</i>						
$K_L$ (L·mg <sup>-1</sup> )	0.0469	0.0467	0.0719	0.0040	0.0134	0.0192
$q_m$ (mg·g <sup>-1</sup> )	1.0562	1.1732	1.3802	4.4985	2.1845	2.5184
$R^2$	0.8973	0.8652	0.8172	0.8597	0.8720	0.9587
$R_L$						
<i>Freundlich</i>						
$K_F$ (mg·g <sup>-1</sup> )	0.3796	0.0051	0.5210	0.4950	0.0776	0.0339
$n$	4.2115	1.9519	3.8028	14.6094	3.3254	2.5677
$R^2$	0.9411	0.9324	0.9077	0.8791	0.8856	0.9609

The Langmuir adsorption isotherm describes the distribution of heavy metal ions between the liquid and solid phases, based on the assumption that many active adsorption sites are on the surface of the sorbents, creating a monolayer, each site can only adsorb one ion and there is no interaction between the adsorbed species (Li *et al.*, 2008). Both models had a good fitting, notwithstanding, the biosorbent used is a mixture of two different materials, which can result in a heterogeneous surface, agreeing with the Freundlich equation, which had the best fitting with the data analyzed ( $R^2 = 0.9609$ ). The isotherm gives an expression that defines the surface heterogeneity and the exponential distribution of active sites and their energies (Ayawei *et al.*, 2017). The values of  $n > 1$  represent a favorable nature of adsorption. This study is considered as a favorable adsorption process since the values of  $n > 1$ . The non-linear fitting curves of the Langmuir and Freundlich models are plotted in Figure 15.

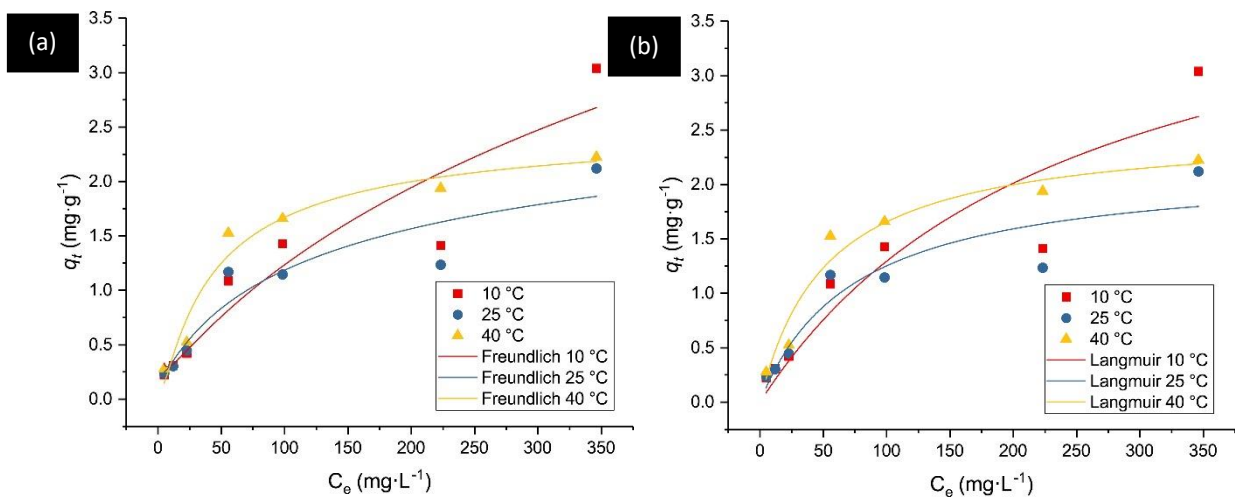


Figure 15. Non-linear isotherm adsorption of Cr(VI) onto immobilized *Rhizopus* sp. biomass. (a) Freundlich; (b) Langmuir.

### 5.3.4. Thermodynamic analysis

The thermodynamic analysis of the adsorption results provides relevant information about the nature of the process, such as feasibility and spontaneity, which are imperative in engineering practice (Seo *et al.*, 2013). The values of  $\Delta G^0$ ,  $\Delta H^0$  and  $\Delta S^0$  are shown in Table 11. The positive value of the enthalpy ( $\Delta H$ ) indicates that the adsorption process of Cr(VI) onto immobilized *Rhizopus* sp. biomass in alginate beads is endothermic. The negative value of  $\Delta G^0$  indicate that the sorption process is spontaneous and the increase in the negative value of  $\Delta G^0$  with a rise in the temperature makes the biosorption of Cr(VI) favorable.

Table 11. Thermodynamic parameters for Cr(VI) adsorption onto immobilized *Rhizopus* sp. biomass.

<b>Thermodynamic parameters</b>			
<i>Rhizopus</i> sp. immobilized in calcium alginate			
Isotherm model	10 °C	25 °C	40 °C
$\ln K_L$	7.74	7.78	8.37
$\Delta G^0$ (kJ·mol <sup>-1</sup> )	-179.99	-190.66	-215.36
$\Delta S^0$ (J·mol <sup>-1</sup> ·K <sup>-1</sup> )		-1.17	
$\Delta H^0$ (kJ·mol <sup>-1</sup> )		156.17	



### 5.3.5. Biosorbent characterization

The FT-IR analysis of the alginate beads along with the immobilized biomass of *Rhizopus* sp. before and after biosorption were studied (Figure 16). The bands at 2924 and 2854  $\text{cm}^{-1}$  were found also in the biomass of *Phanerochaete chrysosporium*, indicating a stretching of  $-\text{CH}$  group (Verma *et al.*, 2014). As it was shown in Chapter 3, the peak at 1713  $\text{cm}^{-1}$  can be associated with a  $\text{C}=\text{O}$  of the carboxyl groups, the peak at 1622  $\text{cm}^{-1}$  is an amide band corresponding to a  $\text{C}=\text{O}$  stretch, this was found studying the  $\text{Cr}(\text{VI})$  removal onto free sterile *Rhizopus* sp. biomass. The peak at 1740  $\text{cm}^{-1}$  represents the stretching band of the free carbonyl double bond from the carboxyl functional group. The peak around 1630  $\text{cm}^{-1}$  is a chelated stretching bond of  $\text{C}=\text{O}$ . It is reported that the carboxyl groups on biological polymers such as Ca-alginate beads have  $\text{pK}_\text{H}$  values from 3.5 to 5.0 (Kim *et al.*, 2008).

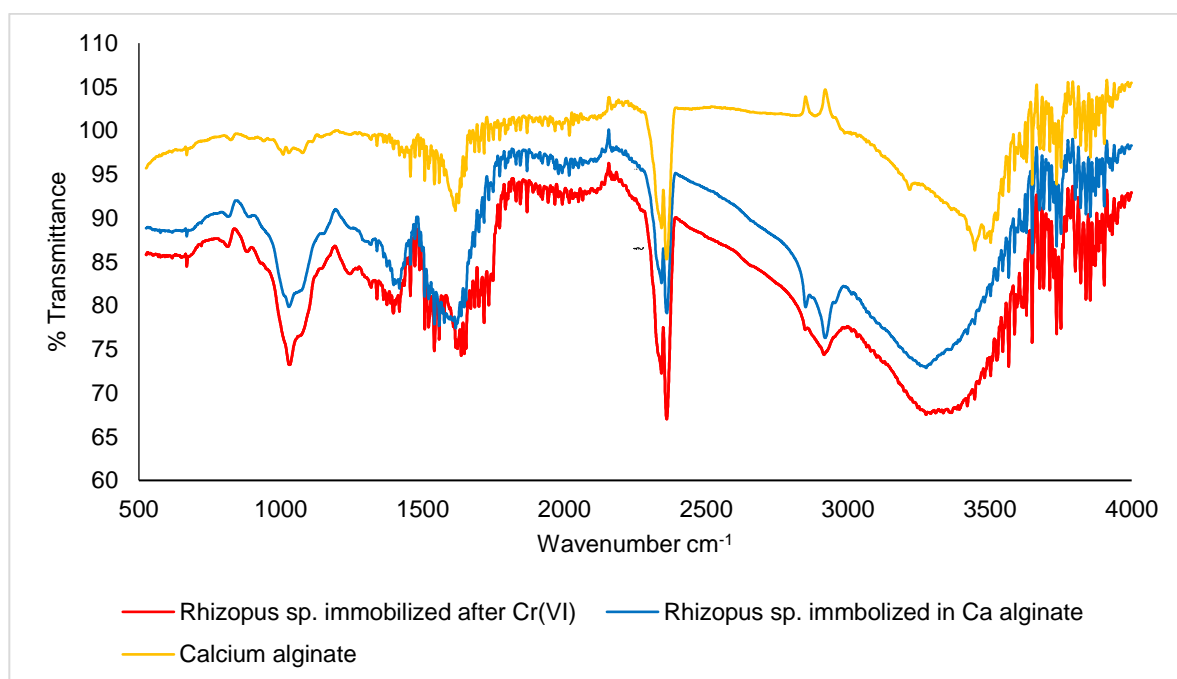


Figure 16. FTIR spectra of calcium alginate, *Rhizopus* sp. biomass immobilized in Ca-alg beads before and after biosorption.

### 5.4. Conclusions

In this study, the  $\text{Cr}(\text{VI})$  adsorption properties of dead *Rhizopus* sp. biomass immobilized in Ca-alginate beads were studied. The results showed that the removal of the ion was affected by the immobilizing matrix. Previous results showed that free *Rhizopus* sp. biomass could remove 99% of the metal, however, the use of alginate to

entrap the powdered biomass reduces the removal capability of the fungal strain to a maximum of 62% in a time period of 7 days. The isotherm studies were best described by the Freundlich isotherm and the thermodynamic analysis revealed that the adsorption process was endothermic and favorable. The biomass characterization allowed the comprehension of the mechanisms involved between the functional groups of the matrix and the target anion. Even though the biosorption capacity of the strain using dead free biomass is good, it is impractical when it comes to an industrial application due to the management of the free biomass.

## 5.5. References

1. APHA, AWWA, WEF, 2012. Standard Methods for the Examination of Water and Wastewater. Twentieth ed. United Book Press, Inc., Baltimore.
2. Arica, M.Y., Arpa, Ç., Ergene, A., Bayramoğlu, G.U., Genç, Ö., 2003. Ca-alginate as a support for Pb(II) and Zn(II) biosorption with immobilized *Phanerochaete chrysosporium*. Carbohydr. Polym. 52, 167–174. [https://doi.org/10.1016/S0144-8617\(02\)00307-7](https://doi.org/10.1016/S0144-8617(02)00307-7)
3. Arica, M.Y., Bayramoğlu, G., Yilmaz, M., Bektaş, S., Genç, Ö., 2004. Biosorption of  $Hg^{2+}$ ,  $Cd^{2+}$ , and  $Zn^{2+}$  by Ca-alginate and immobilized wood-rotting fungus *Funalia trogii*. J. Hazard. Mater. 109, 1–199. <https://doi.org/10.1016/j.jhazmat.2004.03.017>
4. Ayawei, N., Ebelgi, A.N., Wankasi, D., 2017. Modelling and interpretation of adsorption isotherms. J. Chem. 2017. <https://doi.org/10.1155/2017/3039817>
5. Bai, R.S., Abraham, T.E., 2003. Studies on chromium(VI) adsorption-desorption using immobilized fungal biomass. Bioresour. Technol. 87, 17–26. [https://doi.org/10.1016/S0960-8524\(02\)00222-5](https://doi.org/10.1016/S0960-8524(02)00222-5)
6. Bishnoi, N.R., Kumar, R., Bishnoi, K., 2007. Biosorption of Cr(VI) with *Trichoderma viride* immobilized fungal biomass and cell free Ca-alginate beads. Indian J. Exp. Biol. 45, 657–664.
7. Castro-González, I., Rojas-Verde, G., Quintero-Zapata, I., Almaguer-Cantú, V., 2017. A comparative study on removal efficiency of Cr(VI) in aqueous solution by *Fusarium* sp. and *Myrothecium* sp. Water Air Soil Pollut. 228:301–310.
8. Dewangan, T., Tiwari, A., Bajpai, A.K., 2011. Removal of chromium(VI) ions by adsorption onto binary biopolymeric beads of sodium alginate and carboxymethyl cellulose. J. Disper. Sci. Technol. 32(8), 1075–1082.
9. Escudero, C., Fiol, N., Villaescusa, I., Bollinger, J.C., 2017. Effect of chromium speciation on its sorption mechanism onto grape stalks entrapped into alginate beads. Arab. J. Chem. 10, S1293–S1302. <https://doi.org/10.1016/j.arabjc.2013.03.011>

10. Gadd, G.M., 2009. Biosorption: critical review of scientific rationale, environmental importance and significance for pollution treatment. *J. Chem. Technol. Biotechnol.* 84, 13–28. <https://doi.org/10.1002/jctb.1999>
11. Gasemloo, S., Khosravi, M., Sohrabi, M.R., Dastmalchi, S., Gharbani, P., 2019. Response surface methodology (RSM) modeling to improve removal of Cr (VI) ions from tannery wastewater using sulfated carboxymethyl cellulose nanofilter. *J. Clean. Prod.* 208, 736–742. <https://doi.org/10.1016/j.jclepro.2018.10.177>
12. Gopalakannan, V., Viswanathan, N., 2015. Synthesis of magnetic alginate hybrid beads for efficient chromium (VI) removal. *Int. J. Biol. Macromol.* 72, 862–867. <https://doi.org/10.1016/j.ijbiomac.2014.09.024>
13. K.V.G., R., Sudakaran, S.V., Pulimi, M., Natarajan, C., Mukherjee, A., 2018. Removal of hexavalent chromium using nano zero valent iron and bacterial consortium immobilized alginate beads in a continuous flow reactor. *Environ. Technol. Innov.* 12, 104–114. <https://doi.org/10.1016/j.eti.2018.08.004>
14. Katircioğlu, H., Aslim, B., Tunçeli, A., 2012. Chromium (VI) biosorption from aqueous solutions by free and immobilized biomass of *Oscillatoria* sp. H1 isolated from freshwater. *ISIJ Int.* 52, 1173–1178. <https://doi.org/10.2355/isijinternational.52.1173>
15. Kim, T.Y., Chung, J.H., Choi, S.Y., Cho, S.Y., Kim, S.J., 2008. Adsorption characteristics of chromium ions onto composite alginate bead. *Lect. Notes Eng. Comput. Sci.* 2173, 131–136.
16. Li, H., Liu, T., Li, Z., Deng, L., 2008. Low-cost supports used to immobilize fungi and reliable technique for removal hexavalent chromium in wastewater. *Bioresour. Technol.* 99, 2234–2241. <https://doi.org/10.1016/j.biortech.2007.05.033>
17. Munagapati, V.S., Kim, D.S., 2017. Equilibrium isotherms, kinetics, and thermodynamics studies for congo red adsorption using calcium alginate beads impregnated with nano-goethite. *Ecotoxicol. Environ. Saf.* 141, 226–234. <https://doi.org/10.1016/j.ecoenv.2017.03.036>
18. Nasullah, A., Bhat, A.H., Naeem, A., Isa, M.H., Danish, M., 2018. High surface area mesoporous activated carbon-alginate beads for efficient removal of methylene blue. *Int. J. Biol. Macromol.* 107, 1792–1799. <https://doi.org/10.1016/j.ijbiomac.2017.10.045>
19. Seo, H., Lee, M., Wang, S., 2013. Equilibrium and kinetic studies of the biosorption of dissolved metals on *Bacillus drentensis* immobilized in biocarrier beads. *Environ. Eng. Res.* 18, 45–53. <https://doi.org/10.4491/eer.2013.18.1.045>
20. Shroff, K.A., Vaidya, V.K., 2012. Effect of pre-treatments on the biosorption of chromium (VI) ions by the dead biomass of *Rhizopus arrhizus*. *J. Chem. Technol. Biotechnol.* 87, 294–304. <https://doi.org/10.1002/jctb.271>
21. Tsekova, K., Todorova, D., Dencheva, V., Ganeva, S., 2010. Biosorption of copper(II) and cadmium(II) from aqueous solutions by free and immobilized biomass of

- Aspergillus niger*. *Bioresour. Technol.* 101, 1727–1731. <https://doi.org/10.1016/j.biortech.2009.10.012>
22. Valentín-Reyes, J., García-Reyes, R.B., García-González, A., Soto-Regalado, E., Cerino-Córdova, F., 2019. Adsorption mechanisms of hexavalent chromium from aqueous solutions on modified activated carbons. *J. Environ. Manage.* 236, 815–822. <https://doi.org/10.1016/j.jenvman.2019.02.014>
23. Verma, D.K., Hasan, S.H., Ranjan, D., Banik, R.M., 2014. Modified biomass of *Phanerochaete chrysosporium* immobilized on luffa sponge for biosorption of hexavalent chromium. *Int. J. Environ. Sci. Technol.* 11, 1927–1938. <https://doi.org/10.1007/s13762-013-0345-6>
24. Yu, J., Wang, J., Jiang, Y., 2017. Removal of uranium from aqueous solution by alginate beads. *Nucl. Eng. Technol.* 49, 534–540. <https://doi.org/10.1016/j.net.2016.09.004>
25. Zhitkovich, A., 2011. Chromium in drinking water: sources, metabolism, and cancer risks. *Chem. Res. Toxicol.* 24, 1617–1629. <https://doi.org/10.1021/tx200251t>

**CHAPTER 6**  
**FUNGAL PELLETTED SEQUENCING BATCH REACTORS: GROWTH**  
**AND Cr(VI) REMOVAL**

## **Abstract**

Hexavalent chromium in its chromate and dichromate forms are extensively used in anthropogenic activities and are considered highly toxic to most of live organisms. The biological alternative of using fungi as a potential wastewater treatment has caught attention, especially in its immobilized form as aggregates. Fungal pellets of *Trichoderma* sp. were cultivated in a sequencing batch reactor (SBR) to study its potential to remove Cr(VI) from aqueous solutions. Two fungal pelleted reactors operated in SB mode were used (R1 and R2): 1) to produce the fungal pellets appraising its growth and 2) to evaluate the Cr(VI) removal capabilities of the fungal pellets. Each reactor was operated in cycles of 6 h. Fungal pellets were able to grow in an SBR with minimal culture media. Contamination from other organisms in the reactor affected the growth of the pellets. The fungal pellets showed high sensitivity to Cr(VI), which inhibited the substrate consumption in the presence of  $10 \text{ mg}\cdot\text{L}^{-1}$  of Cr(VI). Morphological changes were observed using SEM-EDX analysis, were ruptures were shown in the hyphae of the fungal pellets that were in contact with Cr(VI).

## 6.1. Introduction

Water contamination is an increasing concern across the world, the natural sources of clean water are decreasing at a frightening rate. Among the inorganic pollutants that are discharged in water bodies, heavy metals are a major risk to humans, animals, and plants (Sen *et al.*, 2018). Heavy metals are dispersed naturally in rock formations, yet, increasing industrialization has elevated their concentrations on a threatening level. Their distribution and accumulation, as well as its persistence and toxicity possess potential harm to living beings (Bhattacharya *et al.*, 2019). Hexavalent chromium has had a big impact on different aspects of modern society, like social, economic, environmental and even reaching public health (García-Hernández *et al.*, 2017). Nowadays the co-existence of oxidized pollutants such as nitrate and chromate is a growing problem and challenge for wastewater treatment, the bioremediation of this pollutants into harmless or immobile forms is considered a cost-effective alternative to chemical process, especially for concentrations of Cr(VI) ranging from (10-200 mg·L<sup>-1</sup>) (Jin *et al.*, 2017).

It is well known that conventional activated sludge is the most popular biological process used as a secondary treatment, either way, classical processes as fixed bed, moving bed or even rising technologies as granular sludge are used (Vu and Vu, 2017). Aerobic granular sludge (AGS) has been the focus of many works on wastewater treatment with domestic and high organic loads, its capacity for bioremediating toxic aromatic pollutants, industrial effluents, adsorption of heavy metals and recovery of high value added products makes this technology a promising technology for wastewater treatment, along with the low space requirement and costs reduction compared with activated sludge systems (de Sousa Rollemberg *et al.*, 2018). It has been well established that sequencing batch reactors are an entrenched model for the cultivation of aerobic granular sludge (Nancharaiah *et al.*, 2012). The cultivation of AGS is usually in column reactors where the inoculum is AG, the reactor is operated in SBR mode using bubble aeration and short settling times. The growth is promoted to form dense aggregates, the settling time range between 2-10 min, this time encourages the selection of the densest aggregates (Nancharaiah and Kiran Kumar Reddy, 2018). The most promising feature of aerobic granules in treating emerging contaminants is that they can simultaneously treat

pollutants by three environmentally friendly methods: biodegradation, bioaccumulation and biosorption (Sarma *et al.*, 2017).

Living organisms including bacteria, fungi, yeast, algae, and plants have shown remediation capabilities, but primarily bacteria and fungi have proven to be more efficient in remediation (Jobby *et al.*, 2018). There is an increase in the research of microorganisms capable of transforming the highly toxic and water-soluble form of Cr(VI) into the less toxic and stable form of Cr(III) (Morales-Barrera and Cristiani-Urbina, 2006). Diverse fungal strains have shown their capability to degrade a wide range of contaminants from the environment. Among these pollutants the case of dyes, pharmaceutical compounds, heavy metals, trace organic contaminants have gotten attention by the scientific community. The potential use of fungal pellets in bioreactors in order to remove contaminants has increased the attention of bioengineers, especially for its settleability properties which reduce the operational difficulties caused by fungal dispersed mycelium (Espinosa-Ortiz *et al.*, 2016a). A pellet is considered as a spherical mass of non-growing mycelia surrounded by an outer shell of active hyphae (Papagianni, 2004). Due to high settling velocities, aerobic microbial granules eliminate the use of large settling tanks and allow high biomass concentrations in the reactor leading to higher conversion rates (de Bruin *et al.*, 2004). The effects of Cr(VI) have been studied by Zheng *et al.*, (2016) in AGS cultivation with a sequencing batch reactor (SBR), putting focus on the variations in the pollutant removal and nitrification capability, along with the microbial activity of the aerobic granules. However, the extent of Cr(VI) bioremediation by a fungal pelleted sequencing batch reactor as well as its growth in this configuration is still unclear, which leads to the objective of the present work, to assess the growth and Cr(VI) removal using fungal pellets in SBR.

## **6.2. Materials and methods**

### **6.2.1. Pre culture, medium, and growth**

The fungal strain used in this study was grown in 250 mL Erlenmeyer flasks containing 100 mL of liquid medium (glucose 10 g·L<sup>-1</sup>, K<sub>2</sub>HPO<sub>4</sub> 4 g·L<sup>-1</sup>, MgSO<sub>4</sub> 0.75 g·L<sup>-1</sup>, NH<sub>4</sub>Cl 2.5 g·L<sup>-1</sup>, citric acid 3 g·L<sup>-1</sup>, cysteine 0.5 g·L<sup>-1</sup>, yeast extract 1.5 g·L<sup>-1</sup>, NaCl 1 g·L<sup>-1</sup>, and CaCl 0.010 g·L<sup>-1</sup>), the media was autoclaved for 15 min at 121 ± 2 °C. The



inoculum was a 2 old day flask with pellets. Figure 17 and 18 show the growth of the fungal strain on PDA and in liquid medium, respectively.

The flasks were retired from the experiment every 24 h for a duration of 3 days. The supernatant was filtered with 0.45  $\mu\text{m}$  and the fungal biomass was dried at 105 °C for an hour and afterwards weighted to get the TSS (Total Suspended Solids). The glucose consumption was determined using the DNS reactive agent and the reducing sugar methodology.

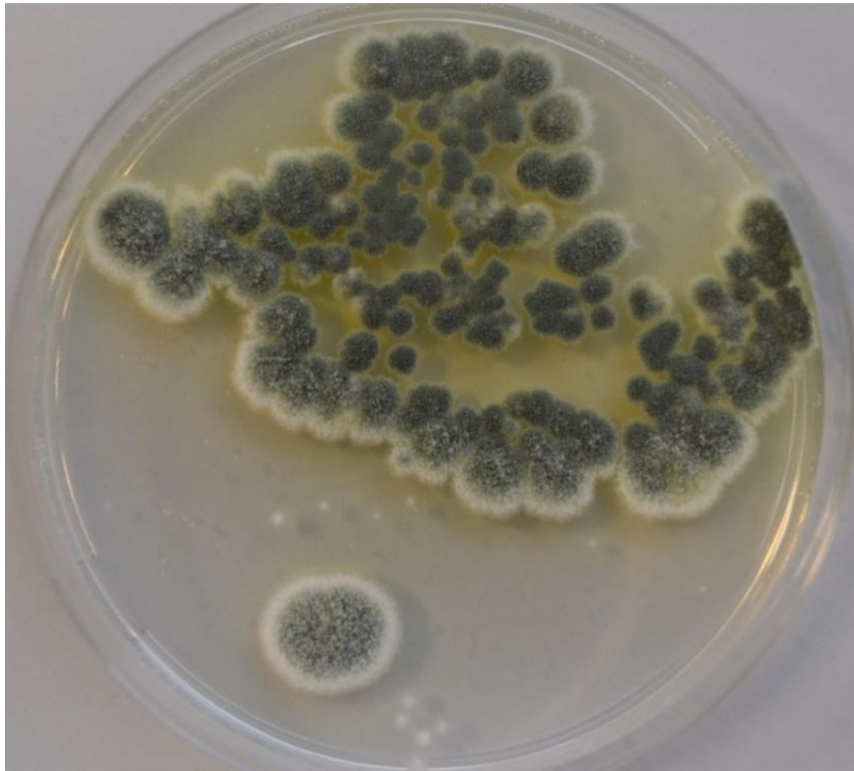


Figure 17. Macroscopic morphology of fungi on solid media (PDA)



Figure 18. Macroscopic morphology of fungi on liquid medium

### 6.2.2. Cr(VI) bioaccumulation

After two days of incubating the adapted culture, the fungal pellets were transferred to fresh liquid media containing different concentrations of Cr(VI) from 10 to 50 mg·L<sup>-1</sup>.

The fungal strain was grown in centrifuge 15 mL tubes containing 10 mL of liquid media ranging the concentration of glucose [0.25-10 g·L<sup>-1</sup>], K<sub>2</sub>HPO<sub>4</sub> 4 g·L<sup>-1</sup>, MgSO<sub>4</sub> 0.75 g·L<sup>-1</sup>, NH<sub>4</sub>Cl 2.5 g·L<sup>-1</sup>, citric acid 3 g·L<sup>-1</sup>, cysteine 0.5 g·L<sup>-1</sup>, yeast extract 1.5 g·L<sup>-1</sup>, NaCl 1 g·L<sup>-1</sup> and CaCl 0.010 g·L<sup>-1</sup>), the media was autoclaved for 15 min at 121 ± 2 °C. The inoculum was a 2 old day flask with pellets. The experimental design consisted in a Central Composite Design (CCD) with biotic and abiotic controls, where the biomass yield and Cr(VI) accumulation were evaluated.

The tubes were centrifuged at 15 000 g for 10 minutes. The supernatant was filtered with 0.45 µm and the fungal biomass was dried at 105 °C for an hour, afterwards, it was weighed to get the total suspended solids (TSS) and put in a muffle furnace for 3 h at 520 °C for the measurement of volatile suspended solids (VSS). The glucose consumption was determined using the DNS reactive agent and the reducing sugar methodology (Miller, 1959).

The determination of the residual Cr(VI) ions after contact with fungal biomass were quantified spectrophotometrically using a UV-VIS Spectrophotometer at 540 nm after complexation with 1,5- diphenyl carbazide agent, following the 3500-Cr B. Colorimetric Method (APHA/AWWA/WEF, 2012).

### 6.2.3. Bioreactor configuration and operating conditions (continuous experiments)

The continuous experiments were performed in two sequencing batch reactors (Figure 19), where each one of the reactors consisted in one supply tank containing the influent, two peristaltic pumps, a cylindrical glass reactor, air supply, effluent tank, pH and dO<sub>2</sub> were monitored during the operation through a controller (Applikon Bio controller ADI 1030) operated by a computer. The program used to configure the sequential process is found in the Appendix E. The reactor was a 1 L cylindrical glass container with a working volume of 0.8 L (Figure 20), it was operated as a sequencing batch reactor with cycles of 6 h, this cycles consisted in 5 min filling, 340 min reactor, 10 min settling, 5 min effluent decanting and 1 min idle period.

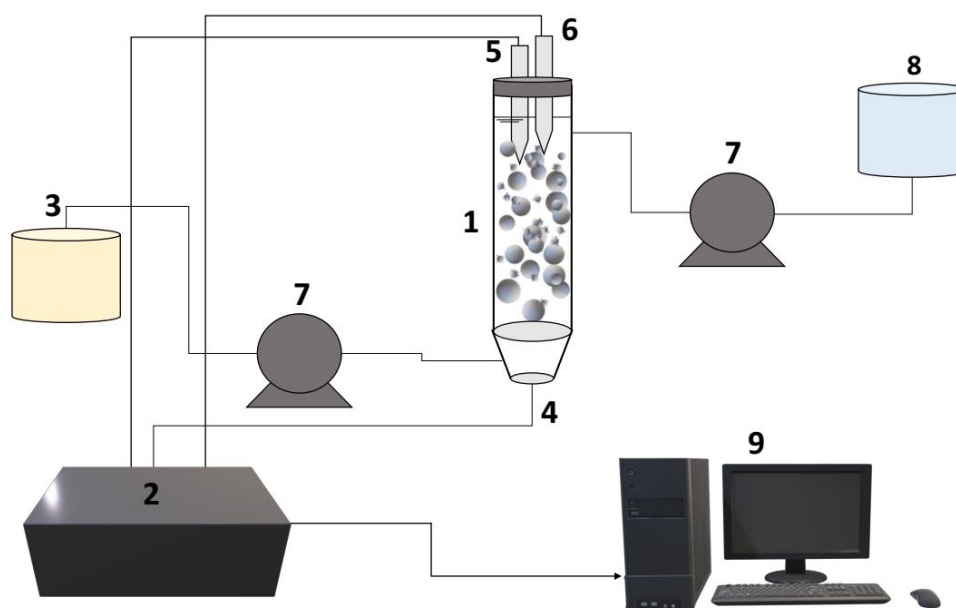


Figure 19. Experimental set up for fungal pelleted reactor: 1) reactor; 2) biocontroller; 3) influent tank; 4) air supply; 5) pH meter; 6) dO<sub>2</sub> meter; 7) peristaltic pumps; 8) effluent tank; 9) computer

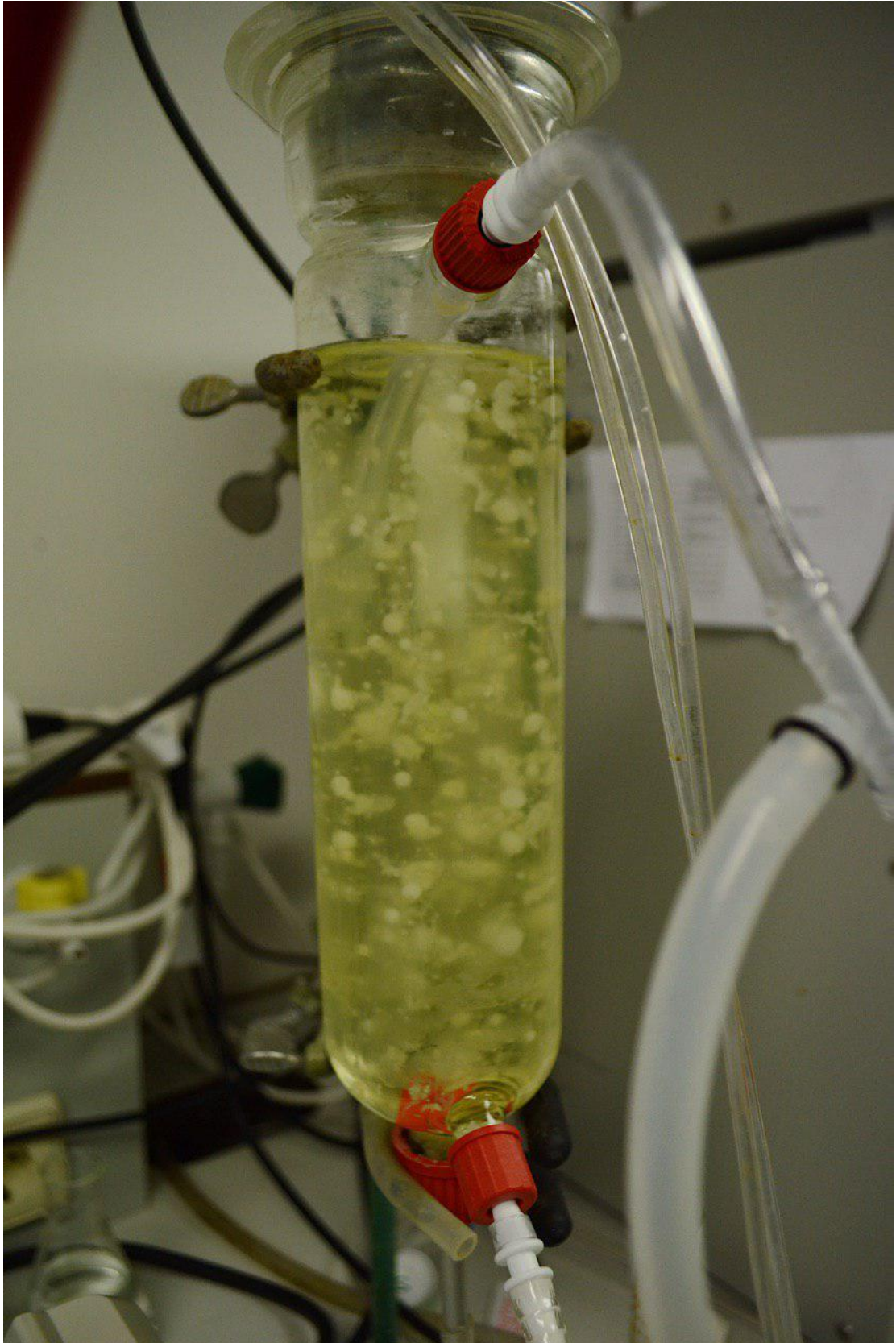


Figure 20. Fungal pelleted reactor

### **6.2.3.1. Cultivation of fungal pellets in SBR**

Reactor 1 (R1) was inoculated with pre-cultured fungal pellets, the working volume of the reactor was 0.8 L bioreactor. The influent tank contained 1:10 diluted culture medium containing glucose [ $10 \text{ g}\cdot\text{L}^{-1}$ ],  $\text{KH}_2\text{PO}_4$   $2 \text{ g}\cdot\text{L}^{-1}$ ,  $\text{MgSO}_4$   $0.5 \text{ g}\cdot\text{L}^{-1}$ ,  $\text{NH}_4\text{Cl}$   $1 \text{ g}\cdot\text{L}^{-1}$ , yeast extract  $1 \text{ g}\cdot\text{L}^{-1}$ ,  $\text{NaCl}$   $1 \text{ g}\cdot\text{L}^{-1}$ , and  $\text{CaCl}$   $0.10 \text{ g}\cdot\text{L}^{-1}$ ), the media was autoclaved for 15 min at  $121 \pm 2 \text{ }^\circ\text{C}$ . After 7 days of cultivation the glucose concentration was changed to 0.5 g/L.

Samples were withdrawn to analyze substrate consumption and dry weight. The supernatant was filtered with  $1.2 \mu\text{m}$  Whatman paper and the fungal biomass was dried at  $105 \text{ }^\circ\text{C}$  for an hour, afterwards the biomass was weighted to measure total suspended solids (TSS) and put in muffle furnace for 3 h at  $520 \text{ }^\circ\text{C}$  for volatile suspended solids (VSS). The glucose consumption was determined using the DNS reactive agent and the reducing sugar methodology (Miller, 1959).

### **6.2.3.2. Cr(VI) removal in SBPR**

Reactor 2 (R2) was operated with a Cr(VI) influent concentration of  $10 \text{ g}\cdot\text{L}^{-1}$ . After day 10 glucose was added at a concentration of  $1 \text{ g}\cdot\text{L}^{-1}$ , by day 23, the glucose concentration was minimized to  $0.5 \text{ g}\cdot\text{L}^{-1}$  to keep feeding substrate to the reactor. Samples were withdrawn and the supernatant was filtered as mentioned in the previous methodology, to measure the glucose consumption and Cr(VI) removal the spectrophotometric techniques of DNS and the DPC methods were used with the same methodology as mentioned above.

The biosorption of the adsorption was calculated using Eq. (1). The removal efficiency of metals was calculated based on Eq. (2).

### **6.2.3.3. Characterization of the dead fungal biomass**

In order to analyze the morphology of the fungal pellets, the samples were rinsed three times using a phosphate buffer with similar pH to the sample in order to keep the sample as it was in its previous environment. A fixation phosphate buffer solution with 0.5% of formaldehyde and 2.5% of glutaraldehyde was used to leave the sample for 16 hours. For the dehydration process, the samples were rinsed with different concentrations

of ethanol [30, 50, 70, 80, 90, 100%] EtOH (in water). The replacement of solvent was executed with concentrations of [25, 50, 75 and 100%] acetone in EtOH. The samples were kept in a fume hood until the acetone was completely evaporated and the samples were completely dry. The samples were prepared in aluminum stabs followed by a gold coat performed under vacuum.

The biomass surface characteristics before and after Cr(VI) adsorption were analyzed using SEM coupled with EDX using JEOL JSM 600 LA.

### 6.3. Results and discussion

#### 6.3.1. Batch glucose growth experiments

The relationship between glucose consumption, TSS and VSS is shown in Figure 21. In the batch experiments where the glucose was varied, the flasks got contaminated with bacteria, since the TSS was affected by this, the data collected was for the first 48 h.

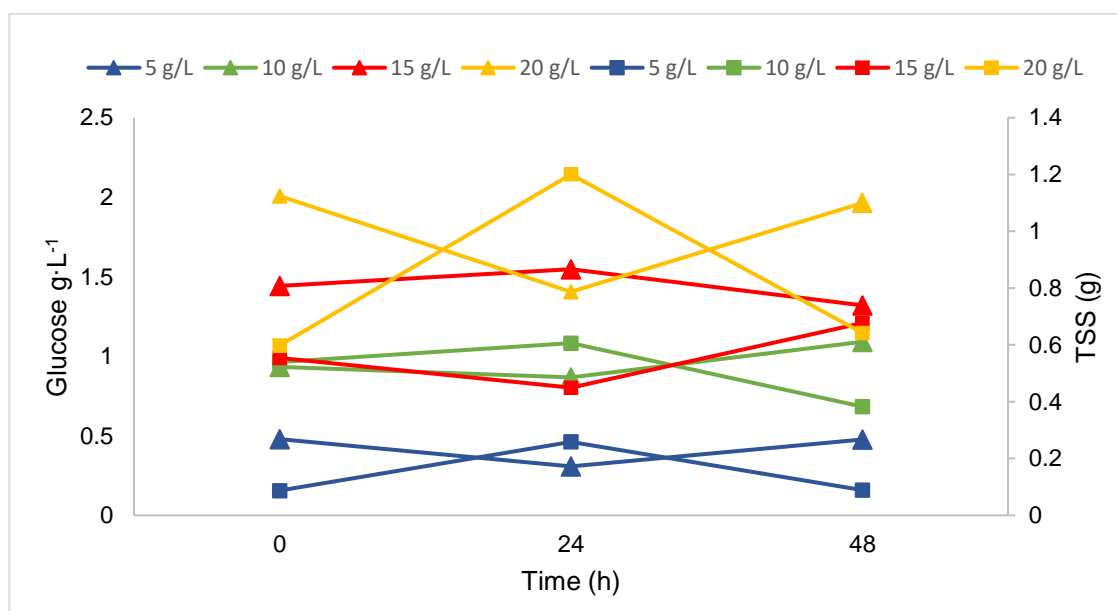


Figure 21. Fungal growth and glucose consumption at different glucose concentrations (■ TSS (g); ▲ glucose consumption (g·L<sup>-1</sup>))

The presented growth kinetics do not give enough information to use the mathematical models, however, it does give some information about the sugar consumption along with the growth of the strain. The dry weight of the fungal pellets was affected by the concentration of glucose, the direct relationship between the fungal growth and glucose consumption is shown in Figure 21. Where the highest growth was at the 20

$\text{g}\cdot\text{L}^{-1}$  of glucose, this agrees with the work of Osadolor *et al.* (2017), where they studied the effect of glucose ranging from 10 to 200  $\text{g}\cdot\text{L}^{-1}$  using *Neurospora intermedia* as model organism, the highest amount of pellets was collected at 20  $\text{g}\cdot\text{L}^{-1}$ , at higher concentrations of substrate the growth was not inhibited, nonetheless the pellets were bigger.

### **6.3.2. Cr(VI) bioaccumulation experiment**

The results for the Cr(VI) determination were quantified with zero Cr(VI) in the samples, the ones with biomass growth, since the control with Cr(VI) is dissolved with the liquid medium, the reduction or removal of Cr(VI) onto another specie is due to a chemical reaction with the salts in the liquid medium and not from a biological process as the main focus of this work is. Bioreduction of Cr(VI) to Cr(III) has been determined in different conditions such as (a) without biomass (b) with biomass (c) with autoclaved biomass and (d) without electron donor (acetate) (Kiran Kumar Reddy and Nancharaiah, 2018), notwithstanding, the controls do not lack the salts in the medium. The analytical determination for Cr(VI) and Cr(III) with the DPC technique has been studied under different liquid media, suspecting that glucose may act as a reducing agent since the tendency of the values are to increase when Cr(VI+III) mixtures are present, in the work of Fernández *et al.* (2010) this tendency was inverted in the case of glucose, confirming that the marked decrease of Cr(VI) titers after oxidation of culture media in the presence of glucose, this could indicate a false significant Cr(VI) removal. Hence, the interferences of the media composition with the Cr(VI) determination should not be ignored, since there are a lot of studies where this analytical technique is used to assess biological removal of the ion, this could lead to misleading results and interpretations. Thereby, this work also encourages the use of AAS (Atomic Absorption Spectroscopy) to confirm the results obtained by the DPC technique.

### **6.3.3. Cultivation of fungal pellets in SBR**

In Figure 22, the dry weight, glucose consumption, and VSS are displayed. The glucose consumption remained constant in each glucose concentration, the  $\text{dO}_2$  profiles (Figure 23) showed that before the cycle was over, dissolved oxygen was already reaching its saturation point, hence, it can be assumed that glucose consumption is related to the dissolved oxygen saturation, since the oxygen consumption rate in aerobic processes is a

comprehensible manifestation of the metabolic activity (Henze *et al.*, 2008). The dropdown of glucose consumption at day 8 was due to the minimization of inlet concentration, nonetheless, the pellets continued to grow and the TSS and VSS reached the same level as at the beginning of the operation with twice the substrate. Maintenance and cleaning of R1 were carried out on days 7 and 12. On day 9 of operation, the pellets in the reactor started to change from a yellow to soft pink color, this could be caused by contamination of other organisms, also the values of dry weight and VSS had their minimum, which could also be explained by the adaptation of the organisms in the culture. Hai *et al.*, (2013) reported two MBRs with fungal pellets in which bacterial contamination could be observed by day 26.

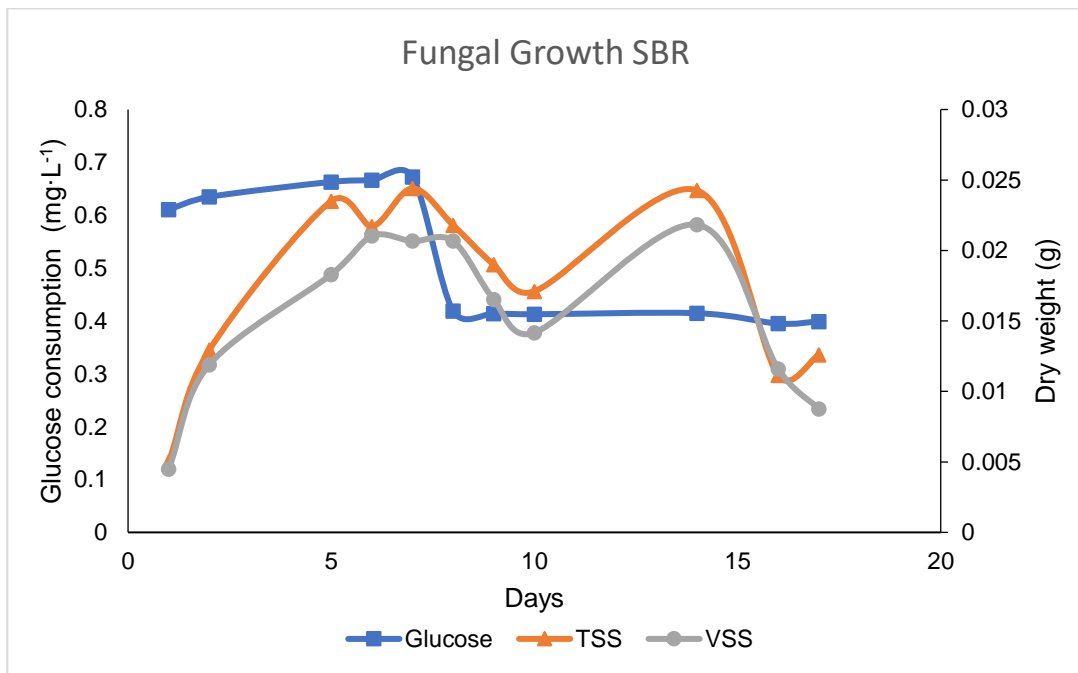


Figure 22. Glucose consumption and dry weight of R1.



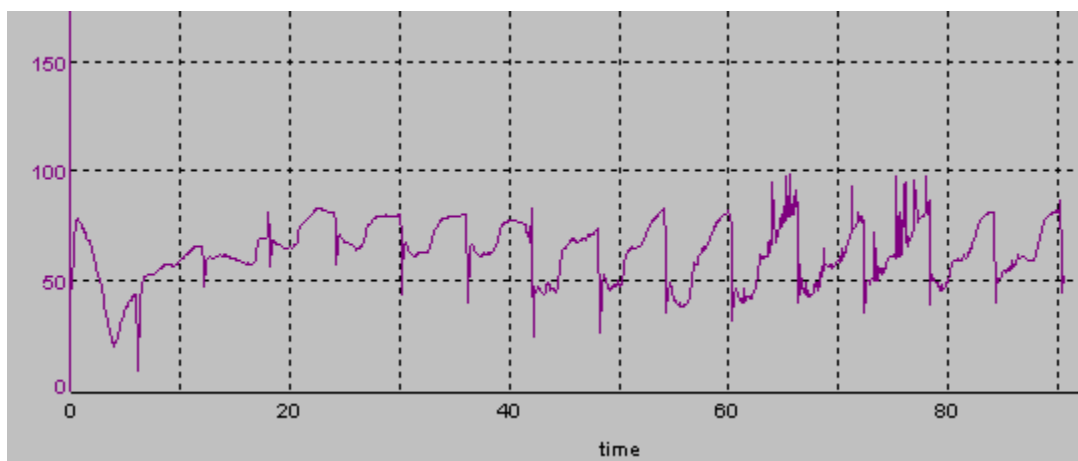


Figure 23. dO<sub>2</sub> profile cycles of R1.

#### 6.3.4. Cr(VI) removal in SBR using fungal pellets

Removal of Cr(VI) in the first 12 days of operation reached a maximum of 11%. On day 14, a known amount of pellets were added to the system and removal reached 18%, nonetheless, the removal dropped down to 6% on day 16. On day 21, pellets were added again and the system reached 29% Cr(VI) removal. The addition of glucose to the system in day 24 did not have any effect on the ion's removal, in fact, the organism did not consume the substrate. It is well known that when a microorganism is exposed to toxic substances, its activity, which is measured on the substrate degradation rate, decreases to the point where all activity ceases (Henze *et al.*, 2008). In this way, the presence of Cr(VI) in biological treatment systems can affect substrate removal (Wang *et al.*, 2015). On day 29, pellets were added to the system and the difference between the cycles changed from a 12% removal to 29%.

Cycles of the system have been monitored at different days and the results are shown in Figure 26, along with the glucose consumption of R2 from day 24 to 28 (Figure 25). The glucose consumption on R2 reached almost 0.1 g·L<sup>-1</sup>, after the second day the substrate consumption did not reach even 0.002 g, which means that glucose was not being consumed.

Oxygen transfer performance is a crucial point when it comes to assessing the metabolic characteristics of aerobic fungal pellets. According to Fernández *et al.* (2017), when working with lower agitation the biomass obtained decreased, relating this phenomenon to the limiting effect of dissolved oxygen in the culture medium. In the previously mentioned study, the effect of limited dissolved oxygen decreased Cr(VI)

removal. The  $dO_2$  profiles of R2 did not show the same trend as the  $dO_2$  profile on R1, where the substrate was being consumed completely and the fungal pellets were metabolically active. In the work of Morales-Barrera *et al.* (2015), the incubation of *Hypocrea tawa* in a culture media without any carbon or energy source, but in the presence of Cr(VI), the concentrations of Cr(VI) and total chromium did not present a measurable change, assuming that the carbon and source in the fungal growth media are required to transform Cr(VI) to Cr(III). Similarly, no decrease in the concentration of Cr(VI) was observed in a cell-free control and in the absence of an electron donor, where aerobic microbial granules were used in aerobic and anoxic conditions to remove Cr(VI) and U(VI) (Nancharaiah *et al.*, 2012).

The chromium effects on the microbial activity of aerobic granular sludge in a sequencing batch reactor were studied by Zheng *et al.*, (2016), where Cr(VI) inhibited the  $NH_4^+$ -N removal rate of the aerobic granules, this inhibition increased as the concentration of Cr(VI) increased. In the work mentioned above, the AG showed high and stable removal efficiency at concentration below  $10 \text{ mg}\cdot\text{L}^{-1}$  and the mechanism of Cr(VI) removal was complex, including physical, chemical, and biological functions. Nonetheless, in this particular study the removal of Cr(VI) could be due to the interaction of the fungal cell wall and the ion, only as a chemical interaction, and not a biological one. Since there was no proof that the Cr(VI) was being removed through the metabolism of the fungi. The addition of fresh biomass was also as a part of maintenance because there was evident lysis in the fungal pellets, hence, also in the fungal cells. Unlike the work of Jin *et al.*, (2017) where anaerobic activated sludge was used in a sequencing batch reactor to remove nitrate and chromate, the results demonstrated that the reduction process was enzyme-mediated and membrane-associated with chromate reductase as the responsible for Cr(VI) reduction. The characteristics of fungi survival in Cr(VI) depends mostly on their structural and biochemical properties as well as their genetic and physiological adaptations. The mechanisms of fungi interaction with chromium have been usually characterized as extracellular, mainly as a linkage to the cell wall or chelation, otherwise as intracellular detoxification where the linkage is with non-proteic thiols and introduced to intracellular compartments (García-Hernández *et al.*, 2017).

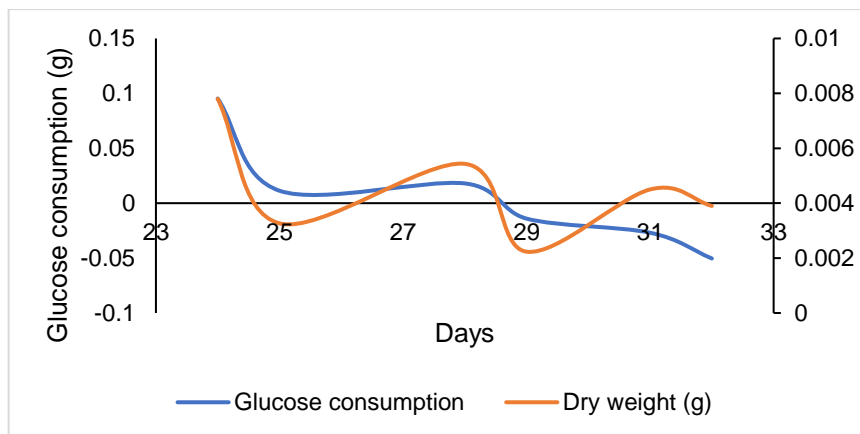


Figure 24. Glucose consumption from day 24 to 32 on SBR with Cr(VI).

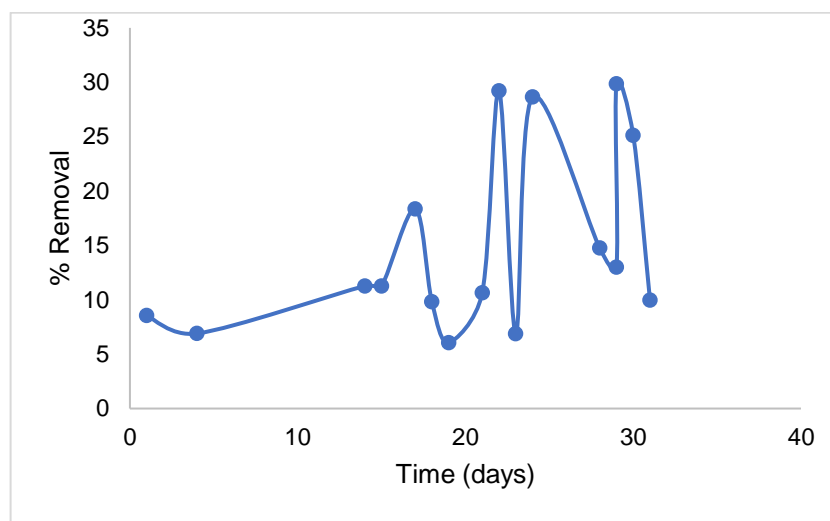


Figure 25. Removal of Cr(VI) in SBR reactor.

### 6.3.5. SEM-EDX

Morphological changes resulting from metal stress can be approached by electronic microscopy, samples of fungal pellets with Cr(VI) were prepared in order to know the physiological effect of the metal with the biomass. In the images of the fungal biomass without Cr(VI) shown in Figure 26, the hyphae of the microorganism looked uniform, nonetheless, in the images for the fungal biomass with Cr(VI), shown in Figure 27, the mycelium shows holes and disruptions inside the hyphae and also disruptions in the biomass, similar alterations in the matrix of the biomass are found in the work of Manorama *et al.* (2016), where a plaster looking like structure is found after the biomass

was in contact with the metal. The removal mechanism of Cr(VI) could be by biosorption since the EDX analysis showed presence of Cr(VI) in the biomass.

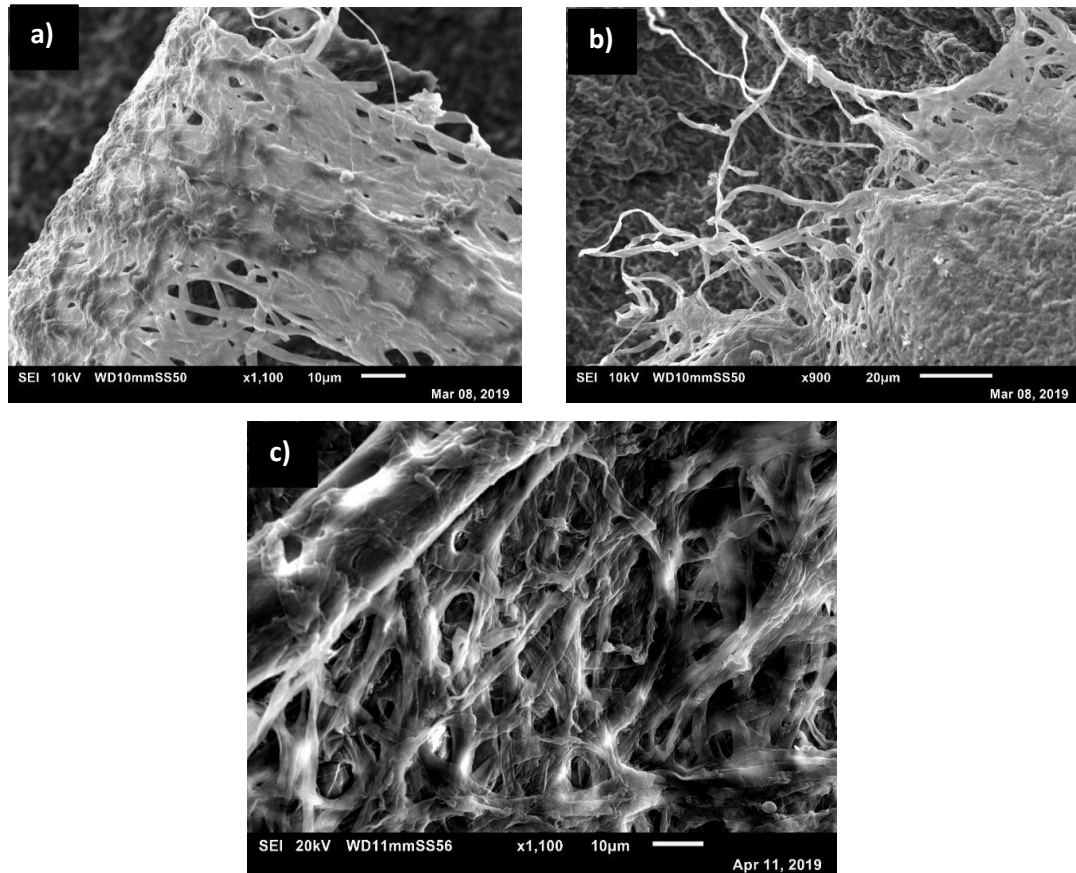


Figure 26. SEM of fungal pellets grown in SBR

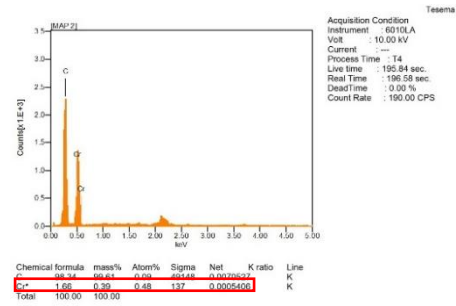
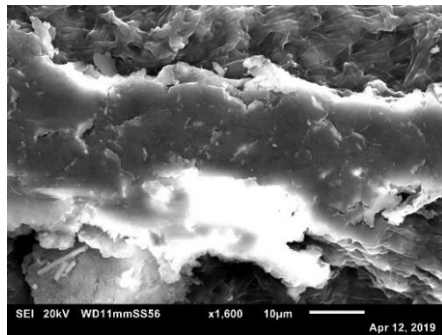
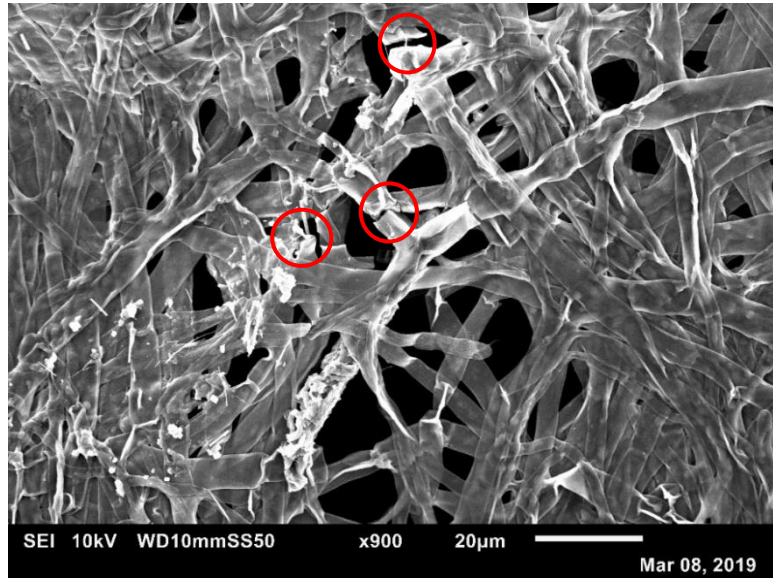


Figure 27. SEM and EDX analysis of fungal biomass after being in contact with Cr(VI).

#### 6.4. Conclusions

Fungal pellets can be cultured in an SBR with a cycle time of 6 h. The settling properties of the fungal pellets give a promising future on the use of these microbial aggregates as a biotechnological approach to treat wastewater effluents. Cr(VI) at a concentration of  $10 \text{ mg} \cdot \text{L}^{-1}$  inhibits the growth of fungal pellets since its substrate was not consumed.

#### 6.5. References

1. APHA/AWWA/WEF, 2012. Standard Methods for the Examination of Water and Wastewater. Stand. Methods 541. <https://doi.org/ISBN 9780875532356>

2. Bhattacharya, A., Gupta, A., Kaur, A., Malik, D., 2019. Alleviation of hexavalent chromium by using microorganisms: Insight into the strategies and complications. *Water Sci. Technol.* 79, 411–424. <https://doi.org/10.2166/wst.2019.060>
3. de Bruin, L.M.M., de Kreuk, M.K., van der Roest, H.F.R., Uijterlinde, C., van Loosdrecht, M.C.M., 2004. Aerobic granular sludge technology: An alternative to activated sludge? *Water Sci. Technol.* 49, 1–7. <https://doi.org/10.2166/wst.2004.0790>
4. de Sousa Rollemberg, S.L., Mendes Barros, A.R., Milen Firmino, P.I., Bezerra dos Santos, A., 2018. Aerobic granular sludge: Cultivation parameters and removal mechanisms. *Bioresour. Technol.* 270, 678–688. <https://doi.org/10.1016/j.biortech.2018.08.130>
5. Espinosa-Ortiz, E.J., Rene, E.R., Pakshirajan, K., van Hullebusch, E.D., Lens, P.N.L., 2016. Fungal pelleted reactors in wastewater treatment: Applications and perspectives. *Chem. Eng. J.* 283, 553–571. <https://doi.org/10.1016/j.cej.2015.07.068>
6. Fernández, P.M., Cruz, E.L., Viñarta, S.C., Castellanos de Figueroa, L.I., 2017. Optimization of culture conditions for growth associated with Cr(VI) removal by *Wickerhamomyces anomalus* M10. *bull. Environ. Contam. Toxicol.* 98, 400–406. <https://doi.org/10.1007/s00128-016-1958-5>
7. Fernández, P.M., Figueroa, L.I.C., Fariña, J.I., 2010. Critical influence of culture medium and Cr(III) quantification protocols on the interpretation of Cr(VI) bioremediation by environmental fungal isolates. *Water. Air. Soil Pollut.* 206, 283–293. <https://doi.org/10.1007/s11270-009-0105-x>
8. García-Hernández, M.A., Villarreal-Chiu, J.F., Garza-González, M.T., 2017. Metallophilic fungi research: an alternative for its use in the bioremediation of hexavalent chromium. *Int. J. Environ. Sci. Technol.* 14, 2023–2038. <https://doi.org/10.1007/s13762-017-1348-5>
9. Hai, F.I., Yamamoto, K., Nakajima, F., Fukushi, K., Nghiem, L.D., Price, W.E., Jin, B., 2013. Degradation of azo dye acid orange 7 in a membrane bioreactor by pellets and attached growth of *Coriolus versicolour*. *Bioresour. Technol.* 141, 29–34. <https://doi.org/10.1016/J.BIORTECH.2013.02.020>
10. Henze, M., van Loosdrecht, M., Ekama, G., Brdjanovic, D., 2008. *Biological Wastewater Treatment: Principles, Modeling and Design*. <https://doi.org/10.2166/9781780408613>
11. Jin, R., Liu, Y., Liu, G., Tian, T., Qiao, S., Zhou, J., 2017. Characterization of product and potential mechanism of Cr ( VI ) reduction by anaerobic activated sludge in a sequencing batch reactor. *Sci. Rep.* 1–12. <https://doi.org/10.1038/s41598-017-01885-z>
12. Jobby, R., Jha, P., Yadav, A.K., Desai, N., 2018. Biosorption and biotransformation of hexavalent chromium [Cr(VI)]: A comprehensive review. *Chemosphere* 207, 255–266. <https://doi.org/10.1016/j.chemosphere.2018.05.050>

13. Kiran Kumar Reddy, G., Nancharaiah, Y. V., 2018. Sustainable bioreduction of toxic levels of chromate in a denitrifying granular sludge reactor. *Environ. Sci. Pollut. Res.* 25, 1969–1979. <https://doi.org/10.1007/s11356-017-0600-3>
14. Manorama, B.A., Sucharita, P.S., Aradhana, B., Kumar, D.N., 2016. Kinetics and surface studies on biosorption of Cr (VI) by using dead fungal biomass from chromium mine waste, Sukinda, India. *Res. J. Chem. Environ.* 20, 42–50.
15. Miller, G.L., 1959. Use of Dinitrosalicylic Acid Reagent for Determination of Reducing Sugar. *Anal. Chem.* 31, 426–428. <https://doi.org/10.1021/ac60147a030>
16. Morales-Barrera, L., Cristiani-Urbina, E., 2015. Bioreduction of hexavalent chromium by *Hypocrea tawa* in a concentric draft-tube airlift bioreactor. *J. Environ. Biotechnol. Res.* 1, 37–44.
17. Morales-Barrera, L., Cristiani-Urbina, E., 2006. Removal of hexavalent chromium by *Trichoderma viride* in an airlift bioreactor. *Enzyme Microb. Technol.* 40, 107–113. <https://doi.org/10.1016/j.enzmictec.2005.10.044>
18. Nancharaiah, Y. V., Kiran Kumar Reddy, G., 2018. Aerobic granular sludge technology: Mechanisms of granulation and biotechnological applications. *Bioresour. Technol.* 247, 1128–1143. <https://doi.org/10.1016/j.biortech.2017.09.131>
19. Nancharaiah, Y.V., Venugopalan, V.P., Francis, A.J., 2012. Removal and biotransformation of U(VI) and Cr(VI) by aerobically grown mixed microbial granules. *Desalin. Water Treat.* 38, 90–95. <https://doi.org/10.1080/19443994.2012.664269>
20. Osadolor, O.A., Nair, R.B., Lennartsson, P.R., Taherzadeh, M.J., 2017. Empirical and experimental determination of the kinetics of pellet growth in filamentous fungi: A case study using *Neurospora intermedia*. *Biochem. Eng. J.* 124, 115–121. <https://doi.org/10.1016/j.bej.2017.05.012>
21. Papagianni, M., 2004. Fungal morphology and metabolite production in submerged mycelial processes. *Biotechnol. Adv.* 22, 189–259. <https://doi.org/10.1016/J.BIOTECHADV.2003.09.005>
22. Sarma, S.J., Tay, J.H., Chu, A., 2017. Finding knowledge gaps in aerobic granulation technology. *Trends Biotechnol.* 35, 66–78. <https://doi.org/10.1016/j.tibtech.2016.07.003>
23. Sen, G., Sen, S., Thakurta, S.G., Chakrabarty, J., Dutta, S., 2018. Bioremediation of Cr(VI) using live cyanobacteria: Experimentation and kinetic Modeling. *J. Environ. Eng. (United States)* 144, 1–12. [https://doi.org/10.1061/\(ASCE\)EE.1943-7870.0001425](https://doi.org/10.1061/(ASCE)EE.1943-7870.0001425)
24. Vu, C.T., Vu, C.T., 2017. Comparison between granular and conventional activated sludge for trace metal elements sorption/desorption. Case of copper for landspreading application in France and in Vietnam. Thèse Université de Limog.

25. Wang, Z., Gao, M., She, Z., Jin, C., 2015. Effects of hexavalent chromium on performance and microbial community of an aerobic granular sequencing batch reactor 4575–4586. <https://doi.org/10.1007/s11356-014-3704-z>



**CHAPTER 7**  
**CONCLUSIONS AND**  
**FUTURE PERSPECTIVES**

## 7.1. Introduction

This dissertation focusses on the use of fungal biomass for heavy metal removal in aqueous solutions. Furthermore, the use of different fungal species was evaluated in batch and continuous experiments. The treatment is based on the adsorption of the metal ions in passive mode (biosorption), where usually the functional groups present in the biosorbent are the ones interacting with the contaminant. Otherwise, the active uptake (metabolic-dependent) by microorganisms is known as bioaccumulation (Kapoor and Viraraghavan, 1995).

## 7.2. Fungal biosorption of Cu(II) and Cr(VI) in aqueous solutions

The need of new treatments for wastewater has made fungi a target to study their potential as heavy metal biosorbents. The biosorption potential of *Aspergillus* sp. and *Rhizopus* sp. using Cu(II) as the contaminant was evaluated in *Chapter 3*. Biosorption of both strains was higher at pH = 5.0. The biomass of *Rhizopus* sp. showed a better affinity to the ion, reaching a 48.63% removal, consequently, the biomass of *Aspergillus* sp. was excluded for the following kinetic and isotherm experiments. The linear and non-linear analysis of the kinetic experiments showed that the ID model fit with the experimental data ( $R^2 = 0.97$ ). As for the isotherm modelling, the data fitted with the Freundlich model. The removal of this ion onto the biomass was not higher enough to continue with further analysis on this phenomenon.

In *Chapter 4*, the metal to remove was Cr(VI). The two strains mentioned above were the same used for this metal. The removal of Cr(VI) showed a 99% removal with both strains at pH = 2.0. Pre-treatment using NaCl was studied with the fungal biomass. In this case both were analyzed by the kinetic models, showing that the PSO and Elovich models were fitting the analyzed data. The Langmuir model ruled the equilibrium studies, implying that the adsorption energy was equally distributed in the surface. *Rhizopus* sp. pre-treated biomass was chosen to be immobilized in Ca-alginate matrixes. The results of Cr(VI) removal with the immobilized biomass are shown in *Chapter 5*. The experiments exhibited that the entrapped biomass decreased the removal obtained with pre-treated *Rhizopus* sp. to a 62.5%. In this case the ID model had the greater coefficient of determination, and the Freundlich model demonstrated the heterogeneity of the biosorbent.

Finally, two SBR using *Trichoderma* sp. were analyzed. The first one, had the goal to produce fungal pellets in the SB mode, since there is no work reporting the growth of fungal pellets under this set up. The self-immobilization was the main purpose, since the previous experiments showed that the Ca-alginate decreased the metal removal. The second reactor was meant to assess the removal of Cr(VI). The maximum removal was of 30%. Evidently, the removal of the metal was not high enough under this specific set-up. However, the production of fungal pellets was achieved using minimum nutrients, also, it was shown that the biomass had good settleability properties, which gives a good potential for this kind of systems.

### **7.3. Scope for future applications in heavy metal biosorption**

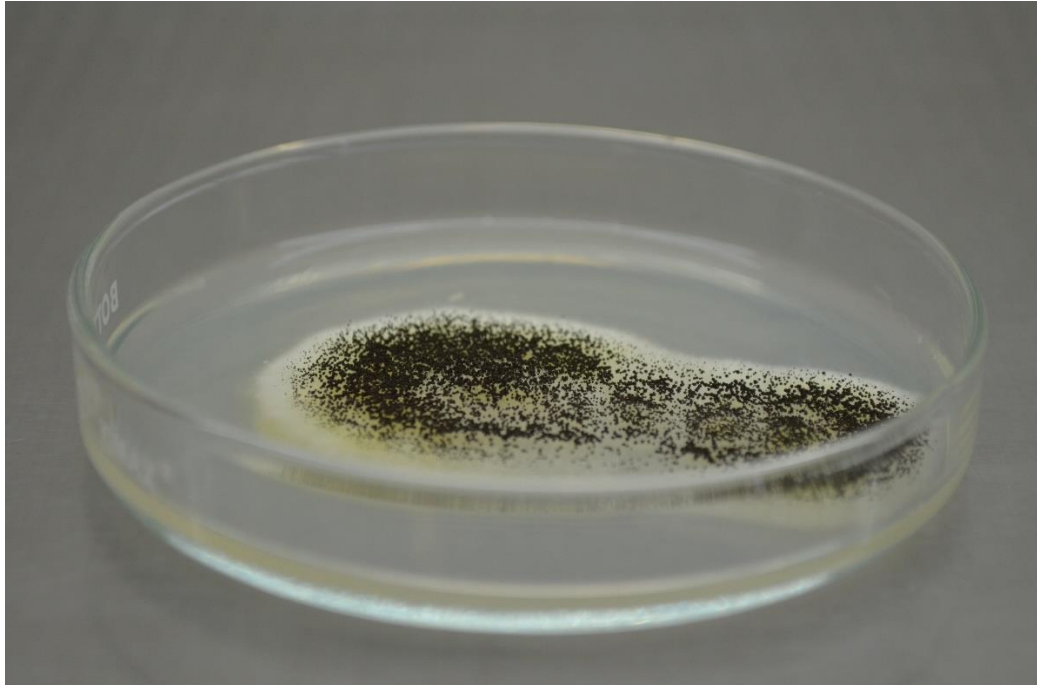
The removal of chromate species in acid aqueous solutions is a promising treatment for effluents in which pH is low. *Rhizopus* sp. dead biomass has the property to remove Cr(VI) efficiently from aqueous solution at low pH. Pre-treatment of the fungal biomass with NaCl increases the capacity of the Cr(VI) adsorption, nonetheless, studies using acid digestion to reach desorption in order to remove Cr(VI) from the biomass need to be taken into account to extend the use of the biomass by reutilizing it. By adopting the view of an industrial application, the immobilization of the dead biomass must be reached. The cell immobilization and the application of bioreactor technologies in continuous operating systems are restrictions that are frequently found in the biosorption processes (Vendruscolo *et al.*, 2017). The lack of quantity and quality of reports containing scale-up processes for Cr(VI) bioremediation advocate for more focus on a pilot and industrial scale (Pradhan *et al.*, 2017).

### **7.4. References**

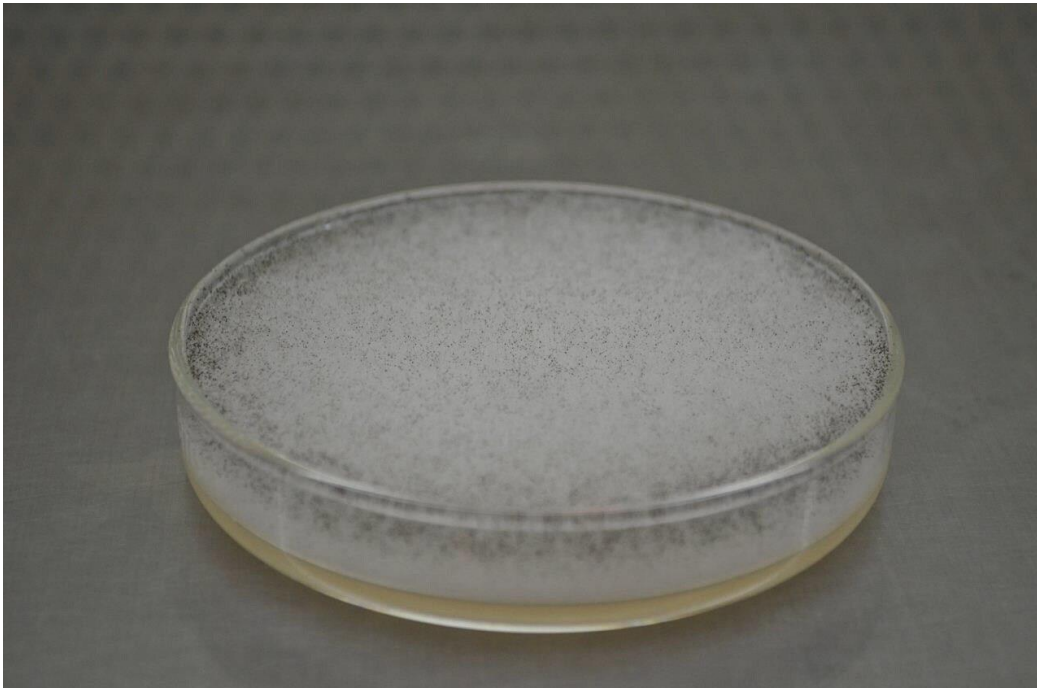
1. Kapoor, A., Viraraghavan, T., 1995. Fungal biosorption - an alternative treatment option for heavy metal bearing wastewaters: a review. *Bioresour. Technol.* 53, 195–206. [https://doi.org/10.1016/0960-8524\(95\)00072-M](https://doi.org/10.1016/0960-8524(95)00072-M).
2. Pradhan, D., Sukla, L.B., Sawyer, M., Rahman, P.K.S.M., 2017. Recent bioreduction of hexavalent chromium in wastewater treatment: A review. *J. Ind. Eng. Chem.* 55, 1–20.
3. Vendruscolo, F., Rocha Ferreira, G.L., Antoniosi Filho, N.R., 2017. Biosorption of hexavalent chromium by microorganisms. *Int. Biodeterior. Biodegrad.* 119, 87–95.

## APPENDIX

**Appendix A. *Aspergillus* sp. on PDA.**



**Appendix B. *Rhizopus* sp. on PDA.**



**Appendix C. ANOVA results of Cu(II) removal screening using *Aspergillus* sp.**

Origen	Tipo III de suma de cuadrados	gl	Cuadrático promedio	F	Sig.	Eta parcial al cuadrado	Parámetro de no centralidad	Potencia observada <sup>b</sup>
Modelo corregido	5706.002 <sup>a</sup>	7	815.143	305.050	.000	.993	2135.349	1.000
Interceptación	118790.861	1	118790.861	44454.925	.000	1.000	44454.925	1.000
pH	5681.438	1	5681.438	2126.156	.000	.993	2126.156	1.000
Temperatura	5.471	1	5.471	2.047	.172	.113	2.047	.270
Agitación	1.342	1	1.342	.502	.489	.030	.502	.102
Error	42.755	16	2.672					
Total	124539.618	24						
Total corregido	5748.757	23						

a. R al cuadrado = .993 (R al cuadrado ajustada = .989)

b. Se ha calculado utilizando alpha = .05

**Appendix D. ANOVA results of Cu(II) removal screening using *Rhizopus* sp.**

Origen	Tipo III de suma de cuadrados	gl	Cuadrático promedio	F	Sig.	Eta parcial al cuadrado	Parámetro de no centralidad	Potencia observada <sup>b</sup>
Modelo corregido	793.783 <sup>a</sup>	7	113.398	40.338	.000	.946	282.367	1.000
Interceptación	148949.052	1	148949.052	52984.672	.000	1.000	52984.672	1.000
pH	779.724	1	779.724	277.366	.000	.945	277.366	1.000
Temperatura	1.045	1	1.045	.372	.551	.023	.372	.088
Agitación	1.837	1	1.837	.654	.431	.039	.654	.118
Error	44.979	16	2.811					
Total	149787.813	24						
Total corregido	838.762	23						

a. R al cuadrado = .946 (R al cuadrado ajustada = .923)

b. Se ha calculado utilizando alpha = .05

**Appendix E. ANOVA results of Cr(VI) removal screening using *Aspergillus* sp.**

Origen	Tipo III de suma de cuadrados	gl	Cuadrático promedio	F	Sig.	Eta parcial al cuadrado	Parámetro de no centralidad	Potencia observada <sup>b</sup>
Modelo corregido	5628.395 <sup>a</sup>	7	804.056	237.689	.000	.990	1663.820	1.000
Interceptación	6011.080	1	6011.080	1776.946	.000	.991	1776.946	1.000
pH	5602.132	1	5602.132	1656.056	.000	.990	1656.056	1.000
Temperatura	4.638	1	4.638	1.371	.259	.079	1.371	.196
Agitación	1.861	1	1.861	.550	.469	.033	.550	.107
Error	54.125	16	3.383					
Total	11693.600	24						
Total corregido	5682.520	23						

a. R al cuadrado = .990 (R al cuadrado ajustada = .986)

b. Se ha calculado utilizando alpha = .05

**Appendix F. ANOVA results of Cr(VI) removal screening using *Rhizopus* sp.**

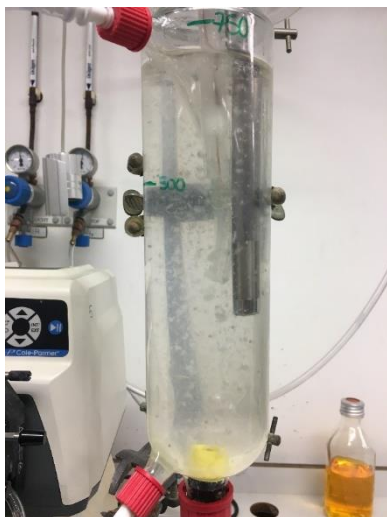
Origen	Tipo III de suma de cuadrados	gl	Cuadrático promedio	F	Sig.	Eta parcial al cuadrado	Parámetro de no centralidad	Potencia observada <sup>b</sup>
Modelo corregido	767.911 <sup>a</sup>	7	109.702	60.540	.000	.964	423.780	1.000
Interceptación	929.786	1	929.786	513.112	.000	.970	513.112	1.000
pH	766.608	1	766.608	423.061	.000	.964	423.061	1.000
Temperatura	.042	1	.042	.023	.882	.001	.023	.052
Agitación	.496	1	.496	.274	.608	.017	.274	.078
Error	28.993	16	1.812					
Total	1726.690	24						
Total corregido	796.904	23						

a. R al cuadrado = .964 (R al cuadrado ajustada = .948)

b. Se ha calculado utilizando alpha = .05



**Appendix G. Reactor 1 through continuous operation for 20 days**



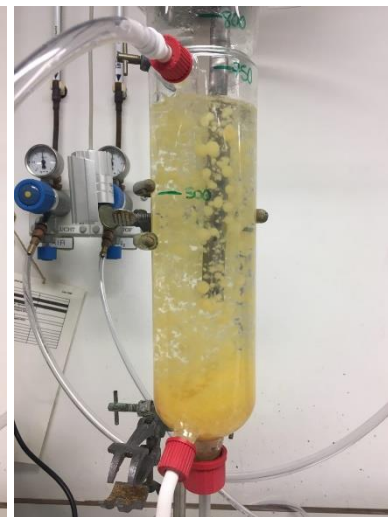
Day 2



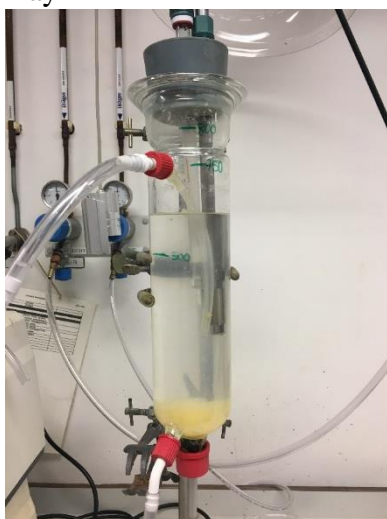
Day 3



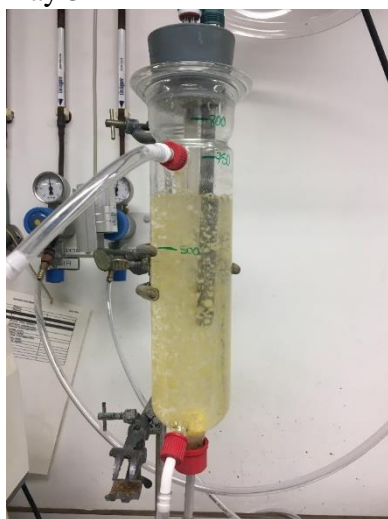
Day 4



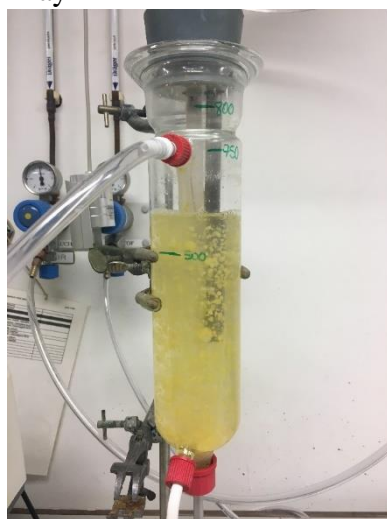
Day 6



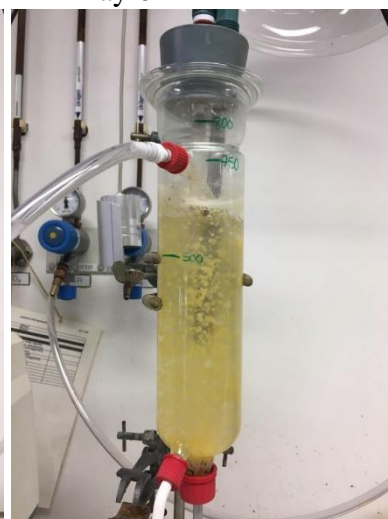
Day 6 (after maintenance)



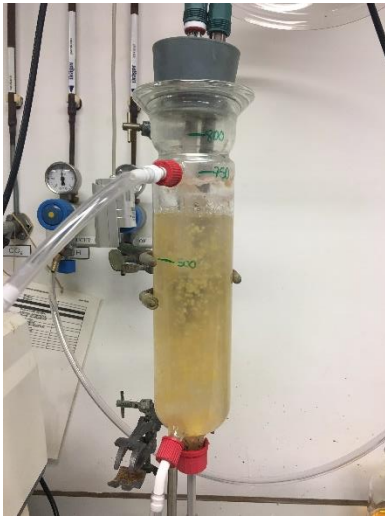
Day 7



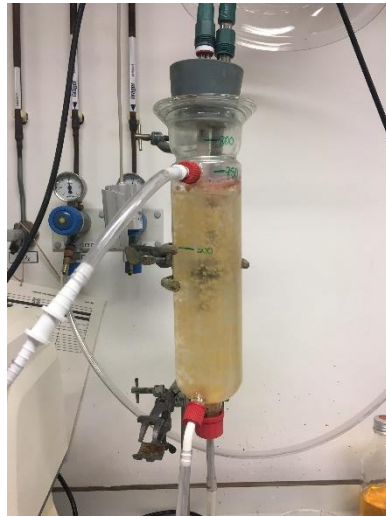
Day 8



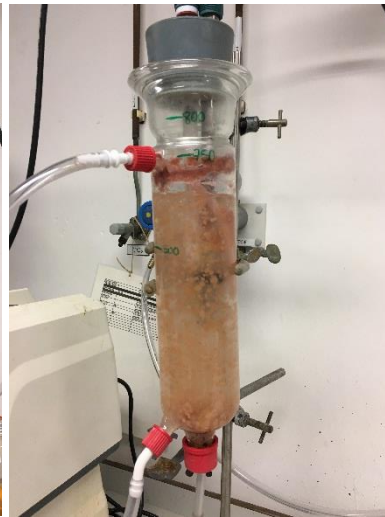
Day 9



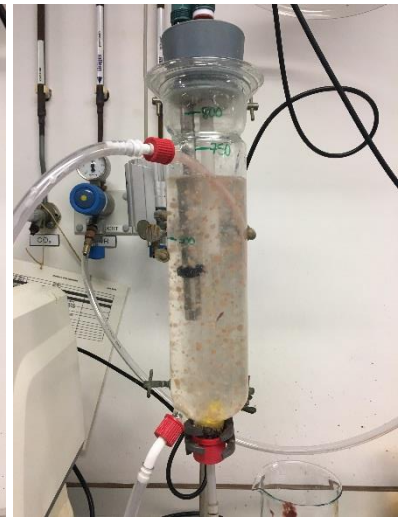
Day 10



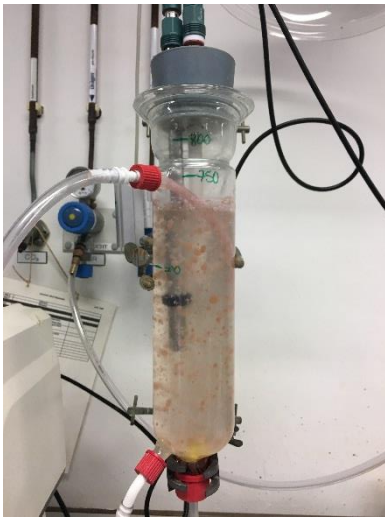
Day 11



Day 13



Day 14 (after m)

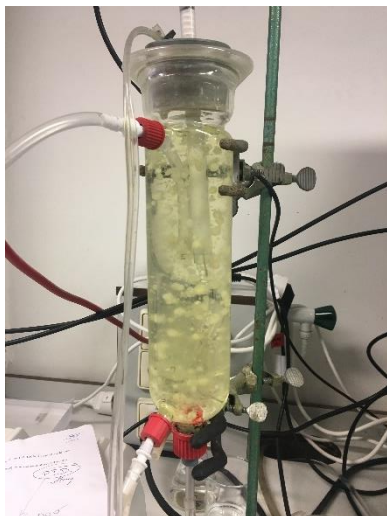


Day 15

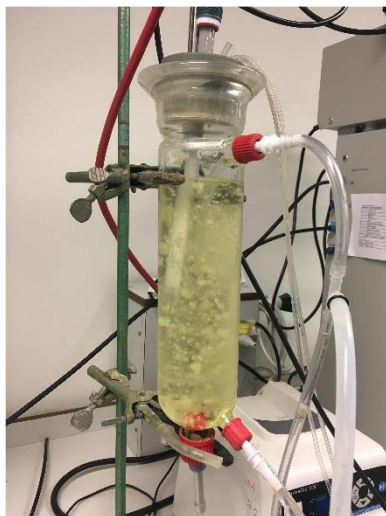


Day 20

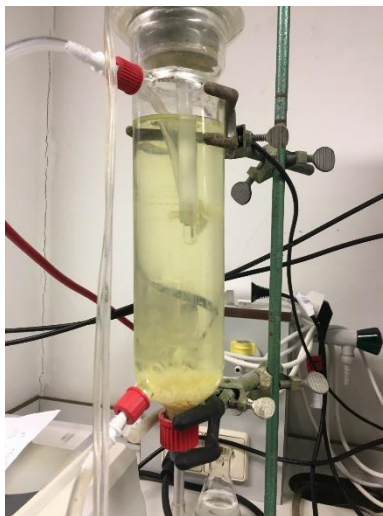
## Appendix H. Reactor 2 through continuous operation for 35 days



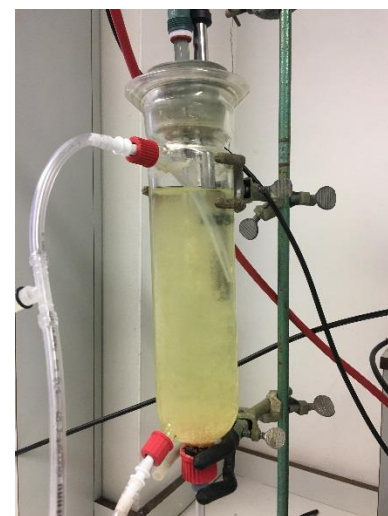
Day 1



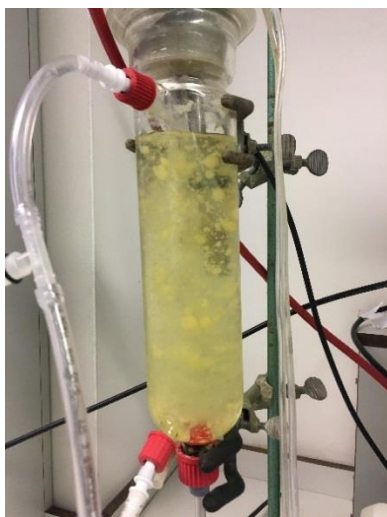
Day 2



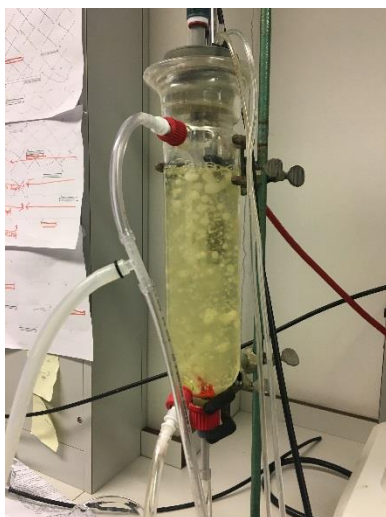
Day 14



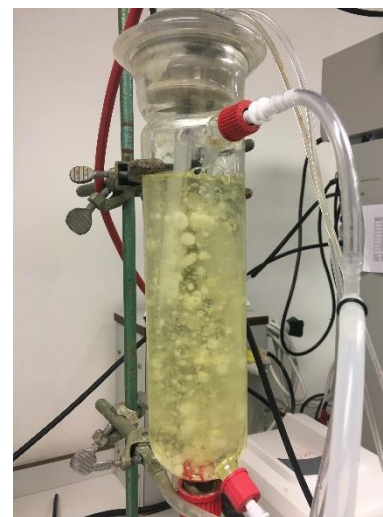
Day 19



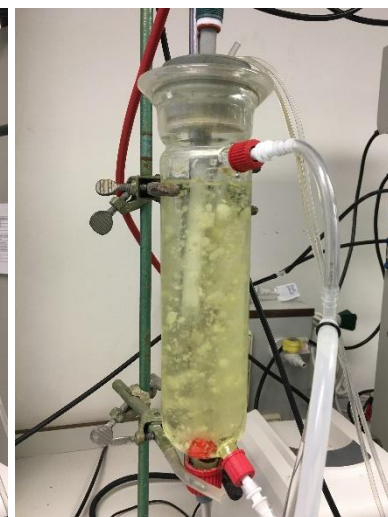
Day 21



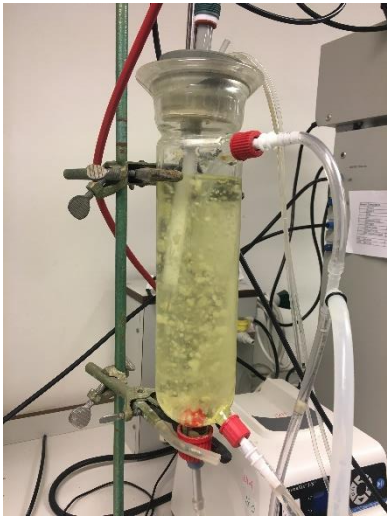
Day 22



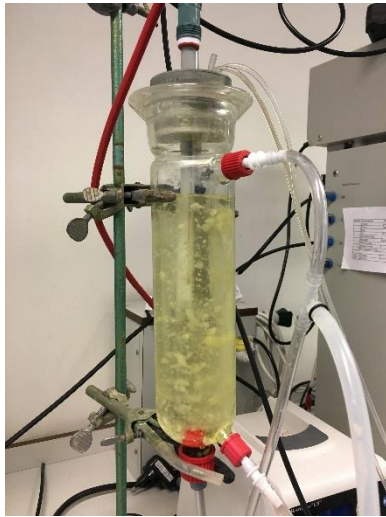
Day 23



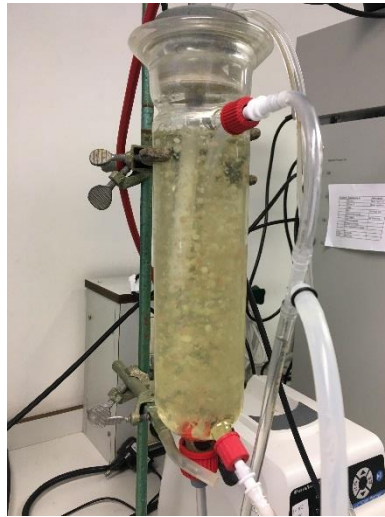
Day 24



Day 25



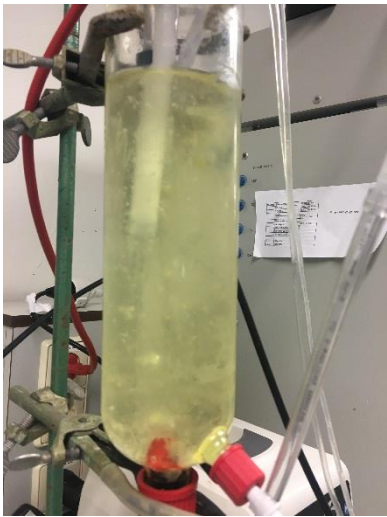
Day 28



Day 29

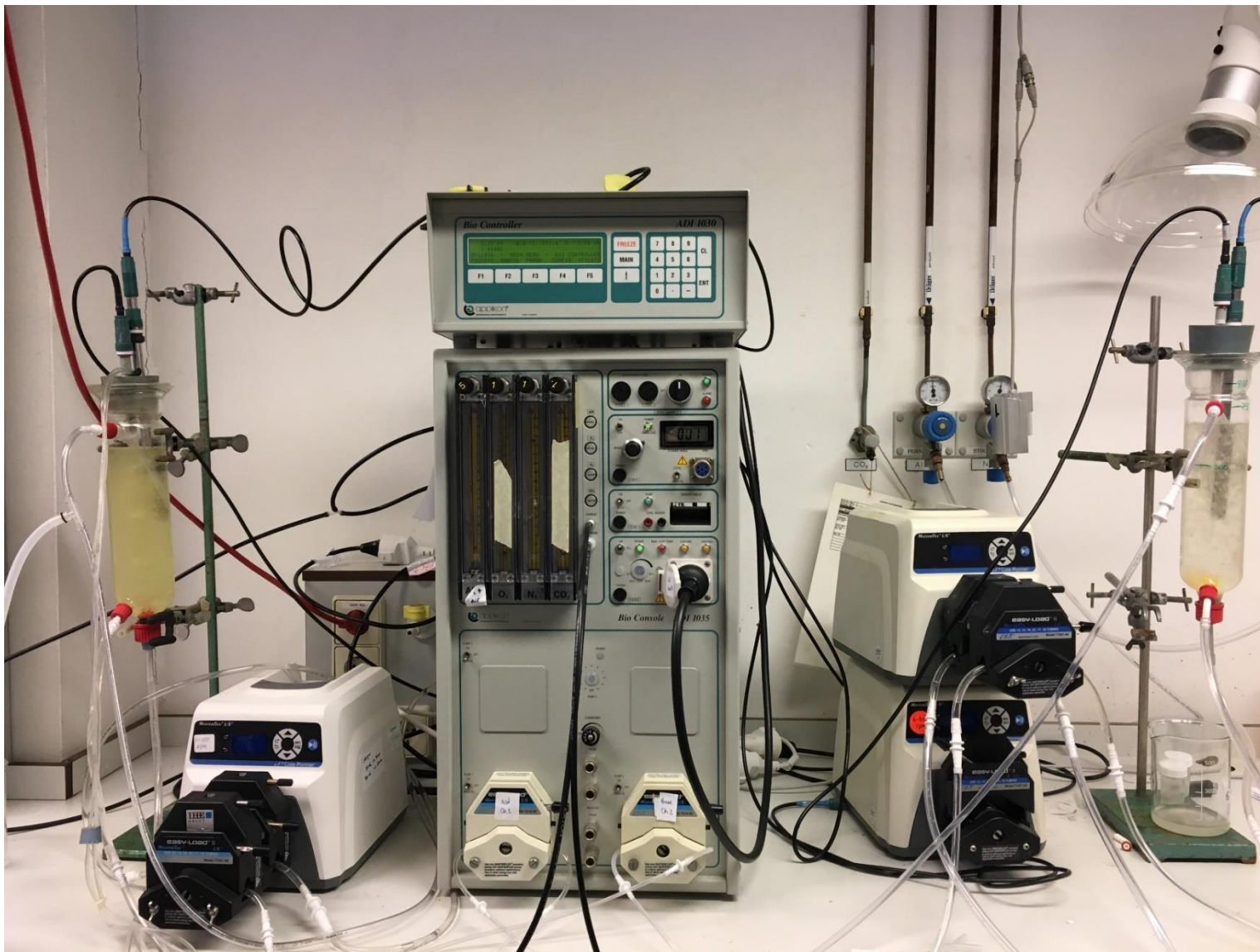


Day 30



Day 35

## Appendix I. Reactors setup



## Appendix J. Script of program used for SBR

-----1. group-----

```
#Stage 0 (Phase 0)
pumpin=0
pumpout=0
NEXTTIME=0
NTT=0
PROCSTEP=0
```

-----2. group-----

```
#Stage 1 (Phase 1)
#phase=1.1
IF PROCSTEP=0 AND TIME>=NEXTTIME
  phase=1.1
  pumpin=1
  air=0
  NEXTTIME=NTT+5
  NTT=NEXTTIME
  PROCSTEP=1.1
ENDIF
```

-----3. group-----

```
#phase=1.2
IF PROCSTEP=1.1 AND TIME>=NEXTTIME
  phase=1.2
  pumpin=0
  air=1
  air2=1
  sppH=3
  NEXTTIME=NTT+700
  NTT=NEXTTIME
  PROCSTEP=1.2
ENDIF
```

-----4. group-----

```
#phase1.3
IF PROCSTEP=1.2 AND TIME>=NEXTTIME
  phase=1.3
  air=0
  air2=0
  sppH=NA
  NEXTTIME=NTT+10
  NTT=NEXTTIME
  PROCSTEP=1.3
ENDIF
```

-----5. group-----

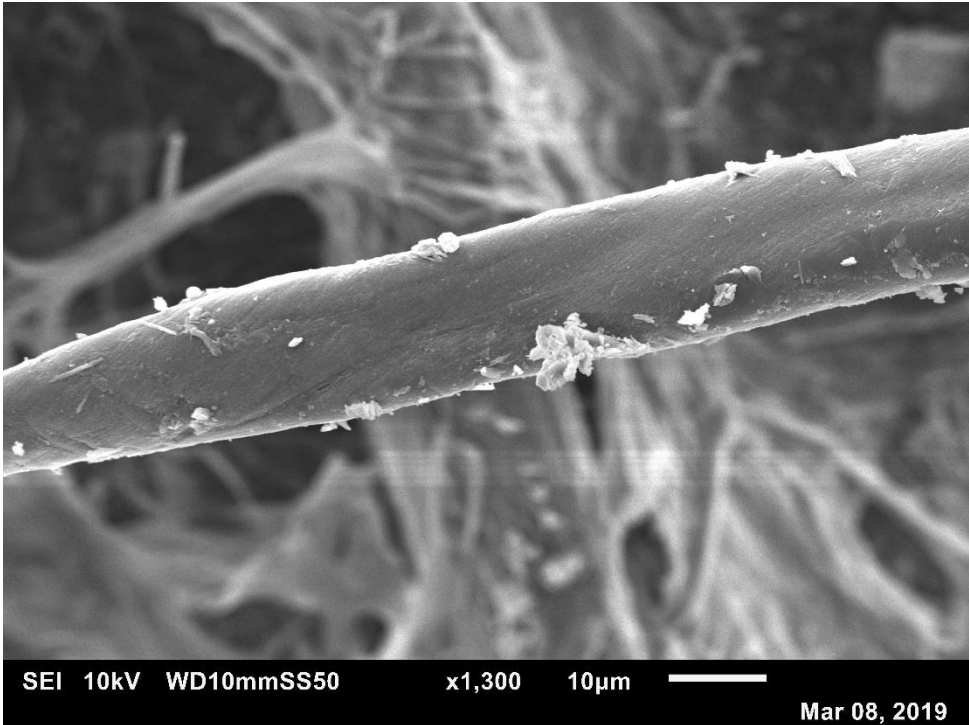
```
#phase1.4
IF PROCSTEP=1.3 AND TIME>=NEXTTIME
  pumpout=1
```

```
air=0
NEXTTIME=NTT+5
NTT=NEXTTIME
PROSTEP=1.4
ENDIF
```

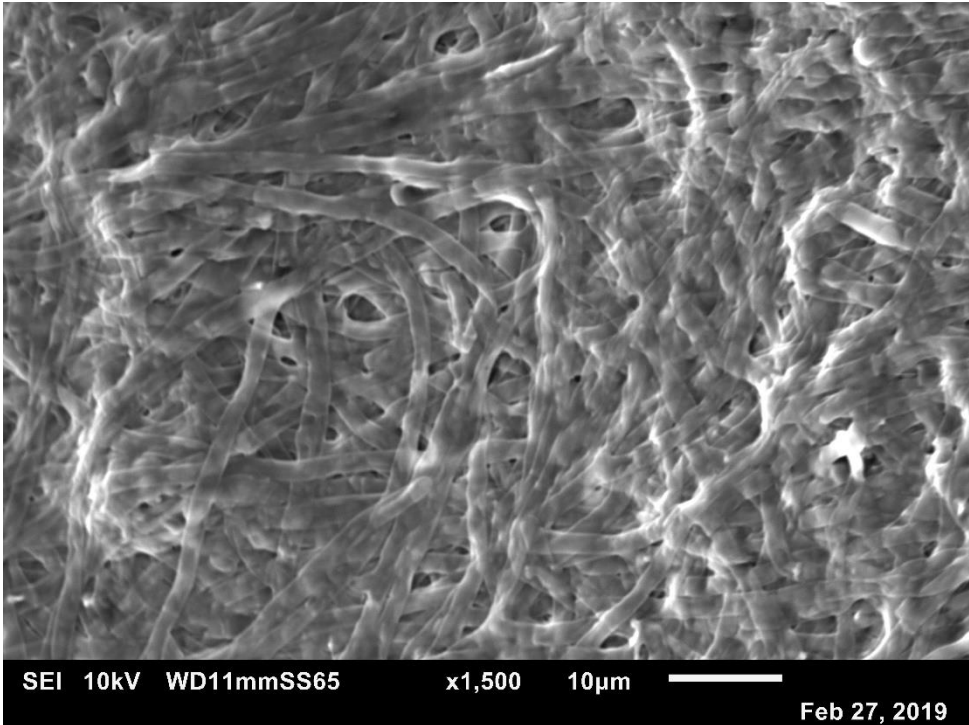
-----**5. group**-----

```
#phase1.5
IF PROCSTEP=1.4 AND TIME>=NEXTTIME
  pumpout=0
  NEXTTIME=NTT+1
  NTT=NEXTTIME
  PROCSTEP=0
ENDIF
```

**Appendix K.1. SEM image of fungal biomass**



**Appendix K.2. SEM image of fungal biomass**





## Appendix L.1 Conference certificate



UNIVERSITÉ  
— PARIS-EST



UNESCO-IHE  
Institute for Water Education



TAMPERE  
UNIVERSITY OF  
TECHNOLOGY

### CERTIFICATE OF ATTENDANCE

*This is to certify that*

**MARTHA ESPINOZA-SÁNCHEZ**

*attended the*

**Joint G16 and final ABWET conference  
on chalcogens and waste-to-energy technologies**

*Naples, Italy*

*6 – 7 December 2018*

Prof. Giovanni Esposito

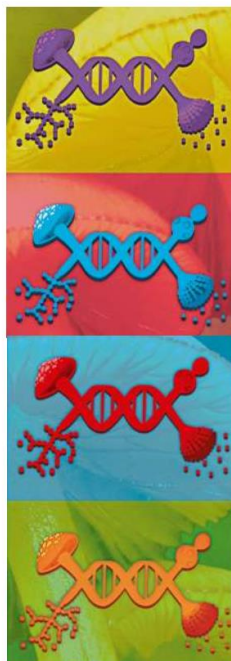
Prof. Eric van Hullebusch

Prof. Piet Lens

Prof. Aino-Maija Lakaniemi



## Appendix L.2 Congress certificate



La Sociedad Mexicana de Bioquímica y el  
Centro de Investigación Científica y Educación Superior de  
Ensenada

Otorgan la presente

## CONSTANCIA

A:

**Martha Alicia Espinoza Sánchez**

Por su asistencia al

**XIII Congreso Nacional de Biología Molecular y  
Celular de Hongos**

Ensenada, Baja California

del 1 al 5 de octubre de 2019

**Dra. Rosa R. Mouriño Pérez**  
Comité Organizador

## Appendix L.3 Congress certificate



### XII Congreso Nacional de Biología Molecular y Celular de Hongos



Otorga la presente **CONSTANCIA** a

**Espinoza Sánchez Martha Alicia**

Quien asistió y presentó el trabajo:

**Characterization of a column biorreactor for the biosorption of Cr(VI) and Cu(II) using fungal biomass**

Por:

Martha Alicia Espinoza Sánchez, Verónica Almaguer Cantú

En la modalidad de cartel durante el XII Congreso Nacional de Biología Molecular y Celular de Hongos del 22 al 26 de octubre de 2017 en Querétaro, Qro.

**Atentamente**

**Por el Comité Organizador**

  
Dr. José Antonio Cervantes Chávez

  
Dr. Edgardo Ulises Esquivel Naranjo



## Biography

Martha Alicia Espinoza Sánchez

PhD Candidate for the degree of  
Doctor in Biotechnology

**Thesis:** Cr(VI) AND Cu(II) BIOREMEDIATION USING  
FUNGAL BIOMASS

**Field of Study:** Environmental Biotechnology

**Personal information:** Born in Delicias, Chihuahua on May 18<sup>th</sup> 1992, daughter of Marco Antonio Espinoza Beltrán and Alicia Sánchez Mendoza.

**Education:** Received her Bachelor's degree on Physics Engineering from the Autonomous University of Chihuahua (UACH).

**Professional experience:** In 2013 started to work as research assistant at CIMAV (CUU) involved in the characterization of different flame retardants nanocomposites. In 2015 worked as Failure and Reliability Analysis Technician in JABIL Circuit Chihuahua. From September 2016 until December 2019 worked as a teacher at the Autonomous University of Nuevo León.

**Congress presentations:** “Characterization of a column bioreactor for the biosorption of Cr(VI) and Cu(II) using fungal biomass” in the *XII Congreso Nacional de Biología Molecular y Celular de Hongos* (2017). “Biosorption of Cr(VI) from water using fungal biomass: a kinetic study” in the *XVII Congreso Internacional y XXIII Congreso nacional de Ciencias Ambientales* (2018). “Cr(VI) biosorption by dead fungal biomass” in the *ABWET Conference on chalcogens and waste to energy technologies*” (2018). “Fungal pelleted reactors in sequencing batch mode, growth and Cr(VI) removal” at the *XIII Congreso Nacional de Biología Molecular y Celular de Hongos* (2019).